

ÇUKUROVA UNIVERSITY
INSTITUTE OF NATURAL AND APPLIED SCIENCES

PhD THESIS

Kerimcan ÇELEBİ

VIBRATION ANALYSIS OF HETEROGENEOUS RODS AND BEAMS

DEPARTMENT OF MECHANICAL ENGINEERING

ADANA, 2010

ÇUKUROVA UNIVERSITY
INSTITUTE OF NATURAL AND APPLIED SCIENCES

**VIBRATION ANALYSIS OF HETEROGENEOUS RODS
AND BEAMS**

Kerimean ÇELEBİ

PhD THESIS

DEPARTMENT OF MECHANICAL ENGINEERING

We certify that the thesis titled above was reviewed and approved for the award of degree of the Doctor of Philosophy by the board of jury on/..../2010.

.....
Prof. Dr. Naki TÛTÛNCÛ
SUPERVISOR

.....
Prof. Dr. Vebil YILDIRIM
MEMBER

.....
Prof. Dr. A. Kamil TANRIKULU
MEMBER

.....
Assoc. Prof. Dr. Ahmet PINARBAŞI
MEMBER

.....
Asst. Prof. Dr. İbrahim KELEŞ
MEMBER

This PhD Thesis is written at the Department of Institute of Natural And Applied Sciences of Çukurova University.

Registration Number:

Prof. Dr. İlhami YEĞİNGİL
Director
Institute of Natural and Applied Sciences

Not:The usage of the presented specific declarations, tables, figures, and photographs either in this thesis or in any other reference without citation is subject to "The law of Arts and Intellectual Products" number of 5846 of Turkish Republic

ABSTRACT

Ph.D. THESIS

VIBRATION ANALYSIS OF HETEROGENEOUS RODS AND BEAMS

Kerimcan ÇELEBİ

**ÇUKUROVA UNIVERSITY
INSTITUTE OF NATURAL AND APPLIED SCIENCES
DEPARTMENT OF MECHANICAL ENGINEERING**

Supervisor : Prof. Dr. Naki TÛTÛNCÛ
Year: 2010, Pages: 133
Jury : Prof. Dr. Naki TÛTÛNCÛ
Prof. Dr. Vebil YILDIRIM
Prof. Dr. A. Kamil TANRIKULU
Assoc. Prof. Dr. Ahmet PINARBAŞI
Asst. Prof. Dr. İbrahim KELEŞ

In the first part, the longitudinal motion of a rod with varying cross-section and elastic properties will be examined. The longitudinal vibration of non-uniform rods is a subject of considerable scientific and practical interest that has been studied extensively. The methods of formulation and solution of an axially loaded rod modeled as a continuous system will be analyzed. The motions of continuous systems will be obtained from the superposition of the modes. In superposition analysis, Duhamel's integral equation will be used to evaluate the response of the system to any form of dynamic loading. The transient response of an axially-loaded bar will also be studied by performing the formulation in the Laplace transform space. The solution in the time domain will be obtained by an appropriate numerical inverse Laplace transformation method. The results will be compared with superposition analysis.

In the second part, free vibration analysis of functionally graded (FG) beam will be performed. Young's modulus of the beam varies in thickness direction according to an exponential law. Using plane strain equation of elasticity, governing equation of axial and transverse motion are solved and exact natural frequencies are obtained. The results are compared with those of various beam theories.

Keywords: FGM beam, Non-uniform rod, Vibration analysis, Laplace transform, Elasticity analysis.

ÖZ

DOKTORA TEZİ

HETEROJEN ÇUBUK VE KİRİŞLERDE TİTREŞİM ANALİZİ

Kerimcan ÇELEBİ

ÇUKUROVA ÜNİVERSİTESİ
FEN BİLİMLERİ ENSTİTÜSÜ
MAKİNA MÜHENDİSLİĞİ ANABİLİM DALI

Danışman : Prof. Dr. Naki TÜTÜNCÜ
Yıl: 2010, Sayfa: 133
Jüri : Prof. Dr. Naki TÜTÜNCÜ
Prof. Dr. Vebil YILDIRIM
Prof. Dr. A. Kamil TANRIKULU
Doç. Dr. Ahmet PINARBAŞI
Yrd. Doç. Dr. İbrahim KELEŞ

Bu tezin ilk bölümünde, değişken kesit ve elastik özelliğe sahip bir çubuğun eksenel titreşimi ele alınacaktır. Değişken kesitli çubukların eksenel titreşimleri bilimsel ve pratik anlamda kayda değer bir ilgi görmüş ve derinlemesine incelenmiştir. Sürekli bir sistem olarak modellenmiş eksenel dinamik yüklü bir çubuğun titreşim analizi yapılacaktır. Devamlı sistemlerin hareketleri, serbest titreşim modları yardımı ile elde edilecektir. Superpozisyon analizinde, sistemin her tür dinamik yüke olan tepkisini değerlendirmek için Duhamel integral denklemi kullanılacaktır. Eksenel yüklü bir çubuğun titreşimi, ayrıca, Laplace transform uzayında gerçekleştirerek incelenecektir. Zaman uzayındaki çözüm uygun bir nümerik ters Laplace transformasyonu ile elde edilecektir. Sonuçlar Superpozisyon analizi ile karşılaştırılacaktır.

İkinci bölümde, fonksiyonel derecelendirilmiş kirişe ait serbest titreşim analizi yapılmıştır. Kirişe ait Young modülü kalınlık doğrultusunda eksponansiyel olarak değişmektedir. Düzlem şekil değiştirme kabulü ile kirişin eksenel ve enine titreşim denklemleri analitik olarak çözülmüş ve kesin doğal frekans değerleri hesaplanmıştır. Sonuçlar değişik kiriş teorileri sonuçları ile karşılaştırılmıştır.

Anahtar kelimeler: FGM kiriş, Değişken kesitli çubuk, Titreşim analizi, Laplace transformasyonu, Elastisite Analizi.

ACKNOWLEDGEMENT

I am truly grateful to my research supervisor, Prof. Dr. Naki TTNC, for his invaluable guidance and support throughout the preparation of this thesis.

I would like to express my special thanks to Advisory Committee Members, Prof. Dr. Vebil YILDIRIM, Prof. Dr. A. Kamil TANRIKULU, for their devotion of invaluable time throughout my research activities.

Another point that should be emphasized here is the continuous moral support, motivation, encouragement and patience of my parents during my studies.

LIST OF CONTENTS	PAGE
ABSTRACT.....	I
ÖZ.....	II
ACKNOWLEDGMENT.....	III
LIST OF CONTENTS.....	IV
LIST OF TABLES	VIII
LIST OF FIGURES	IX
NOMENCLATURE.....	XI
1.INTRODUCTION.....	1
2.PREVIOUS STUDIES.....	3
2.1. Non-uniform and Heterogeneous Rods.....	3
2.2. Application of Laplace Transform to Dynamic Problems.....	5
2.3. FGM Beams.....	6
3.MATERIAL AND METHOD.....	9
3.1. An Overview of the Differential Equation.....	9
3.1.1. Classical Solution.....	9
3.1.2. Duhamel’s Integral.....	9
3.1.3. Transform Methods.....	10
3.2. Partial Differential Equations of Motion of an Axially-Loaded Bar.....	11
3.2.1 Axial Deformations (Undamped).....	11
3.2.2. Orthogonality of Axial Vibrations Modes.....	12
3.2.3. Analysis of Dynamic response (Normal Coordinates).....	14
3.2.4. Uncoupled Axial Equations of Motion.....	14
3.2.5. Formulation of Duhamel Integral.....	16
3.3. Free Vibration Analysis of Non-uniform and Heterogeneous Rods.....	18
3.3.1. Free Vibration Analysis of Non-uniform Rods.....	18
3.3.1.1. Solution for Area Variation of the Form	
$A(h) = A_0(1 + ah)^2$	18

3.3.1.2. Solution for Area Variation of the Form	20
$A = A_0 \sin^2[ah + b]$	
3.3.1.3. Solution for Area Variation of the Form $A(h) = A_0 e^{-ah}$	22
3.3.2. Free Vibration Analysis of Heterogeneous Rods.....	24
3.3.2.1 Solution for $E(h) = E_0(1 + ah)^2$ and $r(h) = r_0(1 + ah)^2$	25
3.3.2.2. Solution for $E(h) = E_0 \sin^2[ah + b]$ and	
$r(h) = r_0 \sin^2[ah + b]$	26
3.3.2.3. Solution for $E(h) = E_0 e^{-ah}$ and $r(h) = r_0 e^{-ah}$	27
3.4. Forced Vibration Analysis of Non-uniform and Heterogeneous Rods....	28
3.4.1. Laplace Transformation.....	28
3.4.1.1. Solution of Boundary-Value Problems by Laplace	
Transforms.....	30
3.4.1.2. Displacement Solution of Axially Loaded Non-Uniform	
Rods Using Laplace Transform Technique.....	30
3.4.1.2.(1). Displacement Solution for Area Variation of	
the Form $A(h) = A_0(1 + ah)^2$	31
3.4.1.2.(2). Displacement Solution for Area Variation of	
the Form $A(h) = A_0 \sin^2[ah + b]$	33
3.4.1.2.(3). Displacement Solution for Area Variation of	
the Form $A(h) = A_0 e^{-ah}$	36
3.4.1.3 Displacement Solution of Axially Loaded Heterogeneous	
Rods Using Laplace Transform Technique.....	38
3.4.1.3.(1). Displacement Solution for $E(h) = E_0(1 + ah)^2$	
and $r(h) = r_0(1 + ah)^2$	38
3.4.1.3.(2). Displacement Solution for $E(h) = E_0 \sin^2[ah + b]$	
and $r(h) = r_0 \sin^2[ah + b]$	40

3.4.1.3.(3). Displacement Solution for $E(h) = E_0 e^{-ah}$ and $r(h) = r_0 e^{-ah}$	41
3.4.2. Numerical Direct Laplace Transform Methods.....	43
3.4.2.1. Direct Laplace Transform which Utilizes FFT.....	43
3.4.3. Numerical Inverse Laplace Transform Methods.....	44
3.4.3.1. Durbin's Inverse Transform Method.....	45
3.4.4. Use of Residue Theorem in Finding Inverse Laplace Transforms..	46
3.4.4.1. Solutions for the form $(1 + ah)^2$	48
3.4.4.1.(1). Displacements due to the Cosine Type Force.....	48
3.4.4.1.(2). Displacements due to the Step Force.....	50
3.4.4.1.(3). Displacements due to the Exponential Type Force.....	53
3.4.4.2. Solutions for the form $\sin^2[ah + b]$	55
3.4.4.2.(1). Displacements due to the Cosine Type Force.....	56
3.4.4.2.(2). Displacements due to the Step Force.....	58
3.4.4.2.(3). Displacements due to the Exponential Type Force.....	61
3.4.4.3 Solutions for the form e^{-ah}	64
3.4.4.3.(1). Displacements due to the Cosine Type Force.....	64
3.4.4.3.(2). Displacements due to the Step Force.....	67
3.4.4.3.(3). Displacements due to the Exponential Type Force.....	69
3.4.5 Mode-Superposition Analysis.....	72
3.5 Free Vibration Analysis of FGM Beam.....	78
3.5.1 Elasticity Analysis.....	79
3.5.2 Mode Shapes.....	85
3.5.3 Beam Theory.....	87
4.RESULTS AND DISCUSSIONS.....	93
5. CONCLUSIONS.....	112

REFERENCES.....	114
CURRICULUM VITAE	118
APPENDIX A.....	120
APPENDIX B.....	124

LIST OF TABLES	PAGE
Table 3.1. Natural frequencies of fixed-free rods with $A(h) = A_0(1 + ah)^2$	20
Table 3.2. Natural frequencies of fixed-free rods with $A(h) = A_0 \sin^2[ah + b]$	22
Table 3.3. Natural frequencies of fixed-free rods with $A(h) = A_0 e^{-ah}$	24
Table 3.4. Axial displacement expressions of the end point in Laplace space for $A(h) = A_0(1 + ah)^2$	33
Table 3.5. Axial displacement expressions of the end point in Laplace space for $A(h) = A_0 \sin^2[ah + b]$	35
Table 3.6. Axial displacement expressions of the end point in Laplace space for $A(h) = A_0 e^{-ah}$	38
Table 3.7. Displacements due to $P_1(t), P_2(t)$ and $P_3(t)$ for the form $(1 + ah)^2$	55
Table 3.8. Displacements due to $P_1(t), P_2(t)$ and $P_3(t)$ for the form $\sin^2[ah + b]$	63
Table 3.9. Displacements due to $P_1(t), P_2(t)$ and $P_3(t)$ for the form e^{-ah}	72
Table 3.10. Mode-Superposition analysis expressions for step-type loading.....	75
Table 3.11. Mode-Superposition analysis expressions for cosine-type loading.....	76
Table 3.12. Mode-Superposition analysis expressions for exponential-type loading.....	77
Table 3.13. Exact natural frequencies for FGM beam, using elasticity theory.....	86
Table 3.14. Natural frequencies for FGM beam from beam theories.....	92

LIST OF FIGURES**PAGE**

Figure 3.1. Two modes of vibration for the same rod.	13
Figure 3.2 Derivation of the Duhamel integral (undamped).	16
Figure 3.3 Integration contour C	47
Figure 3.4. An FGM beam	78
Figure 3.5. Variation of Young's modulus in the thickness direction.	79
Figure 4.1. End displacement for the form $\sin^2[ah + b]$ under $P_2(t) = P_0$, $a=0$, $m=10$.	94
Figure 4.2. End displacement for the form $\sin^2[ah + b]$ under $P_2(t) = P_0$, $a=1$, $m=10$.	94
Figure 4.3. End displacement for the form $\sin^2[ah + b]$ under $P_2(t) = P_0$, $a=2$, $m=10$.	95
Figure 4.4. End displacement for the form $\sin^2[ah + b]$ under $P_1(t) = P_0(1 - \cos[gt])$, $a=0$, $m=10$, $g=0.6$.	95
Figure 4.5. End displacement for the form $\sin^2[ah + b]$ under $P_1(t) = P_0(1 - \cos[gt])$, $a=1$, $m=10$, $g=0.6$.	96
Figure 4.6. End displacement for the form $\sin^2[ah + b]$ under $P_1(t) = P_0(1 - \cos[gt])$, $a=2$, $m=10$, $g=0.6$.	96
Figure 4.7. End displacement for the form $\sin^2[ah + b]$ under $P_3(t) = P_0(1 - e^{-gt})$, $a=0$, $m=10$, $g=0.6$.	97
Figure 4.8. End displacement for the form $\sin^2[ah + b]$ under $P_3(t) = P_0(1 - e^{-gt})$, $a=1$, $m=10$, $g=0.6$.	97
Figure 4.9. End displacement for the form $\sin^2[ah + b]$ under $P_3(t) = P_0(1 - e^{-gt})$, $a=2$, $m=10$, $g=0.6$.	98
Figure 4.10. End displacement for the form $(1 + ah)^2$ under $P_2(t) = P_0$, $a=0$, $m=10$.	98
Figure 4.11. End displacement for the form $(1 + ah)^2$ under $P_2(t) = P_0$, $a=1$, $m=10$.	99
Figure 4.12. End displacement for the form $(1 + ah)^2$ under $P_2(t) = P_0$, $a=2$, $m=10$.	99
Figure 4.13. End displacement for the form $(1 + ah)^2$ under $P_1(t) = P_0(1 - \cos[gt])$, $a=0$, $m=10$, $g=0.6$.	100
Figure 4.14. End displacement for the form $(1 + ah)^2$ under $P_1(t) = P_0(1 - \cos[gt])$, $a=1$, $m=10$, $g=0.6$.	100

Figure 4.15. End displacement for the form $(1 + ah)^2$ under $P_1(t) = P_0(1 - \cos[gt])$, $a=2, m=10, g=0.6$.	101
Figure 4.16. End displacement for the form $(1 + ah)^2$ under $P_3(t) = P_0(1 - e^{-gt})$, $a=0, m=10, g=0.6$.	101
Figure 4.17. End displacement for the form $(1 + ah)^2$ under $P_3(t) = P_0(1 - e^{-gt})$, $a=1, m=10, g=0.6$.	102
Figure 4.18. End displacement for the form $(1 + ah)^2$ under $P_3(t) = P_0(1 - e^{-gt})$, $a=2, m=10, g=0.6$.	102
Figure 4.19. End displacement for the form e^{-ah} under $P_2(t) = P_0$, $a=0, m=10$.	103
Figure 4.20. End displacement for the form e^{-ah} under $P_2(t) = P_0$, $a=1, m=10$.	103
Figure 4.21. End displacement for the form e^{-ah} under $P_2(t) = P_0$, $a=2, m=10$.	104
Figure 4.22. End displacement for the form e^{-ah} under $P_1(t) = P_0(1 - \cos[gt])$, $a=0, m=10, g=0.6$.	104
Figure 4.23. End displacement for the form e^{-ah} under $P_1(t) = P_0(1 - \cos[gt])$, $a=1, m=10, g=0.6$.	105
Figure 4.24. End displacement for the form e^{-ah} under $P_1(t) = P_0(1 - \cos[gt])$, $a=2, m=10, g=0.6$.	105
Figure 4.25. End displacement for the form e^{-ah} under $P_3(t) = P_0(1 - e^{-gt})$, $a=0, m=10, g=0.6$	106
Figure 4.26. End displacement for the form e^{-ah} under $P_3(t) = P_0(1 - e^{-gt})$, $a=1, m=10, g=0.6$.	106
Figure 4.27. End displacement for the form e^{-ah} under $P_3(t) = P_0(1 - e^{-gt})$, $a=2, m=10, g=0.6$.	107
Figure 4.28. Variation of the fundamental frequency of FGM beam with L/h ratio for $n=1$	108
Figure 4.29. Variation of the fundamental frequency of FGM beam with L/h ratio for $n=3$	108
Figure 4.30. Variation of the fundamental frequency of FGM beam with L/h ratio for $n=5$	109
Figure 4.31. Variation of the fundamental frequency of FGM beam with n for $L/h=5$	109
Figure 4.32. Variation of the fundamental frequency of FGM beam with n for $L/h=10$	110
Figure 4.33. Variation of the fundamental frequency of FGM beam with n for $L/h=20$	110
Figure 4.34. Flexural mode shapes at the bottom surface and upper surface of the FGM beam.	111

NOMENCLATURE

a	Inhomogeneity parameter
A	Area
c	Velocity of the Propagation of the Displacement
E	Young's Modulus
$f_I(x,t)$	Inertial Force
FFT	Fast Fourier Transform
Im	Imaginary
h	Thickness
k	Spring Constant
L	Length
n	Wave number
m	Mass
M_n	Generalized Mass of n'th Normal Mode
P_o	Load
$P(x,t)$	Applied Axial Loading
$P_n(t)$	Generalized Loading of n'th Normal Mode in Time Domain
Re	Real
p	Laplace Constant
SDOF	Single Degree of Freedom
t	Time
u	Displacement in x direction
Q_{ij}	Transformed stiffness constants
a	Undamped Natural Circular Frequencies
$Y(t)$	Displacement in Time Domain
Δt	Time Interval
e	Normal Strain
s	Normal Stress
r	Mass per Unit Volume
t	Time (dimensionless)
h	Coordinate in x direction (dimensionless)
b	Free Vibration Frequencies
Φ	Shape Function

1. INTRODUCTION

Longitudinal vibrations of non-uniform bars have attracted considerable scientific and practical attention in the study of composite structures subjected to high velocity impact and the study of foundations. The use of variable cross-section members can help the designer reduce the weight, improve strength and stability of structures. Free vibration analysis and presentation of fundamental frequencies along with mode shapes constitute most of the archival works. The researchers are expected to subsequently obtain the forced vibration response through other methods such as mode superposition.

In the first part of this thesis, the dynamic response of non-uniform rods subjected at the end point to various time-dependent axial forces will be presented as closed-form equations. The need for exact solutions is obvious: they give adequate insight into the physics of the problem as well as establishing the accuracy of the approximate or numerical solutions. In optimization problems using closed-form solutions will greatly reduce the solution time. Laplace transformation will be employed in the analysis. The inversion into the time domain is performed analytically using calculus of residues and numerically by Durbin's inverse transform method. Free vibration behavior is readily obtained since substituting the complex Laplace parameter in the governing equation directly gives natural frequencies. Uniform mass and stiffness are assumed along the rod. The cross section is assumed to vary along the non-dimensional axial coordinate in the forms $A(h) = A_o \sin^2[ah + b]$, $A(h) = A_o (1 + ah)^2$ and $A(h) = A_o e^{-ah}$. Natural frequencies for these cross sections are given in tabular form and good agreement with other benchmark results are observed. The first ten fundamental frequencies are listed. Using only the first ten frequencies in the forced vibration response provided six-digit accuracy. The results are compared to those obtained via Mode Superposition Method (MSM). Among other advantages, the efficiency of analytical results is obvious: for some cases, up to a hundred frequencies were needed in MSM to achieve the same accuracy.

Also, free and forced vibration of heterogeneous rod, which exhibit inhomogeneity both in material density and in elastic modulus, is studied. These inhomogeneities are described in forms of $\sin^2[ah+b]$, $(1+ah)^2$ and e^{-ah} . Closed-form expressions for the fundamental natural frequencies are derived. It is noted that if the nonuniform cross-sectional area and heterogeneous material properties vary according to the same functional form, the governing equation for both cases will be in the same form.

The materials with elastic properties varying in the coordinate direction are termed as functionally graded materials (FGM). FGM can be fabricated by continuously intermixing several materials without generating a boundary. Thus, it was named for this feature of the gradual changes (gradient) of functions.

Beams are incontestably the simplest and the most commonly used of all structural elements. Consequently, many researches have been involved in modeling behavior of beams. In the last part of this study, we analyze the free vibration of an FGM beam. The plane elasticity equations are solved exactly to obtain natural frequencies by using Laplace transform method. Different higher order shear deformation theories and classical beam theories were also used in the literature where, governing equations were found by applying Hamilton's principle. Navier type solution method was used to obtain frequencies. The beam theory results are compared with elasticity solutions.

The aim of the present thesis may be stated as the efforts to obtain analytical benchmark solution for vibration behaviour of rods and beams.

2. PREVIOUS STUDIES

2.1. Non-uniform Rods and Heterogeneous Rods

The vibration of beams and rods has been studied extensively, and continues to receive considerable attention in the literature.

Raj and Sujith (2005) have presented exact solutions for the longitudinal vibration of variable area-rods. The eigen frequencies of rods with certain area variations are obtained.

Li et al. (1999) have presented exact analytical solutions for longitudinal vibration of non-uniform rods with concentrated masses coupled by translational springs. The governing differential equation for longitudinal vibration of a rod with varying cross-section is reduced to Bessel's equation or an ordinary differential equation with constant coefficients by selecting suitable expressions such as power function for the area variation. They have shown in their research that the proposed methods were in good agreement with the full-scale measured data and it is applicable to engineering practices.

Abrate (1994) has shown that for some non-uniform rods and beams the equation of motion can be transformed into the equation of motion for a uniform rod or beam. Also, when the ends were completely fixed, the eigenvalues of the non-uniform continuum were the same as those of uniform rods or beams. They used an efficient procedure to analyze the free vibration of non-uniform beams with general shape and arbitrary boundary conditions. Simple formulas were presented for predicting the fundamental natural frequency of non-uniform beams with various end support conditions.

Qiusheng et al. (1996) have determined the natural frequencies and mode shapes of multi-storey buildings and high-rise structures with variably distributed stiffness and variably distributed mass.

Horgan and Chan (1999) have obtained exact solutions for polynomial and exponential variations of strings, rods and membranes.

Li, Fang and Jeary (1997) have established the differential equations of free longitudinal vibrations of bars with variably distributed mass and stiffness considering damping effects. They proposed an approach to determine the natural frequencies and mode shapes in vertical direction for tall buildings with variably distributed stiffness and variably distributed mass. The numerical examples showed that the computed values of the fundamental longitudinal natural frequency and mode shape by the proposed method were close to the full-scale measured data.

Eisenberg (1991) has presented the solution for exact longitudinal vibration frequencies of a variable cross-section rod. The solution is found using the exact element method, where the dynamic axial stiffness for the rod is found. The natural frequencies for the variable cross-section member are those for which the stiffness is equal to zero. These values can be found up to any desired accuracy. This method is good for any polynomial variation in the cross-sectional area and the mass distribution along the member. The results of several examples are compared with results obtained from finite element analysis.

Kumar and Sujith (1997) have presented exact analytical solutions for the longitudinal vibration of rods with non-uniform cross section. Using appropriate transformations, the equation of motion of axial vibration of a rod with varying cross section was reduced to analytically-solvable standard differential equations whose form depend upon the specific area variation. The governing equation for the problem was the same as that of wave propagation through ducts with non-uniform cross sections. Therefore, solutions they have presented could be used to investigate such problems.

Li (2000) has presented exact analytical solutions for the free longitudinal vibrations of bar with variably distributed stiffness and mass. By using appropriate transformations, the differential equations of free longitudinal vibrations of bars with variably distributed stiffness and mass are reduced to Bessel's equations or ordinary differential equations with constant coefficients.

Candan and Elishakoff (2001) have presented close-form solutions of nonhomogeneous rod under two sets of boundary conditions. Closed-form expressions for the natural frequency can serve as benchmark solutions.

Elishakoff and Candan (2001) used the inverse method and obtained the exact natural frequencies in rods and beams with polynomially varying material and geometrical properties.

Nachum and Altus (2007) found the natural frequencies and mode-shapes of the k-th-order of non-homogeneous rods and beams. The solution is based on the functional perturbation method.

Celebi, Keles and Tütüncü (2009) have obtained the exact displacement solutions of heterogeneous rods under dynamic axial load by using the Laplace transform method. Inverse transformation into the time domain is performed using modified Durbin's method.

2.2. Application of Laplace Transform to Dynamic Problems

Many of the works obtained through a literature survey on vibration analysis have been about the Laplace transform and Fourier transform methods applied to dynamic problems.

Durbin (1974) has presented an accurate method for the numerical inversion of Laplace transform which was a natural continuation to Dubner and Abate's method.

Narayanan (1977) has described the use and importance of dynamic stiffness influence coefficients in flexural forced vibrations of structures composed of beams. The dynamic problem was formulated in terms of dynamic influence coefficients and reduced to a static form. They used the Fourier transform plane and a numerical inversion based on the Cooley-Tukey algorithm of the transformed solution.

Beskos and Narayanan (1981) have presented a general method for determining the dynamic response of complex three dimensional frameworks to dynamic shocks, wind forces or earthquake excitations. The method consisted of formulating and solving the dynamic problem in the Laplace transform domain by the finite element method and of obtaining the response by a numerical inversion of the transformed solution. They provided a basis for comparing the accuracy of other approximate methods such as conventional finite element method. The proposed

method appeared to be better than the conventional finite element method in conjunction with either modal analysis or numerical integration.

Manolis and Beskos (1981) used the Laplace transform in the free vibration analysis. They replaced the complex Laplace parameter with ia in the transient formulation which directly gives the natural frequency a with no inversion required.

Calim (2009) studied the forced vibration of non-uniform composite beams subjected to impulsive loads in the Laplace domain. The solutions obtained are transformed to the time domain using the Durbin's numerical inverse Laplace transform method.

2.3. FGM Beams

Functionally graded materials (FGM) are composite materials intentionally designed so that they possess desirable properties for specific applications. As the application of FGM increases, new methodologies have to be developed to characterize them, and to design and analyze structural components made of these materials. The literature on the response of FGM beam to mechanical and other loadings are mostly inclusive of beam theories.

Sankar (2001) gave an elasticity solution based on the Euler-Bernoulli beam theory for functionally graded beam subjected to static transverse loads by assuming that Young's modulus of the beam vary exponentially through the thickness. Sankar found that beam theory results agree quite well with elasticity solution for beams with large length-to-thickness ratio subjected to more uniform loading characterized by longer wave length of the sinusoidal loading.

Zhong and Yu (2007) presented a general two-dimensional solution for a cantilever FG beam in terms of the Airy stress function.

Sankar and Tzeng (2002) developed a simple Euler-Bernoulli type beam theory to obtain elasticity solution FGM beams subjected to temperature gradients. They found that the thermoelastic properties of the beam can be tailored to reduce thermal stresses for a given temperature distribution.

Aydogdu and Taskin (2007) investigated free vibration of simply supported FGM beams. They used different higher order shear deformation theories and classical beam theory (CBT) and showed that CBT gives higher results and the difference between CBT and higher order theories is increased with increasing mode number.

Calio and Elishakoff (2005) derived closed-form solutions for the natural frequencies for axially graded beam-columns on elastic foundations with guided end conditions.

Ying et al. (2008) obtained the exact solutions for bending and free vibration of FGM beams resting on a Winkler-Pasternak elastic foundation based on the two-dimensional elasticity theory by assuming that the beam is orthotropic at any point and the material properties vary exponentially along the thickness direction.

Sina et al. (2009) used a new beam theory different from the traditional first-order shear deformation beam theory to analyze the free vibration of FGM beams.

Simsek and Kocaturk (2009) have investigated the forced and free vibration characteristics of an FGM Euler-Bernoulli beam under a moving harmonic load.

Kadoli et al. (2008) studied the static behaviour of an FGM beam by using higher-order shear deformation theory and finite element method.

Simsek (2010) has studied the dynamic deflections and the stresses of an FGM simply-supported beam subjected to a moving mass by using Euler-Bernoulli, Timoshenko and the parabolic shear deformation beam theories.

Li (2008) proposed a new unified approach to investigate the static and the free vibration behaviour of Euler-Bernoulli and Timoshenko beams.

Aydogdu (2005) has investigated the vibration of cross-ply composite beams for six different boundary conditions by using the Ritz method. Polynomial trial functions are used in the analyses.

Abbasi et al. (2008) have presented the vibration behavior of an FGM Timoshenko beam under lateral thermal shocks with coupled thermoelastic assumption. The solution obtained by transfinite element method where time is eliminated using the Laplace transform.

Soldatos and Sophocleous (2001) have developed some higher-order shear deformation theories in which there is no need to use shear correction factors.

Simsek (2009) has investigated the static analysis of a functionally graded simply supported beam under a uniformly distributed load by Ritz method. The material properties of the beam vary continuously in the thickness direction according to a power law.

3. MATERIAL AND METHOD

3.1. An Overview of the Differential Equation

The equation of motion for a linear single-degree-of-freedom (SDF) system subjected to external force is the second order differential equation for the displacement:

$$m\ddot{u}(t) + c\dot{u}(t) + ku(t) = P(t)$$

The initial displacement $u(0)$ and initial velocity $\dot{u}(0)$ at time zero must be specified to define the problem completely. Typically, the structure is at rest before the onset of dynamic excitation, so that the initial velocity and the displacement are zero. A brief review of three methods of solution is given in the following sections.

3.1.1. Classical Solution

Complete solution of the linear differential equation of motion consists of the sum of the complementary solution $u_c(t)$ and particular solution $u_p(t)$, that is, $u(t) = u_c(t) + u_p(t)$. Since the differential equation is of second order, two constants of integration are involved. They appear in the complementary solution and are evaluated from knowledge of the initial conditions.

3.1.2. Duhamel's Integral

Another well-known approach to the solution of linear differential equations, such as the equation of the motion of an SDF system, is based on representing the applied force as a sequence of infinitesimally short impulses. The response of the system to an applied force, $p(t)$, at time t is obtained by adding the responses to all

impulses up to that time. We develop this method in the next section, leading to the following result for an undamped SDF system:

$$u(t) = \frac{1}{m w_n} \int_0^t p(t) \sin[w_n (t - t)] dt$$

where $w_n = \sqrt{k/m}$. Implicit in this result are “at rest” initial conditions. This equation, known as Duhamel’s integral-the derivation of which will be discussed in subsequent sections- is a special form of the convolution integral.

Duhamel’s integral provides an alternative method to the classical solution if the applied force $p(t)$ is defined analytically by a simple function that permits analytical evaluation of the integral. For complex excitations that are defined only by numerical values of $p(t)$ at discrete time instants, Duhamel’s integral can be evaluated by numerical methods.

3.1.3. Transform Methods

The Laplace and Fourier transforms provide powerful tools for the solution of linear differential equations, in particular the equation of motion for a linear SDF system. Because the transform methods are similar in concept, here we mention only the Laplace transform method, which leads to the frequency-domain method of dynamic analysis. The frequency-domain method, which is an alternative to the time-domain method symbolized by Duhamel’s integral, is especially useful and powerful for dynamic analysis of structures. The solutions in Laplace transform space can be calculated numerically for real problems. For time-space transition, numerical inverse Laplace transforms are needed. Various inverse Laplace transform methods have been improved for this purpose. Exact inversion into the time domain is performed via the theory of Residues and Durbin’s inverse transform method. The analytical results are tractable and allow for parametric studies.

3.2. Partial Differential Equations of Motion of an Axially-Loaded Bar

The analysis of continuous systems leads to governing partial differential equations in displacement.

3.2.1 Axial Deformations (Undamped)

The axial motion of a rod with varying cross-section $A(x)$, uniform density and Young's modulus is governed by the differential equation

$$m(x) \frac{\partial^2 u(x,t)}{\partial t^2} - \frac{\partial}{\partial x} \left[E A(x) \frac{\partial u(x,t)}{\partial x} \right] = q(x,t) \quad (3.1)$$

Using the dimensionless variables

$$v = \frac{u}{L}, \quad h = \frac{x}{L}, \quad t = \frac{ct}{L} \quad (3.2)$$

Renders Eq.(3.1) in the form

$$c^2 m(h) \frac{\partial^2 v(h,t)}{\partial t^2} - \frac{\partial}{\partial h} (E A(h) \frac{\partial v(h,t)}{\partial h}) = L q(h,t) \quad (3.3)$$

where $c^2 = E / r$, c is the velocity of propagation of the displacement.

Usually, the external axial loading consists only of end loads, in which case the right hand side of this equation would be zero. However, when solving Equation (3.3) the boundary conditions imposed at $h = 0$ and $h = 1$ must be satisfied. It should be noted that in this formulation damping is neglected. The free-vibration equation of motion – setting $q(h,t) = 0$ in Equation (3.3) - becomes

$$c^2 m(h) \frac{\partial^2 v(h,t)}{\partial t^2} - \frac{\partial}{\partial h} (E A(h) \frac{\partial v(h,t)}{\partial h}) = 0 \quad (3.4)$$

3.2.2. Orthogonality of Axial Vibrations Modes

The axial vibration mode shapes have orthogonality properties. The orthogonality of the axial mode shapes with respect to the mass distribution can be derived using Betti's law. Consider the beam shown in Figure (3.1). Two different vibration modes, m and n , are shown for the beam. In each mode, the displaced shape and the inertial forces producing the displacements are indicated.

Betti's law applied to these two deflection patterns means that the work done by the inertial forces of mode n acting on the deflection mode m is equal to the work of the forces of mode m acting on the displacement of mode n ; that is,

$$\int_0^1 v_m f_{I_n} dh = \int_0^1 v_n f_{I_m} dh \quad (3.5)$$

Expressing these in terms of the modal shape functions shown in Figure (3.1) gives

$$\begin{aligned} G_m(t)G_n(t)a_n^2 \int_0^1 V_m(h)m(h)V_n(h)dh \\ = G_m(t)G_n(t)w_m^2 \int_0^1 V_n(h)m(h)V_m(h)dh \end{aligned} \quad (3.6)$$

which may be written as

$$(a_n^2 - a_m^2) \int_0^1 V_m(h)V_n(h)m(h)dh = 0 \quad (3.7)$$

Since the frequencies of these two modes are different, their mode shape must satisfy the orthogonality condition

$$\int_0^1 V_m(h)V_n(h)m(h)dh = 0 \quad , \quad a_m \neq a_n \quad (3.8)$$

If the two modes have the same frequency, the orthogonality condition does not apply, but this condition does not occur often in ordinary structural problems.

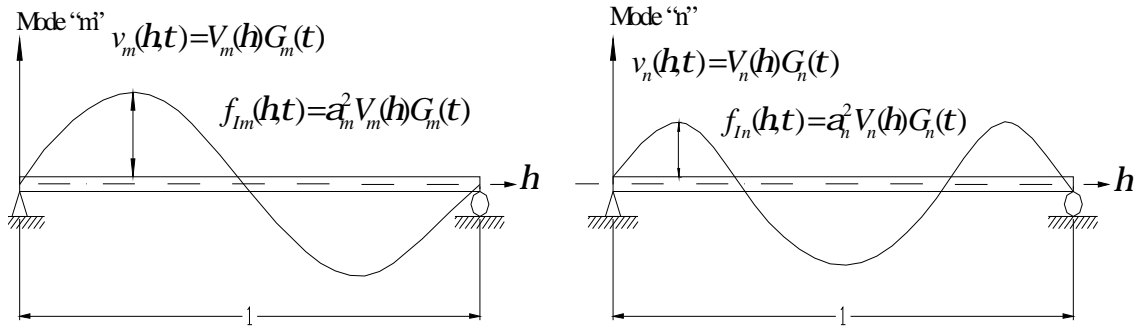


Figure 3.1. Two modes of vibration for the same rod.

The orthogonality relationship with respect to the axial stiffness property can be derived from the homogenous form of the equation of motion [Equation (3.4)] in which the harmonic time variation of free vibration has been substituted. In other words, when the n th-mode displacements are expressed as (Clough and Penzien, 1993)

$$v_n(h, t) = V_n(h) r_n \sin(a_n t + j_n) \quad (3.9)$$

and this displacement expression is substituted into the homogeneous form of Equation (3.4), one obtains

$$c^2 a_n^2 m(h) V_n(h) = -\frac{d}{dh} \left[E A(h) \frac{dV_n}{dh} \right] \quad (3.10)$$

Substituting this relation into both sides of Equation (3.6) and canceling the common term $G_m(t)G_n(t)$ gives

$$-\frac{(a_n^2 - a_m^2)}{a_n^2} \int_0^1 V_m(h) \frac{d}{dh} \left[E A(h) \frac{dV_n}{dh} \right] = 0 \quad (3.11)$$

Since the frequencies are different, modes m and n must satisfy the orthogonality condition

$$\int_0^1 V_m(h) \frac{d}{dh} \left[E A(h) \frac{dV_n(h)}{dh} \right] dh = 0 \quad (3.12)$$

3.2.3. Analysis of Dynamic response (Normal Coordinates)

The essential operation of the mode-superposition analysis is the transformation from the geometric displacement coordinates to the modal-amplitude or normal coordinates. For a one-dimensional system, this transformation is expressed as

$$v(h,t) = \sum_{i=1}^{\infty} V_i(h) G_i(t) \quad (3.13)$$

which is simply a statement that any physically permissible displacement pattern can be made up by superposing appropriate amplitudes of the vibration mode shapes for the structure.

3.2.4. Uncoupled Axial Equations of Motion

The mode-shape (normal) coordinate transformation serves to uncouple the equations of motion of any dynamic system and therefore is applicable to the axial

motion of a one-dimensional member. Introducing Equation (3.13) into the equation of axial motion, Equation (3.3), leads to

$$\sum_{i=1}^{\infty} c^2 m(h) V_i(h) \ddot{G}_i(t) - \sum_{i=1}^{\infty} \frac{d}{dh} \left[E A(h) \frac{dG_i(h)}{dh} \right] G_i(t) = L q(h, t) \quad (3.14)$$

Multiplying each term by $V_n(h)$ and applying the orthogonality relationships [Equation (3.8) and Equation (3.12)] leads to

$$\begin{aligned} \ddot{G}_n(t) \int_0^1 c^2 m(h) V_n(h)^2 dh - G_n(t) \int_0^1 V_n(h) \frac{d}{dh} \left[E A(h) \frac{dV_n(h)}{dh} \right] dh \\ = \int_0^1 L V_n(h) q(h, t) dh \end{aligned} \quad (3.15)$$

multiplying Equation (3.10) by $V_n(h)$ and integrating yields

$$\int_0^1 c^2 a_n^2 m(h) V_n^2(h) dh = - \int_0^1 V_n(h) \frac{d}{dh} \left[E A(h) \frac{dV_n(h)}{dh} \right] dh \quad (3.16)$$

Substituting Equation (3.16) into Equation (3.15), we get uncoupled axial equation of motion

$$M_n \ddot{G}_n(t) + a_n^2 M_n G_n(t) = P_n(t) \quad (3.17)$$

where

$$M_n = \int_0^1 c^2 m(h) V_n^2(h) dh \quad (3.18)$$

is generalized mass of the n'th mode and

$$P_n = L \int_0^1 V_n(h) q(h,t) dh \quad (3.19)$$

is the generalized loading associated with mode shape $V_n(h)$.

From this discussion it is apparent that after the vibration mode shapes have been determined, the reduction to the normal-coordinate form involves exactly the same type of operations for all structures.

3.2.5. Formulation of Duhamel Integral

In theory of vibrations, Duhamel's integral is a way of calculating the response of linear systems and structures to arbitrary time-varying external excitations.

The procedure described in (Clough and Penzien, 1993) for approximating the response of an undamped SDOF structure to short duration impulsive loads can be used as the basis for developing a formula for evaluating response to a general dynamic loading. This formula is:

$$G(t) = \frac{1}{m\alpha} \left(\int_0^{t_1} P(t) dt \right) \sin[\alpha \bar{t}] , \bar{t} = t - t_1 \quad (3.20)$$

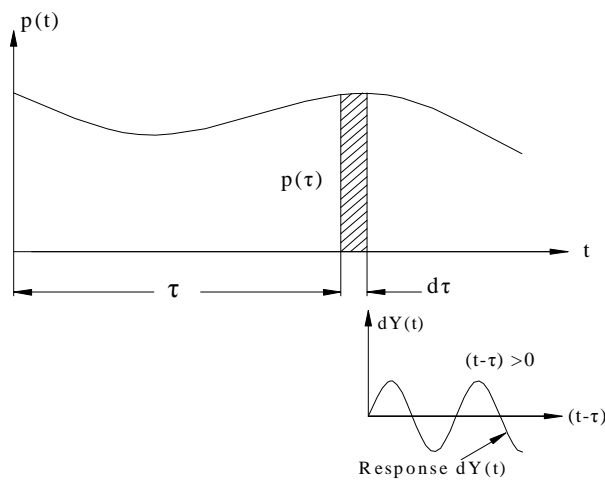


Figure 3.2 Derivation of the Duhamel integral (undamped).

Consider an arbitrary general loading $P(t)$ as illustrated in Figure 3.2 and, for the moment, concentrate on the intensity of loading $P(t^*)$ acting at time $t = t^*$. This loading acting during the interval of time dt^* represents a very short duration impulse $P(t^*)dt^*$ on the structure, so that Equation (3.20) can be used to evaluate the resulting response. It should be noted carefully that although this equation is approximate for impulses of finite duration, it becomes exact as the duration of loading approaches zero. Thus, for the differential time interval dt^* , the response produced by the impulse $P(t^*)d(t^*)$ is exactly equal to

$$dG(t) = \frac{P(t^*)dt^*}{ma} \sin[a(t - t^*)] \quad , \quad t \geq t^* \quad (3.21)$$

In this expression, the term $dG(t)$ represents the time-history response to the differential impulse over the time $t \geq t^*$; it is not change of G during a time interval dt .

The entire loading history can be considered to consist of a succession of such short impulses, each producing its own differential response of the form of Equation (3.21). For this linearly elastic system, the total response can then be obtained by summing all the differential responses developed during the loading history, that is, by integrating Equation (3.21) as follows:

$$G(t) = \frac{1}{ma} \int_0^t P(t^*) \sin[a(t - t^*)] dt^* \quad t \geq 0 \quad (3.22)$$

This relation, generally known as the “Duhamel integral equation”, can be used to evaluate the response of an undamped SDOF system to any form of dynamic loading $P(t)$; however, for arbitrary loadings the evaluation must be performed numerically using procedures described subsequently. Finally we can say that, Equation (3.22) is a Duhamel solution of the Equation (3.17).

3.3. Free Vibration Analysis of Non-uniform and Heterogeneous Rods

By applying the so-called product method, or method of separating variables, we shall obtain ordinary differential equation which satisfies the motion of a rod.

3.3.1. Free Vibration Analysis of Non-uniform Rods

The longitudinal motion of a rod with varying cross-section $A(h)$, uniform density and Young's modulus is governed by the differential equation

$$\frac{\partial^2 v(h, t)}{\partial h^2} + \frac{1}{A(h)} \frac{\partial A(h)}{\partial h} \frac{\partial v(h, t)}{\partial h} = \frac{\partial^2 v(h, t)}{\partial t^2} \quad 0 < h < 1, t > 0 \quad (3.23)$$

Assuming a solution of the form $v(h, t) = V(h)G(t)$, Equation (3.23) reduces to the second order differential equation for the complex amplitude $V(h)$:

$$\frac{d^2 V(h)}{dh^2} + \frac{1}{A(h)} \frac{dA(h)}{dh} \frac{dV(h)}{dh} + a^2 V(h) = 0 \quad (3.24)$$

The above equation will be solved for rods with cross-sections varying as $A(h) = A_0 \sin^2[ah + b]$, $A(h) = A_0(1 + ah)^2$ and $A(h) = A_0 e^{-ah}$.

3.3.1.1. Solution for Area Variation of the Form $A(h) = A_0(1 + ah)^2$

In this section the exact solution for the longitudinal vibration of a rod with an area variation of the form

$$A(h) = A_0(1 + ah)^2 \quad (3.25)$$

is derived. To simplify equation (3.24) a new variable z is introduced (Abrate, 1995):

$$V(h) = \frac{z}{(1+ah)} \quad (3.26)$$

Transforming equation (3.24) from the $U - h$ space to $V - h$ space yields

$$z'' + a^2 z = 0 \quad (3.27)$$

whose solution is given by

$$z = c_1 \cos[kh] + c_2 \sin[kh] \quad (3.28)$$

where

$$k^2 = a^2 \quad (3.29)$$

Therefore,

$$V(h) = \frac{1}{(1+ah)} (c_1 \cos[kh] + c_2 \sin[kh]) \quad (3.30)$$

For fixed-free rods, the boundary conditions are $V(0) = 0$ and $(\partial V / \partial h)[1, t] = 0$ which give the following equation

$$k = \frac{a}{(1+a)} \tan[k] \quad (3.31)$$

The equation (3.31) can be proved by the different values of k . So equation (3.29) can be shown to be:

$$a_n = k_n \quad (3.32)$$

Table 3.1 shows the natural frequencies for tapered rods with $a=0,1,2$ and $L=1$.

Table 3.1. Natural frequencies of fixed-free rods with $A(h) = A_0(1 + ah)^2$

Mode	a=0	a=1	a=2
1	1.57079	1.165561	0.967402
2	4.71239	4.604216	4.567452
3	7.85398	7.789883	7.768373
4	10.9956	10.949943	10.934681
5	14.1372	14.101725	14.089886
6	17.2788	17.249781	17.240109
7	20.4204	20.395842	20.387664
8	23.5619	23.540708	23.533624
9	26.7035	26.684801	26.678553
10	29.8451	29.828369	29.822779

3.3.1.2. Solution for Area Variation of the Form $A = A_0 \sin^2[ah + b]$

In this section the exact solution for the longitudinal vibration of a rod with an area variation of the form

$$A(h) = A_0 \sin^2[ah + b] \quad (3.33)$$

is derived. To simplify equation (3.24) a new variable z is introduced (Kumar and Sujith, 1997):

$$V(h) = \frac{z}{\sin[ah + b]} \quad (3.34)$$

Transforming equation (3.24) from the $V - h$ space to $z - h$ space yields

$$z'' + (a^2 + a^2)z = 0 \quad (3.35)$$

whose solution is given by

$$z = c_1 \sin[kh] + c_2 \cos[kh] \quad (3.36)$$

where

$$k^2 = a^2 + a^2 \quad (3.37)$$

Therefore,

$$V(h) = \frac{1}{\sin[ah + b]} (c_1 \sin[kh] + c_2 \cos[kh]) \quad (3.38)$$

For fixed-free rods, the boundary conditions are $V(0) = 0$ and $(\partial V / \partial h)[l, t] = 0$ which give the following equation

$$k = \tan[k] \frac{a}{\tan[a + b]} \quad (3.39)$$

The equation (3.39) can be proved by the different values of k . So equation (3.37) can be shown to be:

$$a_n^2 = k_n^2 - a^2 \quad (3.40)$$

Table 3.2. shows the natural frequencies for tapered rods with $a=0,1,2$ and $L=1$.

Table 3.2. Natural frequencies of fixed-free rods with $A = A_0 \sin^2[ah + b]$

Mode	a=0	a=1	a=2
1	1.57079	1.51764	2.14856
2	4.71239	4.70214	5.53576
3	7.85398	7.84831	8.63281
4	10.9956	10.9916	11.6946
5	14.1372	14.1341	14.7579
6	17.2788	17.2763	17.8306
7	20.4204	20.4183	20.9137
8	23.5619	23.5601	24.0062
9	26.7035	26.7019	27.1064
10	29.8451	29.8437	30.2129

3.3.1.3. Solution for Area Variation of the Form $A(h) = A_0 e^{-ah}$

In this section the exact solution for the longitudinal vibration of a rod with an area variation of the form

$$A(h) = A_0 e^{-ah} \quad (3.41)$$

is derived. The equation (3.24) becomes

$$\frac{d^2V}{dh^2} - a \frac{dV}{dh} + a^2V = 0 \quad (3.42)$$

it is obvious that if

$$a^2 - 4a^2 \geq 0 \quad (3.43)$$

then, only zero solution exists. When

$$a^2 - 4a^2 \leq 0 \quad (3.44)$$

the general solution of $V(h)$ is given by (Li, 2000)

$$V(h) = e^{\frac{ah}{2}} (c_1 \cos[kh] + c_2 \sin[kh]) \quad (3.45)$$

where

$$k^2 = a^2 - \frac{a^2}{4} \quad (3.46)$$

For fixed-free rods, the boundary conditions are $V(0) = 0$ and $(\partial V / \partial h)[l, t] = 0$ which give the following equation

$$\cot[k] = -\frac{a}{2k} \quad (3.47)$$

The equation (3.47) can be supplied by the different values of k . Equation (3.46) can be shown to be.

$$a_n^2 = k_n^2 + \frac{a^2}{4} \quad (3.48)$$

Table 3.3. shows the natural frequencies for tapered rods with $a=0, 1, 2$ and $L=1$

Table 3.3. Natural frequencies of fixed-free rods with $A(h) = A_0 e^{-ah}$

Mode	a=0	a=1	a=2
1	1.57079	1.90344	2.26183
2	4.71239	4.84173	5.01391
3	7.85398	7.93283	8.04109
4	10.9956	11.0521	11.1306
5	14.1372	14.1812	14.2426
6	17.2788	17.3149	17.3652
7	20.4204	20.4509	20.4936
8	23.5619	23.5884	23.6255
9	26.7035	26.7269	26.7596
10	29.8451	29.8661	29.8953

3.3.2. Free Vibration Analysis of Heterogeneous Rods

The longitudinal motion of a rod with uniform cross-section, varying density $r(h)$ and varying Young's modulus $E(h)$ is governed by the differential equation

$$\frac{\partial^2 v(h,t)}{\partial h^2} + \frac{1}{E(h)} \frac{\partial E(h)}{\partial h} \frac{\partial v(h,t)}{\partial h} = c^2 \frac{r(h)}{E(h)} \frac{\partial^2 v(h,t)}{\partial t^2} \quad 0 < h < 1, t > 0 \quad (3.49)$$

Assuming a solution of the form $v(h,t) = V(h)G(t)$, Equation (3.49) reduces to the second order differential equation for the complex amplitude $V(h)$:

$$\frac{d^2 V(h)}{dh^2} + \frac{1}{E(h)} \frac{dE(h)}{dh} \frac{dV(h)}{dh} + a^2 c^2 \frac{r(h)}{E(h)} V(h) = 0 \quad (3.50)$$

The above equation will be solved for rods with density and Young' modulus varying as $\sin^2[ah+b]$, $(1+ah)^2$ and e^{-ah} . Since the density and elasticity

variations of the heterogeneous rods are of the same form of the area variations of non-uniform rods they have the same natural frequencies.

3.3.2.1 Solution for $E(h) = E_0(1 + ah)^2$ and $r(h) = r_0(1 + ah)^2$

In this section the exact solution for the longitudinal vibration of a rod with a density and elastic modulus variation of the forms

$$\begin{aligned} E(h) &= E_0(1 + ah)^2 \\ r(h) &= r_0(1 + ah)^2 \end{aligned} \quad (3.51)$$

is derived. To simplify equation (3.50) a new variable z is introduced:

$$V(h) = \frac{z}{(1 + ah)} \quad (3.52)$$

Transforming equation (3.50) from the $U - h$ space to $V - h$ space yields

$$z'' + a^2 z = 0 \quad (3.53)$$

whose solution is given by

$$z = c_1 \cos[kh] + c_2 \sin[kh] \quad (3.54)$$

where

$$k^2 = a^2 \quad (3.55)$$

Following the same steps as in the section (3.3.1.1), the same mode shapes and natural frequencies at Table 3.1 can be found for $E(h) = E_0(1+ah)^2$ and $r(h) = r_0(1+ah)^2$.

3.3.2.2. Solution for $E(h) = E_0 \sin^2[ah+b]$ and $r(h) = r_0 \sin^2[ah+b]$

In this section the exact solution for the longitudinal vibration of a rod with a density and elastic modulus variation of the forms

$$\begin{aligned} E(h) &= E_0 \sin^2[ah+b] \\ r(h) &= r_0 \sin^2[ah+b] \end{aligned} \quad (3.56)$$

is derived. To simplify equation (3.50) a new variable z is introduced:

$$V(h) = \frac{z}{\sin[ah+b]} \quad (3.57)$$

Transforming equation (3.50) from the $V-h$ space to $z-h$ space yields

$$z'' + (a^2 + a^2)z = 0 \quad (3.58)$$

whose solution is given by

$$z = c_1 \sin[kh] + c_2 \cos[kh] \quad (3.59)$$

where

$$k^2 = a^2 + a^2 \quad (3.60)$$

Following the same steps as in the section (3.3.1.2), the same mode shapes and natural frequencies at Table 3.2 can be found for $E(h) = E_0 \sin^2[ah + b]$ and $r(h) = r_0 \sin^2[ah + b]$.

3.3.2.3. Solution for $E(h) = E_0 e^{-ah}$ and $r(h) = r_0 e^{-ah}$

In this section the exact solution for the longitudinal vibration of a rod with a density and elastic modulus variation of the forms

$$\begin{aligned} E(h) &= E_0 e^{-ah} \\ r(h) &= r_0 e^{-ah} \end{aligned} \quad (3.61)$$

is derived. The equation (3.50) becomes

$$\frac{d^2V}{dh^2} - a \frac{dV}{dh} + a^2V = 0 \quad (3.62)$$

it is obvious that if

$$a^2 - 4a^2 \geq 0 \quad (3.63)$$

then, only zero solution exists. When

$$a^2 - 4a^2 < 0 \quad (3.64)$$

the general solution of $V(h)$ is given by

$$V(h) = e^{\frac{ah}{2}} (c_1 \cos[kh] + c_2 \sin[kh]) \quad (3.65)$$

where

$$k^2 = a^2 - a^2 / 4 \quad (3.66)$$

Following the same steps as in the section (3.3.1.3), the same mode shapes and natural frequencies at Table 3.3 can be found for $E(h) = E_0 e^{-ah}$ and $r(h) = r_0 e^{-ah}$.

3.4. Forced Vibration Analysis of Non-uniform Rods and Heterogeneous Rods

The main methods employed in the analysis are Mode-superposition method and Laplace transformation method. Inverse transformation into the time domain is performed using calculus of residues and Durbin's numerical inverse method.

3.4.1. Laplace Transformation

Laplace transform is a powerful method for solving differential equations in engineering and science. It can be used to find the response of a system under any type of excitation including the harmonic and periodic types. This method can be used for the efficient solution of linear differential equations, particularly those with constant coefficients. It permits the conversion of differential equations into algebraic ones which are easier to manipulate. The major advantages of the method are that it can treat discontinuous functions without any particular difficulty and that it automatically takes into account the initial conditions.

The Laplace transformation method is widely used in engineering mathematics, where it has numerous applications. It is particularly useful in problems where the (mechanical or electrical) driving force has discontinuities, for instance, acts for a short time only, or is periodic but is not merely a sine or cosine function. Another advantage is that it solves problems directly. Indeed, initial value problems

are solved without first determining a general solution. Similarly, nonhomogeneous equations are solved without first solving the corresponding homogeneous equation.

The Laplace transform of a function $f(t)$, denoted symbolically as $F(p) = L f(t)$, is defined as

$$F(p) = L f(t) = \int_0^{\infty} e^{-pt} f(t) dt \quad (3.67)$$

where p is, in general, a complex quantity and is called the subsidiary variable. The function e^{-pt} is called the kernel of the transformation. Since the integration is with respect to t , the transformation gives a function of p . Here and in the following sections, a capital F will represent the function in the Laplace domain, whose inversion in real time, $f(t)$, is required. It is noted that t can be any independent variable. However, in this thesis, and because of its association with “time”, in many engineering applications we will call it “time”. The inversion integral is defined as follows (Abramowitz and Stegun, 1982).

$$f(t) = \frac{1}{2\pi j} \int_{\partial-j\infty}^{\partial+j\infty} e^{st} F(p) dp \quad (3.68)$$

where ∂ is chosen so that all the singular points of $F(p)$ lie to the left of the line $\text{Re}\{p\} = \partial$ in the complex p -plane.

In order to solve a vibration problem using the Laplace transform method, the following steps are necessary:

1. Write the equation of motion of the system.
2. Transform each term of the equation, using known initial conditions.
3. Solve for the transformed response of the system.

4. Obtain the desired solution (response) by using inverse Laplace transformation.

The Laplace transform method of solving the differential equation provides a complete solution, yielding both transient and forced vibration.

3.4.1.1. Solution of Boundary-Value Problems by Laplace Transforms

Various problems in science and engineering, when formulated mathematically, lead to partial differential equations involving one or more unknown functions together with certain prescribed conditions on the functions which arise from the physical situation.

These conditions are called boundary conditions. The problem of finding solutions to the equations which satisfy the boundary conditions is called a boundary-value problem.

By use of the Laplace transformation (with respect to t or x) in a one-dimensional boundary-value problem, the partial differential equation can be transformed into an ordinary differential equation. The required solution can then be obtained by solving this equation and inverting by use of the inversion formula or any other methods.

3.4.1.2. Displacement Solution of Axially Loaded Non-Uniform Rods Using Laplace Transform Technique

In this section, the same problem in section 3.3.1 will be investigated again. A fixed-free rod with the axial force applied at the free end $h = 1.0$ will be considered. In order to obtain equation of the motion of the system, equation (3.23) can be used again. The above equation is solved for a rods with a same cross-section area variations in section 3.3.1.

3.4.1.2.(1). Displacement Solution for Area Variation of the Form

$$A(h) = A_o(1 + ah)^2$$

If $v(h, t)$ is longitudinal displacement of any point “ h ” of the beam at dimensionless time “ t ”, the boundary value problem is

$$\frac{\partial^2 v(h, t)}{\partial h^2} + \frac{1}{A(h)} \frac{\partial A(h)}{\partial h} \frac{\partial v(h, t)}{\partial h} = \frac{\partial^2 v(h, t)}{\partial t^2}, \quad 0 < h < 1, t > 0 \quad (3.69-a)$$

$$v(h, 0) = 0, \quad \frac{\partial v(h, 0)}{\partial t} = 0, \quad v(0, t) = 0, \quad \left. \frac{\partial v}{\partial h} \right|_{h=1} = \frac{P(t)}{A(1)E} \quad (3.69-b)$$

where E is Young’s modulus. Substituting $A(h) = A_o(1 + ah)^2$ and taking the Laplace transform of equations (3.69-a) and (3.69-b) yields

$$y''(h, p) + \frac{2a}{(1 + ah)} y'(h, p) - p^2 y(h, p) = 0 \quad (3.70-a)$$

$$y(0, p) = 0, \quad \frac{\partial y(1, p)}{\partial h} = \frac{1}{EA(1)} L\{P(t)\} \quad (3.70-b)$$

where $y(h, p) = L\{v(h, t)\}$, p being the complex Laplace parameter. Introducing a new variable z defined as (Abrate, 1995).

$$y(h, p) = \frac{z}{(1 + ah)} \quad (3.71)$$

into equation (3.70-a) results in

$$z'' - p^2 z = 0 \quad (3.72)$$

At this stage free vibration analysis can easily be performed and determination of fundamental frequencies would be in order. If the Laplace parameter p in Eq. (3.72) is replaced by ia , we will get again Eq. (3.27) at “3.3.1.1” and the end we will find the same frequencies at Table-3.1. Note that a corresponds to the natural frequency whose determination will not require inverse transformation (Manolis and Beskos, 1981). The general solution of equation (3.72) is

$$z = c_1 \sin[kh] + c_2 \cos[kh] \quad (3.73)$$

where

$$k^2 = -p^2 \quad (3.74)$$

Therefore,

$$y = \frac{1}{(1+ah)} (c_1 \sin[kh] + c_2 \cos[kh]) \quad (3.75)$$

From the first condition in (3.70-b), $c_2 = 0$ and so

$$y(h, p) = c_1 \frac{\sin[kh]}{(1+ah)} \quad (3.76)$$

From the second condition in (3.70-b), we have

$$\frac{\partial y(1, p)}{\partial h} = c_1 \left[\frac{k(1+a) \cos[k] - a \sin[k]}{(1+a)^2} \right] = \frac{1}{E A_o (1+a)} L\{P(t)\} \quad (3.77)$$

From equation (3.77), we can find “ c_1 ” for the different loading types and then put it into the equation (3.76) to find the displacement in Laplace space. Later, we use

Direct Laplace Transform methods and Theory of Residues for finding displacement of rod under dynamic loading in real time.

Table 3.4. Axial displacement expressions of the end point in laplace space for $A(h) = A_o(1 + ah)^2$

	$P(t)$	$L\{P(t)\}$	$y(1, p)$
STEP FORCE	P_o	$P_o \frac{1}{p}$	$\frac{P_o}{E A_o} \frac{1}{p} \frac{1}{(k(1+a)\cos[k] - a\sin[k])} \frac{\sin[k]}{(1+a)}$
COS. TYPE FORCE	$P_o(1 - \cos[gt])$	$P_o \frac{g^2}{p(p^2 + g^2)}$	$\frac{P_o}{E A_o} \frac{g^2}{p(p^2 + g^2)} \frac{1}{(k(1+a)\cos[k] - a\sin[k])} \frac{\sin[k]}{(1+a)}$
EXP. TYPE FORCE	$P_o(1 - e^{-gt})$	$P_o \frac{g}{p(p+g)}$	$\frac{P_o}{E A_o} \frac{g}{p(p+g)} \frac{1}{(k(1+a)\cos[k] - a\sin[k])} \frac{\sin[k]}{(1+a)}$

3.4.1.2.(2). Displacement Solution for Area Variation of the Form

$$A = A_o \sin^2[ah + b]:$$

If $v(h, t)$ is longitudinal displacement of any point “ h ” of the beam at dimensionless time “ t ”, the boundary value problem is

$$\frac{\partial^2 v(h, t)}{\partial h^2} + \frac{1}{A(h)} \frac{\partial A(h)}{\partial h} \frac{\partial v(h, t)}{\partial h} = \frac{\partial^2 v(h, t)}{\partial t^2}, \quad 0 < h < 1, t > 0 \quad (3.78-a)$$

$$v(h, 0) = 0, \quad \frac{\partial v(h, 0)}{\partial t} = 0, \quad v(0, t) = 0, \quad \left. \frac{\partial v}{\partial h} \right|_{h=1} = \frac{P(t)}{A(1)E} \quad (3.78-b)$$

where E is Young’s modulus. Substituting $A(h) = A_o \sin^2[ah + b]$ and taking the Laplace transform of equations (3.78-a) and (3.78-b) yields

$$y''(h, p) + 2a \cot[ah + b] y'(h, p) - p^2 y(h, p) = 0 \quad (3.79-a)$$

$$y(0, p) = 0, \quad \frac{\partial y(1, p)}{\partial h} = \frac{1}{EA(1)} L\{P(t)\} \quad (3.79-b)$$

where $y(h, p) = L\{v(h, t)\}$, p being the complex Laplace parameter. Introducing a new variable z defined as (Kumar and Sujith, 1997)

$$y(h, p) = \frac{z}{\sin[ah + b]} \quad (3.80)$$

into equation (3.79-a) results in

$$z'' + (a^2 - p^2)z = 0 \quad (3.81)$$

At this stage free vibration analysis can easily be performed and determination of fundamental frequencies would be in order. If the Laplace parameter p in Eq. (3.81) is replaced by ia , we will get again Eq. (3.35) at “3.3.1.2” and the end we will find the same frequencies at Table-3.2. The general solution of equation (3.81) is

$$z = c_1 \sin[kh] + c_2 \cos[kh] \quad (3.82)$$

where

$$k^2 = a^2 - p^2 \quad (3.83)$$

Therefore,

$$y = \frac{1}{\sin[ah + b]} (c_1 \sin[kh] + c_2 \cos[kh]) \quad (3.84)$$

From the first condition in (3.79-b), $c_2 = 0$ and so

$$y(h, p) = c_1 \frac{\sin[kh]}{\sin[ah + b]} \quad (3.85)$$

From the second condition in (3.79-b), we have

$$\begin{aligned} \frac{\partial y(1, p)}{\partial h} &= c_1 [\csc[a + b](k \cos[k] - a \cot[a + b] \sin[k])] \\ &= \frac{1}{E A_o \sin^2[a + b]} L\{P(t)\} \end{aligned} \quad (3.86)$$

From equation (3.86), we can find “ c_1 ” for the different loading types and then put it into the equation (3.85) to find the displacement in Laplace space. Later, we use Direct Laplace Transform methods and Theory of Residues for finding displacement of rod under dynamic loading in real time.

Table 3.5. Axial displacement expressions of the end point in laplace space for a

$$A = A_o \sin^2[ah + b]$$

	$P(t)$	$L\{P(t)\}$	$y(1, p)$
STEP FORCE	P_o	$P_o \frac{1}{p}$	$\frac{P_o}{E A_o} \frac{1}{p} \frac{1}{k \cos[k] \sin[a + b] - a \cos[a + b] \sin[k]} \frac{\sin[k]}{\sin[a + b]}$
COS. TYPE FORCE	$P_o (1 - \cos[gt])$	$P_o \frac{g^2}{p(p^2 + g^2)}$	$\frac{P_o}{E A_o} \frac{g^2}{p(p^2 + g^2)} \frac{1}{k \cos[k] \sin[a + b] - a \cos[a + b] \sin[k]} \frac{\sin[k]}{\sin[a + b]}$
EXP. TYPE FORCE	$P_o (1 - e^{-gt})$	$P_o \frac{g}{p(p + g)}$	$\frac{P_o}{E A_o} \frac{g}{p(p + g)} \frac{1}{k \cos[k] \sin[a + b] - a \cos[a + b] \sin[k]} \frac{\sin[k]}{\sin[a + b]}$

3.4.1.2.(3). Displacement Solution for Area Variation of the Form $A(h) = A_0 e^{-ah}$

If $v(h,t)$ is longitudinal displacement of any point “ h ” of the beam at dimensionless time “ t ”, the boundary value problem is

$$\frac{\partial^2 v(h,t)}{\partial h^2} + \frac{1}{A(h)} \frac{\partial A(h)}{\partial h} \frac{\partial v(h,t)}{\partial h} = \frac{\partial^2 v(h,t)}{\partial t^2}, \quad 0 < h < 1, t > 0 \quad (3.87-a)$$

$$v(h,0) = 0, \quad \frac{\partial v(h,0)}{\partial t} = 0, \quad v(0,t) = 0, \quad \left. \frac{\partial v}{\partial h} \right|_{h=1} = \frac{P(t)}{A(1)E} \quad (3.87-b)$$

where E is Young’s modulus. Substituting $A(h) = A_0 e^{-ah}$ and taking the Laplace transform of equations (3.87-a) and (3.87-b) yields

$$y''(h,p) - a y'(h,p) - p^2 y(h,p) = 0 \quad (3.88-a)$$

$$y(0,p) = 0, \quad \left. \frac{\partial y(1,p)}{\partial h} \right|_{h=1} = \frac{1}{EA(1)} L\{P(t)\} \quad (3.88-b)$$

At this stage free vibration analysis can easily be performed and determination of fundamental frequencies would be in order. If the Laplace parameter p in Eq. (3.88-a) is replaced by ia , we will get again Eq. (3.42) at “3.3.1.3” and the end we will find the same frequencies at Table-3.3. For equation (3.88-a), it is obvious that if

$$a^2 + 4p^2 \leq 0 \quad (3.89)$$

then, only zero solution exists. When

$$a^2 + 4p^2 \neq 0 \quad (3.90)$$

the general solution of $y(h, p)$ is given by

$$y(h, p) = c_1 e^{I_1 h} + c_2 e^{I_2 h} \quad (3.91)$$

where $I_{1,2} = \frac{a \pm \sqrt{\Delta}}{2}$ and $\Delta = a^2 + 4p^2$.

From the first condition in (3.88-b), $c_2 = -c_1$ and so

$$y(h, p) = c_1 e^{\frac{a}{2}h} \left[e^{\frac{\sqrt{\Delta}}{2}h} - e^{-\frac{\sqrt{\Delta}}{2}h} \right] \quad (3.92)$$

Result of the use of hyperbolic equalities, the equation (3.92) becomes

$$y(h, p) = c_3 e^{\frac{a}{2}h} \sinh\left[\frac{\sqrt{\Delta}}{2}h\right] \quad (3.93)$$

From the second condition in (3.88-b), we have

$$\frac{\partial y(1, p)}{\partial x} = c_3 \frac{e^{a/2}}{2} \left[\sqrt{\Delta} \cosh\left[\frac{\sqrt{\Delta}}{2}\right] + a \sinh\left[\frac{\sqrt{\Delta}}{2}\right] \right] = \frac{1}{E A_o e^{-a}} L\{P(t)\} \quad (3.94)$$

From equation (3.94), we can find “ c_3 ” for the different loading types and then put it into the equation (3.93) to find the displacement in Laplace space. Later, we use Direct Laplace Transform methods and Theory of Residues for finding displacement of rod under dynamic loading in real time.

Table 3.6. Axial displacement expressions of the end point in laplace space for

$$A(h) = A_0 e^{-ah}$$

	$P(t)$	$L\{P(t)\}$	$y(1, p)$
STEP FORCE	P_0	$P_0 \frac{1}{p}$	$\frac{2P_0 e^a}{EA_0} \frac{1}{p} \frac{\sinh[\frac{\sqrt{a^2+4p^2}}{2}]}{\sqrt{a^2+4p^2} \cosh[\frac{\sqrt{a^2+4p^2}}{2}] + a \sinh[\frac{\sqrt{a^2+4p^2}}{2}]}$
COS. TYPE FORCE	$P_0 (1 - \cos[gt])$	$P_0 \frac{g^2}{p(p^2+g^2)}$	$\frac{2P_0 e^a}{EA_0} \frac{g^2}{p(p^2+g^2)} \frac{\sinh[\frac{\sqrt{a^2+4p^2}}{2}]}{\sqrt{a^2+4p^2} \cosh[\frac{\sqrt{a^2+4p^2}}{2}] + a \sinh[\frac{\sqrt{a^2+4p^2}}{2}]}$
EXP. TYPE FORCE	$P_0 (1 - e^{-gt})$	$P_0 \frac{g}{p(p+g)}$	$\frac{2P_0 e^a}{EA_0} \frac{g}{p(p+g)} \frac{\sinh[\frac{\sqrt{a^2+4p^2}}{2}]}{\sqrt{a^2+4p^2} \cosh[\frac{\sqrt{a^2+4p^2}}{2}] + a \sinh[\frac{\sqrt{a^2+4p^2}}{2}]}$

3.4.1.3 Displacement Solution of Axially Loaded Heterogeneous Rods Using Laplace Transform Technique

In this section, the same problem in section 3.3.2 will be investigated again. A fixed-free rod with the axial force applied at the free end $h=1.0$ will be considered. In order to obtain equation of the motion of the system, equation (3.49) can be used again. The above equation is solved for a rods with a same density and same Young's modulus variations at (3.3.2). The heterogeneous rod shares the same displacement expressions of the non-uniform one. Since the density and elasticity variations of the heterogeneous rod must be same.

3.4.1.3.(1). Displacement Solution for $E(h) = E_0(1+ah)^2$ and $r(h) = r_0(1+ah)^2$

If $v(h,t)$ is longitudinal displacement of any point “ h ” of the beam at dimensionless time “ t ”, the boundary value problem is

$$\frac{\partial^2 v(h,t)}{\partial h^2} + \frac{1}{E(h)} \frac{\partial E(h)}{\partial h} \frac{\partial v(h,t)}{\partial h} = c^2 \frac{r(h)}{E(h)} \frac{\partial^2 v(h,t)}{\partial t^2}, 0 < h < 1, t > 0 \quad (3.95-a)$$

$$v(h,0) = 0, \quad \frac{\partial v(h,0)}{\partial t} = 0, \quad v(0,t) = 0, \quad \left. \frac{\partial v}{\partial h} \right|_{h=1} = \frac{P(t)}{E(1)A} \quad (3.95-b)$$

where E is Young's modulus. Substituting $E(h) = E_o(1+ah)^2 - r(h) = r_o(1+ah)^2$ and taking the Laplace transform of equations (3.95-a) and (3.95-b) yields

$$y''(h,p) + \frac{2a}{(1+ah)} y'(h,p) - p^2 y(h,p) = 0 \quad (3.96-a)$$

$$y(0,p) = 0, \quad \frac{\partial y(1,p)}{\partial h} = \frac{1}{E(1)A} L\{P(t)\} \quad (3.96-b)$$

where $y(h,p) = L\{v(h,t)\}$, p being the complex Laplace parameter. Introducing a new variable z defined as

$$y(h,p) = \frac{z}{(1+ah)} \quad (3.97)$$

into equation (3.96-a) results in

$$z'' - p^2 z = 0 \quad (3.98)$$

The general solution of equation (3.98) is

$$z = c_1 \sin[kh] + c_2 \cos[kh] \quad (3.99)$$

where

$$k^2 = -p^2 \quad (3.100)$$

Following the same steps as in the section (3.4.1.2.(1)), the same axial displacement expressions of the end point in the Laplace space for $A(h) = A_o(1 + ah)^2$ at Table 3.4 can be found for $E(h) = E_o(1 + ah)^2$ and $r(h) = r_o(1 + ah)^2$.

3.4.1.3.(2). Displacement Solution for $E(h) = E_o \sin^2[ah + b]$ and $r(h) = r_o \sin^2[ah + b]$

If $v(h, t)$ is longitudinal displacement of any point “ h ” of the beam at dimensionless time “ t ”, the boundary value problem is

$$\frac{\partial^2 v(h, t)}{\partial h^2} + \frac{1}{E(h)} \frac{\partial E(h)}{\partial h} \frac{\partial v(h, t)}{\partial h} = c^2 \frac{r(h)}{E(h)} \frac{\partial^2 v(h, t)}{\partial t^2}, 0 < h < 1, t > 0 \quad (3.101-a)$$

$$v(h, 0) = 0, \quad \frac{\partial v(h, 0)}{\partial t} = 0, \quad v(0, t) = 0, \quad \left. \frac{\partial v}{\partial h} \right|_{h=1} = \frac{P(t)}{E(1)A} \quad (3.101-b)$$

where E is Young’s modulus. Substituting $E(h) = E_o \sin^2[ah + b]$ -
 $r(h) = r_o \sin^2[ah + b]$ and taking the Laplace transform of equations (3.101-a) and (3.101-b) yields

$$y''(h, p) + 2a \cot[ah + b] y'(h, p) - p^2 y(h, p) = 0 \quad (3.102-a)$$

$$y(0, p) = 0, \quad \frac{\partial y(1, p)}{\partial h} = \frac{1}{E(1)A} L\{P(t)\} \quad (3.102-b)$$

where $y(h, p) = L\{v(h, t)\}$, p being the complex Laplace parameter. Introducing a new variable z defined as

$$y(h, p) = \frac{z}{\sin[ah + b]} \quad (3.103)$$

into equation (3.102-a) results in

$$z'' + (a^2 - p^2)z = 0 \quad (3.104)$$

The general solution of equation (3.104) is

$$z = c_1 \sin[kh] + c_2 \cos[kh] \quad (3.105)$$

where

$$k^2 = a^2 + a^2 \quad (3.106)$$

Following the same steps as in the section (3.4.1.2.(2)), the same axial displacement expressions of the end point in the Laplace space for $A(h) = A_0 \sin^2[ah + b]$ at Table 3.5 can be found for $E(h) = E_0 \sin^2[ah + b]$ and $r(h) = r_0 \sin^2[ah + b]$.

3.4.1.3.(3). Displacement Solution for $E(h) = E_0 e^{-ah}$ and $r(h) = r_0 e^{-ah}$:

If $v(h, t)$ is longitudinal displacement of any point “ h ” of the beam at dimensionless time “ t ”, the boundary value problem is

$$\frac{\partial^2 v(h, t)}{\partial h^2} + \frac{1}{E(h)} \frac{\partial E(h)}{\partial h} \frac{\partial v(h, t)}{\partial h} = c^2 \frac{r(h)}{E(h)} \frac{\partial^2 v(h, t)}{\partial t^2}, 0 < h < 1, t > 0 \quad (3.107-a)$$

$$v(h, 0) = 0, \quad \frac{\partial v(h, 0)}{\partial t} = 0, \quad v(0, t) = 0, \quad \left. \frac{\partial v}{\partial h} \right|_{h=1} = \frac{P(t)}{E(1)A} \quad (3.107-b)$$

where E is Young's modulus. Substituting $E(h) = E_0 e^{-ah}$ - $r(h) = r_0 e^{-ah}$ and taking the Laplace transform of equations (3.107-a) and (3.107-b) yields

$$y''(h, p) - a y'(h, p) - p^2 y(h, p) = 0 \quad (3.108-a)$$

$$y(0, p) = 0, \quad \frac{\partial y(1, p)}{\partial h} = \frac{1}{E(1)A} L\{P(t)\} \quad (3.108-b)$$

For equation (3.108-a), it is obvious that if

$$a^2 + 4p^2 \leq 0 \quad (3.109)$$

then, only zero solution exists. When

$$a^2 + 4p^2 > 0 \quad (3.110)$$

the general solution of $y(h, p)$ is given by

$$y(h, p) = c_1 e^{I_1 h} + c_2 e^{I_2 h} \quad (3.111)$$

where $I_{1,2} = \frac{a \pm \sqrt{\Delta}}{2}$ and $\Delta = a^2 + 4p^2$.

Following the same steps as in the section (3.4.1.2.(3)), the same axial displacement expressions of the end point in the Laplace space for $A(h) = A_0 e^{-ah}$ at Table 3.6 can be found for $E(h) = E_0 e^{-ah}$ and $r(h) = r_0 e^{-ah}$.

3.4.2. Numerical Direct Laplace Transform Methods

Some load functions analytical expressions are complicated and their Laplace transforms can not be found from tables. In such cases, numerical values of functions should be calculated separately. Their transforms can be obtained by a direct Laplace transform method which depends on Fast Fourier Transform (FFT).

The Fast Fourier Transform (FFT) was developed by (Cooley and Tukey, 1965), which enables us to compute numerically direct and inverse Fourier transforms and convolution integrals. This algorithm, originally developed for electrical engineering needs, has also been successfully applied to various problems of applied mechanics.

3.4.2.1. Direct Laplace Transform which Utilizes FFT

If $f(t)$ function in time space is:

$$\begin{aligned} f(t) &= f(t) \quad \text{for } 0 \leq t \leq T \\ f(t) &= 0 \quad \text{for } t < 0 \text{ and } t > T \end{aligned} \quad (3.112)$$

Laplace transformation of $f(t)$ is

$$\bar{F}(p) = \int_0^T f(t) e^{-pt} dt \quad (3.113)$$

$t = t_n = n \Delta t$ for the separated values of $f(t)$ in separated Equation (3.113) form,

$$f(p_k) = \Delta t \sum_{n=0}^{N-1} [f(t_n) e^{-at_n}] e^{-i \frac{2p n k}{N}} \quad (3.114)$$

Here, $p_k = a + i \frac{2p}{T} k$ (the k 'th Laplace transform parameter) and $N = T / \Delta t$.

Equation (3.114) can be calculated by the help of FFT algorithm. The term in the summation $[f(t_n)e^{-at_n}]$ is input to the FFT algorithm (Clough and Penzien,1993). The FFT algorithm is also given in Appendix-A.

3.4.3. Numerical Inverse Laplace Transform Methods

Using the Laplace transform for solving differential equations, however, sometimes leads to solutions in the Laplace domain that are not readily invertible to the real domain by analytical means. Numerical inversion methods are then used to convert the obtained solution from the Laplace domain into the real domain. Each individual method has its own application and is suitable for a particular type of function. All the inversion methods are based on approximations used to evaluate the integral given in Eq.(3.68).

The solutions in Laplace transform space can be calculated numerically for real problems. For time-space transition, numerical inverse Laplace transforms are needed. Various inverse Laplace transform methods have been improved for this purpose (Canat, 1975) and (Beskos and Narayan, 1982). Three important methods are given below:

- Maximum Degree of Precision Method
- Dubner and Abate Inverse Transform Method
- Durbin's Inverse Transform Method

As it can be seen from (Temel, 1995), the best solution is provided by Durbin's inverse Transform Method, so Modified Durbin's Method is to be used in the prepared program in the present thesis.

3.4.3.1. Durbin's Inverse Transform Method

A numerical inverse Laplace transform technique is necessary to obtain the values in the time domain. For this purpose, Durbin's inverse Laplace transform technique based on the fast fourier transform is used (Durbin,1974). Durbin's formulation for inverse Laplace transform is summarized as follows:

The real-time function $f(t_j)$ is obtained from the corresponding transform values $\bar{F}(p_k)$ as

$$f(t_j) \cong \frac{2e^{aj\Delta t}}{T} \left[-\frac{1}{2} \operatorname{Re}\{\bar{F}(a)\} + \operatorname{Re}\left\{ \sum_{k=0}^{N-1} (A(k) + iB(k))W^{jk} \right\} \right] \quad (3.115)$$

(j=0,1,2,.....,N-1)

where

$$A(k) = \sum_{l=0}^L \operatorname{Re}\left\{ \bar{F}\left(a + i(k + lN) \frac{2p}{T}\right) \right\}$$

$$B(k) = \sum_{l=0}^L \operatorname{Im}\left\{ \bar{F}\left(a + i(k + lN) \frac{2p}{T}\right) \right\} \quad (3.116)$$

$$W = \operatorname{Exp}\left[i \frac{2p}{N}\right]$$

Here, i is the complex number, $p_k = a + i \frac{2p}{T} k$ is the k^{th} Laplace transform parameter. There are N units of equal time intervals and T is the solution interval. $f(t)$ is calculated for all $t_j = j\Delta t = jT/N, (j = 0,1,2,\dots,N-1)$. The selection of constant "a" in numerical direct and inverse Laplace transform is explained in (Durbin, 1974). It is implied that if the value of "aT" is chosen from range 5 to 10, good results are obtained. Therefore, for the numerical examples presented in this thesis the value of "aT" is generally taken as "6". Finally, results can be modified multiplying each term by Fejer (F_k) or Lanczos (L_k) factors to obtain better results

in the Laplace domain (Narayan, 1977). The terms in Equation (3.116) are input to the FFT subprogram as

$$\sum_{k=0}^{N-1} [A(k) + iB(k)] e^{(i \frac{2p}{N})jk} \quad (3.117)$$

As proposed by (Narayan, 1977), the equation (3.116) is modified as follows:

$$f(t_j) \cong \frac{2e^{aj\Delta t}}{T} \left[-\frac{1}{2} \operatorname{Re}\{\overline{F(a)}\} + \operatorname{Re}\left\{ \sum_{k=0}^{N-1} ([A(k) + iB(k)]L_k) e^{(i \frac{2p}{N})jk} \right\} \right] \quad (3.118)$$

Each value calculated in the Laplace space is multiplied by Lanczos correction factor (L_k). This correction factor is;

$$L_k \Rightarrow \left\{ \begin{array}{l} L_0 = 1 \text{ for } k = 0 \\ L_k = \frac{\operatorname{Sin} \frac{kp}{N}}{\frac{kp}{N}} \text{ for } k > 0 \end{array} \right\} \quad (3.119)$$

The inverse transformation outlined above is used in the present thesis work for transforming displacement equations at Table 3.7, Table 3.8 and Table 3.9.

3.4.4. Use of Residue Theorem in Finding Inverse Laplace Transforms

Another way of inverse transformation into the time domain is performed using calculus of residues. We consider the inverse Laplace integral:

$$f(t) = \frac{1}{2\pi i} \int_{c-i\infty}^{c+i\infty} F(p)e^{pt} dp = \frac{1}{2\pi i} \lim_{R \rightarrow \infty} \int_{c-iR}^{c+iR} F(p)e^{pt} dp \quad (3.120)$$

where $t > 0$ and c is to the right of all singularities of $F(p)$.

1. Check that $F(p) \rightarrow 0$ as $R \rightarrow \infty$ on the contour

$$g_R = \left\{ z \in C : z = c + Re^{if}, \frac{p}{2} \leq f \leq \frac{3p}{2} \right\} \quad (3.121)$$

2. Check that $F(p)$ has only isolated singularities to the left of $\text{Re}(p) = c$ and compute residue terms at each singularity.
3. Compute the inverse Laplace integral by the Residue Theorem:

$$f(t) = \sum_{\text{Re}(p_j) < c} \text{Res}[F(p)e^{pt}; p_j] \quad (3.122)$$

If a Laplace transform involves a branch point, the contour in Fig.3.3 must be modified by inserting a branch cut to make the function single valued inside the contour, and this often involves making a cut along the negative real axis. The Residue Theorem and Branch point issue are also given in Appendix-B.

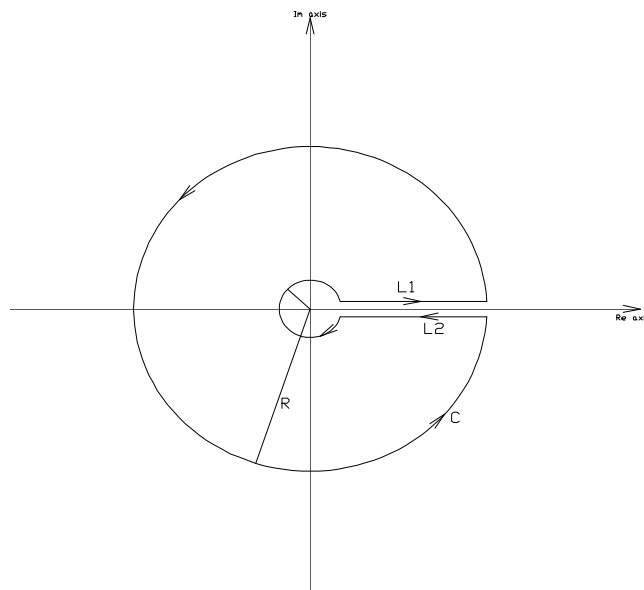


Figure 3.3 Integration contour C

3.4.4.1. Solutions for the form $(1 + ah)^2$

The displacement equations of the rod are almost the same for Case 1 (non-uniform rod with varying cross-section $A(h) = A_o(1 + ah)^2$) and Case 2 (heterogeneous rod with varying density $r(h) = r_o(1 + ah)^2$ and varying Young's modulus $E(h) = E_o(1 + ah)^2$), as shown in Table 3.4. As a result of this, Case 1 and Case 2 will be handled together. A detailed analysis for the load types $P_1(t) = P_o(1 - \cos[gt])$, $P_2(t) = P_o$ and $P_3(t) = P_o(1 - e^{-gt})$ will be presented, and subsequently, the outline of analyses and results will be listed.

3.4.4.1.(1). Displacements due to the Cosine Type Force

Expression given in Table-3.4 can be rewritten as follows;

$$y = \frac{P_o g^2}{E A_o (1 + a)} \frac{F(p)}{p(p^2 + g^2)G(p)} \quad (3.123)$$

where

$$F(p) = \sin[\sqrt{-p^2}] \quad (3.124)$$

$$G(p) = \sqrt{-p^2} (1 + a) \cos[\sqrt{-p^2}] - a \sin[\sqrt{-p^2}] \quad (3.125)$$

and the complex Laplace parameter p has been maintained in the formulation.

Using the inversion theorem we may write the displacement function v in the real time space as

$$v(h, t) = \frac{P_o g^2}{E A_o (1 + a) 2pi} \int_{c - i\infty}^{c + i\infty} \frac{e^{xt} F(x) dx}{(x^2 + g^2)G(x) x} \quad (3.126)$$

Applying the residue theorem yields

$$v(\mathbf{h}, t) = 2\pi i \sum \text{Residues at the poles of } v \quad (3.127)$$

The points of Eq. (3.126) are $x = \pm ig$ and the zeros of the equation $G(x) = 0$ and $x = 0$. These points are singular points, not branch points (see Appendix-B). The residues at the pole ig and $-ig$ can be obtained readily. They are

$$-\frac{e^{igt} F(ig)}{2g^2 G(ig)} \quad \text{and} \quad -\frac{e^{-igt} F(-ig)}{2g^2 G(-ig)} \quad (3.128)$$

Noting that $F(-ig) = F(ig)$ and $G(-ig) = G(ig)$ sum of the residues becomes

$$R_1 = -\frac{F(ig) \cos[gt]}{g^2 G(ig)} \quad (3.129)$$

As for the roots of $G(x) = 0$; in view of Eq. (3.125), replacing x with ia and setting $G(ia) = G(-ia)$ equal to zero gives

$$\sqrt{a_s^2} (1 + a) \cos[\sqrt{a_s^2}] - a \sin[\sqrt{a_s^2}] = 0 \quad (3.130)$$

The roots a_s , $s = 1, 2, \dots$ of Eq.(3.130) correspond to natural frequencies given by Eq. (3.32). Without resorting to lengthy discussions, based on this observation, it can be concluded that these are all real and simple.

The residues of the integrand at the simple poles $x = \pm ia_s$ are

$$\frac{e^{ia_s t} F(ia_s)}{(g^2 - a_s^2) a_s \left. \frac{dG}{dx} \right|_{x=ia_s}} \quad \text{and} \quad \frac{e^{-ia_s t} F(-ia_s)}{(g^2 - a_s^2) a_s \left. \frac{dG}{dx} \right|_{x=-ia_s}} \quad (3.131)$$

The residue sum is expressed explicitly as

$$R_s = \frac{2 \cos[a_s t] \sin[\sqrt{a_s^2}]}{(g^2 - a_s^2)(a_s)(\cos[a_s] - (1+a)a_s \sin[\sqrt{a_s^2}])} \quad (3.132)$$

The sum of the residues at the poles of the zeros of $G(x)$ is

$$R_2 = \sum_{s=1}^{\infty} R_s \quad (3.133)$$

For $x = 0$ the residue is as follows:

$$R_3 = \frac{\sin[0]}{g^2(-a) \sin[0]} \quad (3.134)$$

The result of Eq.(3.134) is 0/0 , so L'Hospital's rule must be used.

$$R_3 = \frac{1}{g^2} \quad (3.135)$$

Final form of the displacement can now be written as

$$v(1,t) = \frac{P_0 g^2}{E A_0 (1+a)} (R_1 + R_2 + R_3) \quad (3.136)$$

3.4.4.1.(2). Displacements due to the Step Force

Expression given in Table-3.4. can be rewritten as follows;

$$y = \frac{P_0}{E A_0 (1+a)} \frac{F(p)}{p G(p)} \quad (3.137)$$

where

$$F(p) = \sin[\sqrt{-p^2}] \quad (3.138)$$

$$G(p) = \sqrt{-p^2} (1+a) \cos[\sqrt{-p^2}] - a \sin[\sqrt{-p^2}] \quad (3.139)$$

Using the inversion theorem we may write the displacement function v in the real time space as

$$v(h,t) = \frac{P_0}{E A_0 (1+a) 2p i} \int_{c-i\infty}^{c+i\infty} \frac{e^{xt} F(x) dx}{G(x) x} \quad (3.140)$$

Applying the residue theorem yields

$$v(h,t) = 2p i \sum \text{Residues at the poles of } v \quad (3.141)$$

The singular points of Eq.(3.140) are $x = 0$ and the zeros of the equation $G(x) = 0$.

As for the roots of $G(x) = 0$; in view of Eq. (3.139), replacing x with ia and setting $G(ia) = G(-ia)$ equal to zero gives

$$\sqrt{a_s^2} (1+a) \cos[\sqrt{a_s^2}] - a \sin[\sqrt{a_s^2}] = 0 \quad (3.142)$$

The roots a_s , $s = 1, 2, \dots$ of Eq.(3.142) correspond to natural frequencies. The residues of the integrand at the simple poles $x = \pm ia_s$ are

$$\frac{e^{ia_s t} F(ia_s)}{a_s \left. \frac{dG}{dx} \right|_{x=a_s}} \quad \text{and} \quad \frac{e^{-ia_s t} F(-ia_s)}{a_s \left. \frac{dG}{dx} \right|_{x=-a_s}} \quad (3.143)$$

The residue sum is expressed explicitly as

$$R_s = \frac{2 \cos[a_s t] \sin[\sqrt{a_s^2}]}{(a_s)(\cos[a_s] - (1+a)a_s \sin[\sqrt{a_s^2}])} \quad (3.144)$$

The sum of the residues at the poles of the zeros of $G(x)$ is

$$R_2 = \sum_{s=1}^{\infty} R_s \quad (3.145)$$

For $x = 0$ the residue is as follows:

$$R_3 = \frac{\sin[0]}{(-a) \sin[0]} \quad (3.146)$$

The result of Eq.(3.146) is 0/0 , so L'Hospital's rule must be used.

$$R_3 = 1 \quad (3.147)$$

Final form of the displacement can now be written as

$$v(1,t) = \frac{P_0}{E A_0 (1+a)} (R_1 + R_2 + R_3) \quad (3.148)$$

3.4.4.1.(3). Displacements due to the Exponential Type Force

Expression given in Table-3.4 can be rewritten as follows;

$$y = \frac{P_0 g}{E A_0 (1+a)} \frac{F(p)}{p(p+g)G(p)} \quad (3.149)$$

where

$$F(p) = \sin[\sqrt{-p^2}] \quad (3.150)$$

$$G(p) = \sqrt{-p^2} (1+a) \cos[\sqrt{-p^2}] - a \sin[\sqrt{-p^2}] \quad (3.151)$$

Using the inversion theorem we may write the displacement function v in the real time space as

$$v(h,t) = \frac{P_0 g}{E A_0 (1+a) 2p i} \int_{c-i\infty}^{c+i\infty} \frac{e^{xt} F(x) dx}{(x+g)G(x) x} \quad (3.152)$$

Applying the residue theorem yields

$$v(h,t) = 2p i \sum \text{Residues at the poles of } v \quad (3.153)$$

The singular points of Eq. (3.152) are $x = -g$ and the zeros of the equation $G(x) = 0$ and $x = 0$. The residues at the pole $-g$ can be obtained readily. It is

$$R_1 = -\frac{F(-g) e^{-gt}}{g G(-g)} \quad (3.154)$$

As for the roots of $G(x) = 0$; in view of Eq. (3.113), replacing x with ia and setting $G(ia) = G(-ia)$ equal to zero gives

$$\sqrt{a_s^2} (1+a) \cos[\sqrt{a_s^2}] - a \sin[\sqrt{a_s^2}] = 0 \quad (3.155)$$

The roots $a_s, s = 1, 2, \dots$ of Eq.(3.155) correspond to natural frequencies. The residues of the integrand at the simple poles $x = \pm ia_s$ are

$$\frac{e^{ia_s t} F(ia_s)}{(g + ia_s) a_s \frac{dG}{dx} \Big|_{x = a_s}} \quad \text{and} \quad \frac{e^{-ia_s t} F(-ia_s)}{(g - ia_s) a_s \frac{dG}{dx} \Big|_{x = -a_s}} \quad (3.156)$$

The residue sum is expressed explicitly as

$$R_s = \frac{\sin[a_s] (2g \cos[a_s t] + 2a_s \sin[a_s t])}{(g^2 + a_s^2)(a_s)(\cos[a_s] - (1+a) a_s \sin[a_s])} \quad (3.157)$$

The sum of the residues at the poles of the zeros of $G(x)$ is

$$R_2 = \sum_{s=1}^{\infty} R_s \quad (3.158)$$

For $x = 0$ the residue is as follows:

$$R_3 = \frac{\sin[0]}{g(-a) \sin[0]} \quad (3.159)$$

The result of Eq.(3.159) is $0/0$, so L'Hospital's rule must be used.

$$R_3 = \frac{1}{g} \quad (3.160)$$

Final form of the displacement can now be written as

$$v(l, t) = \frac{P_0 g}{E A_0 (1+a)} (R_1 + R_2 + R_3) \quad (3.161)$$

Table 3.7. Displacements due to $P_1(t)$, $P_2(t)$ and $P_3(t)$ for the form $(1+ah)^2$

$P_1(t)$	$v(l, t) = \frac{P_0 g^2}{E_0 A_0 (1+a)} (R_1 + R_2 + R_3)$	
	R_1	$-\frac{F(ig) \cos[gt]}{g^2 G(ig)}$
	R_2	$\sum_{s=1}^{\infty} \frac{2F(ia_s) \cos[a_s t]}{(g^2 - a_s^2) a_s (\cos[a_s] - (1+a) a_s \sin[a_s])}$
	R_3	$1/g^2$
$P_2(t)$	$v(l, t) = \frac{P_0}{E_0 A_0 (1+a)} (R_1 + R_2 + R_3)$	
	R_1	0
	R_2	$\sum_{s=1}^{\infty} \frac{2F(ia_s) \cos[a_s t]}{a_s (\cos[a_s] - (1+a) a_s \sin[a_s])}$
	R_3	1
$P_3(t)$	$v(l, t) = \frac{P_0 g}{E_0 A_0 (1+a)} (R_1 + R_2 + R_3)$	
	R_1	$-\frac{F(-g) e^{-gt}}{g G(-g)}$
	R_2	$\sum_{s=1}^{\infty} \frac{F(ia_s) (2a_s \sin[a_s t] + 2g \cos[a_s t])}{(g^2 + a_s^2) a_s (\cos[a_s] - (1+a) a_s \sin[a_s])}$
	R_3	$\frac{1}{g}$

3.4.4.2. Solutions for the form $\sin^2[ah+b]$

The displacement equations of the rod are almost the same for Case 3 (non-uniform rod with varying cross-section $A(h) = A_0 \sin^2[ah+b]$) and Case 4 (heterogeneous rod with varying density $r(h) = r_0 \sin^2[ah+b]$) and varying

Young's modulus $E(h) = E_0 \sin^2[ah + b]$, as shown in Table 3.5. As a result of this, Case 3 and Case 4 will be handled together. A detailed analysis for the load types $P_1(t) = P_0(1 - \cos[gt])$, $P_2(t) = P_0$ and $P_3(t) = P_0(1 - e^{-gt})$ will be presented, and subsequently, the outline of analyses and results will be listed.

3.4.4.2.(1). Displacements due to the Cosine Type Force

Expression given in Table-3.5. can be rewritten as follows;

$$y = \frac{P_0 g^2}{E A_0 \sin[a + b]} \frac{F(p)}{p(p^2 + g^2)G(p)} \quad (3.162)$$

where

$$F(p) = \sin[\sqrt{a^2 - p^2}] \quad (3.163)$$

$$G(p) = \sqrt{a^2 - p^2} \sin[a + b] \cos[\sqrt{a^2 - p^2}] - a \cos[a + b] \sin[\sqrt{a^2 - p^2}] \quad (3.164)$$

Using the inversion theorem we may write the displacement function v in the real time space as

$$v(h, t) = \frac{P_0 g^2}{E A_0 \sin[a + b] 2p i} \int_{c - i\infty}^{c + i\infty} \frac{e^{xt} F(x) dx}{(x^2 + g^2) G(x) x} \quad (3.165)$$

Applying the residue theorem yields

$$v(h, t) = 2p i \sum \text{Residues at the poles of } v \quad (3.166)$$

The singular points of Eq. (3.165) are $x = \pm ig$ and the zeros of the equation $G(x) = 0$ and $x = 0$. The residues at the pole ig and $-ig$ can be obtained readily. They are

$$-\frac{e^{igt} F(ig)}{2g^2 G(ig)} \quad \text{and} \quad -\frac{e^{-igt} F(-ig)}{2g^2 G(-ig)} \quad (3.167)$$

Noting that $F(-ig) = F(ig)$ and $G(-ig) = G(ig)$ sum of the residues becomes

$$R_1 = -\frac{F(ig) \cos[gt]}{g^2 G(ig)} \quad (3.168)$$

As for the roots of $G(x) = 0$; in view of Eq. (3.164), replacing x with ia and setting $G(ia) = G(-ia)$ equal to zero gives

$$\sqrt{a^2 + a_s^2} \sin[a+b] \cos[\sqrt{a^2 + a_s^2}] - a \cos[a+b] \sin[\sqrt{a^2 + a_s^2}] = 0 \quad (3.169)$$

The roots a_s , $s = 1, 2, \dots$ of Eq.(3.169) correspond to natural frequencies given by Eq. (3.40). The residues of the integrand at the simple poles $x = \pm ia_s$ are

$$\frac{e^{ia_s t} F(ia_s)}{(g^2 - a_s^2) a_s \frac{dG}{dx} \Big|_{x=ia_s}} \quad \text{and} \quad \frac{e^{-ia_s t} F(-ia_s)}{(g^2 - a_s^2) a_s \frac{dG}{dx} \Big|_{x=-ia_s}} \quad (3.170)$$

The residue sum is expressed explicitly as

$$R_s = \frac{2 \cos[a_s t] \sin[\sqrt{a^2 + a_s^2}] (\sqrt{a^2 + a_s^2})}{(g^2 - a_s^2)(a_s^2 (a \cos[a + b] \cos[\sqrt{a^2 + a_s^2}] + \sin[a + b] (-\cos[\sqrt{a^2 + a_s^2}] + \sqrt{a^2 + a_s^2} \sin[\sqrt{a^2 + a_s^2}])))} \quad (3.171)$$

The sum of the residues at the poles of the zeros of $G(x)$ is

$$R_2 = \sum_{s=1}^{\infty} R_s \quad (3.172)$$

For $x = 0$ the residue is as follows:

$$R_3 = \frac{\sin[a]}{g^2(a) \sin[b]} \quad (3.173)$$

If parameter “a” is equal to zero, the result of Eq.(3.173) is 0/0 , so L’Hospital’s rule must be used.

$$R_3 = \frac{1}{g^2 \sin[b]} \quad (3.174)$$

Final form of the displacement can now be written as

$$v(l, t) = \frac{P_0 g^2}{E A_0 \sin[a + b]} (R_1 + R_2 + R_3) \quad (3.175)$$

3.4.4.2.(2). Displacements due to the Step Force

Expression given in Table 3.5. can be rewritten as follows;

$$y = \frac{P_0}{E A_0 \sin[a+b]} \frac{F(p)}{p G(p)} \quad (3.176)$$

where

$$F(p) = \sin[\sqrt{a^2 - p^2}] \quad (3.177)$$

$$G(p) = \sqrt{a^2 - p^2} \sin[a+b] \cos[\sqrt{a^2 - p^2}] - a \cos[a+b] \sin[\sqrt{a^2 - p^2}] \quad (3.178)$$

Using the inversion theorem we may write the displacement function v in the real time space as

$$v(h,t) = \frac{P_0}{E A_0 \sin[a+b] 2p i} \int_{c-i\infty}^{c+i\infty} \frac{e^{xt} F(x) dx}{G(x) x} \quad (3.179)$$

Applying the residue theorem yields

$$v(h,t) = 2p i \sum \text{Residues at the poles of } v \quad (3.180)$$

The singular points of Eq. (3.179) are $x = 0$ and the zeros of the equation $G(x) = 0$.

As for the roots of $G(x) = 0$; in view of Eq. (3.178), replacing x with ia and setting $G(ia) = G(-ia)$ equal to zero gives

$$\sqrt{a^2 + a_s^2} \sin[a+b] \cos[\sqrt{a^2 + a_s^2}] - a \cos[a+b] \sin[\sqrt{a^2 + a_s^2}] = 0 \quad (3.181)$$

The roots a_s , $s = 1, 2, \dots$ of Eq.(3.181) correspond to natural frequencies. The residues of the integrand at the simple poles $x = \pm ia_s$ are

$$\frac{e^{ia_s t} F(ia_s)}{a_s \left. \frac{dG}{dx} \right|_{x=a_s}} \quad \text{and} \quad \frac{e^{-ia_s t} F(-ia_s)}{a_s \left. \frac{dG}{dx} \right|_{x=-a_s}} \quad (3.182)$$

The residue sum is expressed explicitly as

$$R_s = - \frac{2 \cos[a_s t] \sin[\sqrt{a^2 + a_s^2}] (\sqrt{a^2 + a_s^2})}{a_s^2 (a \cos[a+b] \cos[\sqrt{a^2 + a_s^2}] + \sin[a+b] (-\cos[\sqrt{a^2 + a_s^2}] + \sqrt{a^2 + a_s^2} \sin[\sqrt{a^2 + a_s^2}]))} \quad (3.183)$$

The sum of the residues at the poles of the zeros of $G(x)$ is

$$R_2 = \sum_{s=1}^{\infty} R_s \quad (3.184)$$

For $x = 0$ the residue is as follows:

$$R_3 = \frac{\sin[a]}{a \sin[b]} \quad (3.185)$$

If parameter “a” is equal to zero, the result of Eq.(3.185) is 0/0 , so L’Hospital’s rule must be used.

$$R_3 = \frac{1}{\sin[b]} \quad (3.186)$$

Final form of the displacement can now be written as

$$v(1,t) = \frac{P_0}{E A_0 \sin[a+b]} (R_1 + R_2 + R_3) \quad (3.187)$$

3.4.4.2.(3). Displacements due to the Exponential Type Force

Expression given in Table 3.5. can be rewritten as follows;

$$y = \frac{P_0 g}{E A_0 \sin[a+b]} \frac{F(p)}{p(p+g)G(p)} \quad (3.188)$$

where

$$F(p) = \sin[\sqrt{a^2 - p^2}] \quad (3.189)$$

$$G(p) = \sqrt{a^2 - p^2} \sin[a+b] \cos[\sqrt{a^2 - p^2}] - a \cos[a+b] \sin[\sqrt{a^2 - p^2}] \quad (3.190)$$

Using the inversion theorem we may write the displacement function v in the real time space as

$$v(h,t) = \frac{P_0 g}{E A_0 \sin[a+b] 2p i} \int_{c-i\infty}^{c+i\infty} \frac{e^{xt} F(x) dx}{(x+g)G(x) x} \quad (3.191)$$

Applying the residue theorem yields

$$v(h,t) = 2p i \sum \text{Residues at the poles of } v \quad (3.192)$$

The singular points of Eq. (3.191) are $x = -g$, the zeros of the equation $G(x) = 0$ and $x = 0$. The residues at the pole $-g$ can be obtained readily. It is

$$R_1 = -\frac{F(-g) e^{-gt}}{g G(-g)} \quad (3.193)$$

As for the roots of $G(x) = 0$; in view of Eq. (3.190), replacing x with ia and setting $G(ia) = G(-ia)$ equal to zero gives

$$\sqrt{a^2 + a_s^2} \sin[a+b] \cos[\sqrt{a^2 + a_s^2}] - a \cos[a+b] \sin[\sqrt{a^2 + a_s^2}] = 0 \quad (3.194)$$

The roots $a_s, s = 1, 2, \dots$ of Eq. (3.194) correspond to natural frequencies. The residues of the integrand at the simple poles $x = \pm ia_s$ are

$$\frac{e^{ia_s t} F(ia_s)}{(g + ia_s) a_s \frac{dG}{dx} \Big|_{x=ia_s}} \quad \text{and} \quad \frac{e^{-ia_s t} F(-ia_s)}{(g - ia_s) a_s \frac{dG}{dx} \Big|_{x=-ia_s}} \quad (3.195)$$

The residue sum is expressed explicitly as

$$R_s = - \frac{(2g \cos[a_s t] + 2a_s \sin[a_s t]) \sin[\sqrt{a^2 + a_s^2}] (\sqrt{a^2 + a_s^2})}{(g^2 + a_s^2) (a_s^2 (a \cos[a+b] \cos[\sqrt{a^2 + a_s^2}] + \sin[a+b] (-\cos[\sqrt{a^2 + a_s^2}] + \sqrt{a^2 + a_s^2} \sin[\sqrt{a^2 + a_s^2}]))} \quad (3.196)$$

The sum of the residues at the poles of the zeros of $G(x)$ is

$$R_2 = \sum_{s=1}^{\infty} R_s \quad (3.197)$$

For $x = 0$ the residue is as follows:

$$R_3 = \frac{\sin[a]}{g(a) \sin[b]} \quad (3.198)$$

If parameter “a” is equal to zero, the result of Eq.(3.198) is 0/0 , so L’Hospital’s rule must be used.

$$R_3 = \frac{1}{g \sin[b]} \tag{3.199}$$

Final form of the displacement can now be written as

$$v(l,t) = \frac{P_0 g}{E A_0 \sin[a+b]} (R_1 + R_2 + R_3) \tag{3.200}$$

Table 3.8. Displacements due to $P_1(t), P_2(t)$ and $P_3(t)$ for the form $\sin^2[ah + b]$

$P_1(t)$	$v(l,t) = \frac{P_0 g^2}{E_0 A_0 \sin[a+b]} (R_1 + R_2 + R_3)$	
	R_1	$-\frac{F(ig) \cos[gt]}{g^2 G(ig)}$
	R_2	$\sum_{s=1}^{\infty} \frac{2 \cos[a_s t] \sin[\sqrt{a^2 + a_s^2}] (\sqrt{a^2 + a_s^2})}{(g^2 - a_s^2) (a_s^2 (a \cos[a+b] \cos[\sqrt{a^2 + a_s^2}] + \sin[a+b] (-\cos[\sqrt{a^2 + a_s^2}] + \sqrt{a^2 + a_s^2} \sin[\sqrt{a^2 + a_s^2}])))}$
	R_3	$\frac{\sin[a]}{g^2(a) \sin[b]}$
$P_2(t)$	$v(l,t) = \frac{P_0}{E_0 A_0 \sin[a+b]} (R_1 + R_2 + R_3)$	
	R_1	0
	R_2	$\sum_{s=1}^{\infty} \frac{2 \cos[a_s t] \sin[\sqrt{a^2 + a_s^2}] (\sqrt{a^2 + a_s^2})}{s^2 a_s^2 (a \cos[a+b] \cos[\sqrt{a^2 + a_s^2}] + \sin[a+b] (-\cos[\sqrt{a^2 + a_s^2}] + \sqrt{a^2 + a_s^2} \sin[\sqrt{a^2 + a_s^2}])))}$
	R_3	$\frac{\sin[a]}{a \sin[b]}$
$P_3(t)$	$v(l,t) = \frac{P_0 g}{E_0 A_0 \sin[a+b]} (R_1 + R_2 + R_3)$	
	R_1	$-\frac{F(-g)e^{-gt}}{g G(-g)}$
	R_2	$\sum_{s=1}^{\infty} \frac{(2g \cos[a_s t] + 2a_s \sin[a_s t]) \sin[\sqrt{a^2 + a_s^2}] (\sqrt{a^2 + a_s^2})}{s^2 (g^2 + a_s^2) (a_s^2 (a \cos[a+b] \cos[\sqrt{a^2 + a_s^2}] + \sin[a+b] (-\cos[\sqrt{a^2 + a_s^2}] + \sqrt{a^2 + a_s^2} \sin[\sqrt{a^2 + a_s^2}])))}$
	R_3	$\frac{\sin[a]}{g(a) \sin[b]}$

3.4.4.3 Solutions for the form e^{-ah}

The displacement equations of the rod are almost the same for Case 5 (non-uniform rod with varying cross-section $A(h) = A_0 e^{-ah}$) and Case 6 (heterogeneous rod with varying density $r(h) = r_0 e^{-ah}$ and varying Young's modulus $E(h) = E_0 e^{-ah}$), as shown in Table 3.6. As a result of this, Case 5 and Case 6 will be handled together. A detailed analysis for the load types $P_1(t) = P_0(1 - \cos[gt])$, $P_2(t) = P_0$ and $P_3(t) = P_0(1 - e^{-gt})$ will be presented, and subsequently, the outline of analyses and results will be listed.

3.4.4.3.(1). Displacements due to the Cosine Type Force

Expression given in Table 3.6. can be rewritten as follows;

$$y = \frac{2P_0 e^a g^2}{E A_0} \frac{F(p)}{p(p^2 + g^2)G(p)} \quad (3.201)$$

where

$$F(p) = \sinh\left[\frac{\sqrt{a^2 + 4p^2}}{2}\right] \quad (3.202)$$

$$G(p) = \sqrt{a^2 + 4p^2} \cosh\left[\frac{\sqrt{a^2 + 4p^2}}{2}\right] + a \sinh\left[\frac{\sqrt{a^2 + 4p^2}}{2}\right] \quad (3.203)$$

Using the inversion theorem we may write the displacement function v in the real time space as

$$v(h, t) = \frac{2P_0 e^a g^2}{E A_0 2pi} \int_{c-i\infty}^{c+i\infty} \frac{e^{xt} F(x) dx}{(x^2 + g^2)G(x) x} \quad (3.204)$$

Applying the residue theorem yields

$$v(\mathbf{h}, t) = 2\pi i \sum \text{Residues at the poles of } v \quad (3.205)$$

The singular points of Eq. (3.204) are $x = \pm ig$ and the zeros of the equation $G(x) = 0$ and $x = 0$. The residues at the pole ig and $-ig$ can be obtained readily. They are

$$-\frac{e^{igt} F(ig)}{2g^2 G(ig)} \quad \text{and} \quad -\frac{e^{-igt} F(-ig)}{2g^2 G(-ig)} \quad (3.206)$$

Noting that $F(-ig) = F(ig)$ and $G(-ig) = G(ig)$ sum of the residues becomes

$$R_1 = -\frac{F(ig) \cos[gt]}{g^2 G(ig)} \quad (3.207)$$

As for the roots of $G(x) = 0$; in view of Eq. (3.203), replacing x with ia and setting $G(ia) = G(-ia)$ equal to zero gives

$$\sqrt{a^2 + 4p^2} \cosh\left[\frac{\sqrt{a^2 + 4p^2}}{2}\right] + a \sinh\left[\frac{\sqrt{a^2 + 4p^2}}{2}\right] = 0 \quad (3.208)$$

The roots a_s , $s = 1, 2, \dots$ of Eq.(3.208) correspond to natural frequencies given by Eq. (3.48). The residues of the integrand at the simple poles $x = \pm ia_s$ are

$$\frac{e^{ia_s t} F(ia_s)}{(g^2 - a_s^2) a_s \left. \frac{dG}{dx} \right|_{x = a_s}} \quad \text{and} \quad \frac{e^{-ia_s t} F(-ia_s)}{(g^2 - a_s^2) a_s \left. \frac{dG}{dx} \right|_{x = -a_s}} \quad (3.209)$$

The residue sum is expressed explicitly as

$$R_s = \frac{2 \cos[a_s t] \sinh\left[\frac{\sqrt{a^2 - 4a_s^2}}{2}\right] (\sqrt{a^2 - 4a_s^2})}{(g^2 - a_s^2)(a_s(-2a_s((2+a) \cosh\left[\frac{\sqrt{a^2 - 4a_s^2}}{2}\right] + \sqrt{a^2 - 4a_s^2}) \sinh\left[\frac{\sqrt{a^2 - 4a_s^2}}{2}\right]))} \quad (3.210)$$

The sum of the residues at the poles of the zeros of $G(x)$ is

$$R_2 = \sum_{s=1}^{\infty} R_s \quad (3.211)$$

For $x = 0$ the residue is as follows:

$$R_3 = \frac{\sinh\left[\frac{a}{2}\right]}{g^2(a) \left(\cosh\left[\frac{a}{2}\right] + \sinh\left[\frac{a}{2}\right]\right)} \quad (3.212)$$

If parameter “a” is equal to zero, the result of Eq.(3.212) is 0/0 , so L’Hospital’s rule must be used.

$$R_3 = \frac{1}{2g^2} \quad (3.213)$$

Final form of the displacement can now be written as

$$v(l, t) = \frac{2P_0 e^a g^2}{EA_0} (R_1 + R_2 + R_3) \quad (3.214)$$

3.4.4.3.(2). Displacements due to the Step Force

Expression given in Table 3.6. can be rewritten as follows;

$$y = \frac{2P_0 e^a}{EA_0} \frac{F(p)}{pG(p)} \quad (3.215)$$

where

$$F(p) = \sinh\left[\frac{\sqrt{a^2 + 4p^2}}{2}\right] \quad (3.216)$$

$$G(p) = \sqrt{a^2 + 4p^2} \cosh\left[\frac{\sqrt{a^2 + 4p^2}}{2}\right] + a \sinh\left[\frac{\sqrt{a^2 + 4p^2}}{2}\right] \quad (3.217)$$

Using the inversion theorem we may write the displacement function v in the real time space as

$$v(h, t) = \frac{2P_0 e^a}{EA_0} \frac{1}{2pi} \int_{c-i\infty}^{c+i\infty} \frac{e^{xt} F(x) dx}{G(x) x} \quad (3.218)$$

Applying the residue theorem yields

$$v(h, t) = 2pi \sum \text{Residues at the poles of } v \quad (3.219)$$

The singular points of Eq. (3.218) are $x = 0$ and the zeros of the equation $G(x) = 0$. As for the roots of $G(x) = 0$; in view of Eq. (3.217), replacing x with ia and setting $G(ia) = G(-ia)$ equal to zero gives

$$\sqrt{a^2 + 4p^2} \cosh\left[\frac{\sqrt{a^2 + 4p^2}}{2}\right] + a \sinh\left[\frac{\sqrt{a^2 + 4p^2}}{2}\right] = 0 \quad (3.220)$$

The roots a_s , $s = 1, 2, \dots$ of Eq. (3.220) correspond to natural frequencies. The residues of the integrand at the simple poles $x = \pm ia_s$ are

$$\frac{e^{ia_s t} F(ia_s)}{a_s \left. \frac{dG}{dx} \right|_{x=a_s}} \quad \text{and} \quad \frac{e^{-ia_s t} F(-ia_s)}{a_s \left. \frac{dG}{dx} \right|_{x=-a_s}} \quad (3.221)$$

The residue sum is expressed explicitly as

$$R_s = \frac{2 \cos[a_s t] \sinh\left[\frac{\sqrt{a^2 - 4a_s^2}}{2}\right] (\sqrt{a^2 - 4a_s^2})}{(a_s (-2a_s ((2+a) \cosh\left[\frac{\sqrt{a^2 - 4a_s^2}}{2}\right] + \sqrt{a^2 - 4a_s^2}) \sinh\left[\frac{\sqrt{a^2 - 4a_s^2}}{2}\right]))} \quad (3.222)$$

The sum of the residues at the poles of the zeros of $G(x)$ is

$$R_2 = \sum_{s=1}^{\infty} R_s \quad (3.223)$$

For $x = 0$ the residue is as follows:

$$R_3 = \frac{\sinh\left[\frac{a}{2}\right]}{a \left(\cosh\left[\frac{a}{2}\right] + \sinh\left[\frac{a}{2}\right] \right)} \quad (3.224)$$

If parameter “a” is equal to zero, the result of Eq.(3.224) is 0/0 , so L’Hospital’s rule must be used.

$$R_3 = \frac{1}{2} \quad (3.225)$$

Final form of the displacement can now be written as

$$v(l,t) = \frac{2P_0 e^a}{EA_0} (R_1 + R_2 + R_3) \quad (3.226)$$

3.4.4.3.(3). Displacements due to the Exponential Type Force

Expression given in Table 3.6. can be rewritten as follows;

$$y = \frac{2P_0 e^a g}{EA_0} \frac{F(p)}{p(p+g)G(p)} \quad (3.227)$$

where

$$F(p) = \sinh \left[\frac{\sqrt{a^2 + 4p^2}}{2} \right] \quad (3.228)$$

$$G(p) = \sqrt{a^2 + 4p^2} \cosh \left[\frac{\sqrt{a^2 + 4p^2}}{2} \right] + a \sinh \left[\frac{\sqrt{a^2 + 4p^2}}{2} \right] \quad (3.229)$$

Using the inversion theorem we may write the displacement function v in the real time space as

$$v(h,t) = \frac{2P_0 e^a g}{EA_0 2pi} \int_{c-i\infty}^{c+i\infty} \frac{e^{xt} F(x) dx}{(x+g)G(x) x} \quad (3.230)$$

Applying the residue theorem yields

$$v(h,t) = 2\pi i \sum \text{Residues at the poles of } v \quad (3.231)$$

The singular points of Eq. (3.230) are $x = -g$ and the zeros of the equation $G(x) = 0$ and $x = 0$. The residues at the pole $-g$ can be obtained readily. It is

$$R_1 = -\frac{F(-g)e^{-gt}}{gG(-g)} \quad (3.232)$$

As for the roots of $G(x) = 0$; in view of Eq. (3.229), replacing x with ia and setting $G(ia) = G(-ia)$ equal to zero gives

$$\sqrt{a^2 + 4p^2} \cosh\left[\frac{\sqrt{a^2 + 4p^2}}{2}\right] + a \sinh\left[\frac{\sqrt{a^2 + 4p^2}}{2}\right] = 0 \quad (3.233)$$

The roots $a_s, s = 1, 2, \dots$ of Eq.(3.233) correspond to natural frequencies. The residues of the integrand at the simple poles $x = \pm ia_s$ are

$$\frac{e^{ia_s t} F(ia_s)}{(g + ia_s) a_s \left. \frac{dG}{dx} \right|_{x = a_s}} \quad \text{and} \quad \frac{e^{-ia_s t} F(-ia_s)}{(g - ia_s) a_s \left. \frac{dG}{dx} \right|_{x = -a_s}} \quad (3.234)$$

The residue sum is expressed explicitly as

$$R_s = \frac{(2a_s \sin[a_s t] + 2g \cos[a_s t]) \sinh\left[\frac{\sqrt{a^2 - 4a_s^2}}{2}\right] (\sqrt{a^2 - 4a_s^2})}{(g^2 + a_s^2) (a_s (-2a_s ((2+a) \cosh\left[\frac{\sqrt{a^2 - 4a_s^2}}{2}\right] + \sqrt{a^2 - 4a_s^2}) \sinh\left[\frac{\sqrt{a^2 - 4a_s^2}}{2}\right]))} \quad (3.235)$$

The sum of the residues at the poles of the zeros of $G(x)$ is

$$R_2 = \sum_{s=1}^{\infty} R_s \quad (3.236)$$

For $x = 0$ the residue is as follows:

$$R_3 = \frac{\sinh\left[\frac{a}{2}\right]}{g(a) (\cosh\left[\frac{a}{2}\right] + \sinh\left[\frac{a}{2}\right])} \quad (3.237)$$

If parameter “a” is equal to zero, the result of Eq.(3.237) is 0/0 , so L’Hospital’s rule must be used.

$$R_3 = \frac{1}{2g} \quad (3.238)$$

Final form of the displacement can now be written as

$$v(1,t) = \frac{2P_0 e^a g}{E A_0} (R_1 + R_2 + R_3) \quad (3.239)$$

Table 3.9. Displacements due to $P_1(t)$, $P_2(t)$ and $P_3(t)$ for the form e^{-ah}

$P_1(t)$	$v(l, t) = \frac{2e^a P_0 g^2}{E_0 A_0} (R_1 + R_2 + R_3)$	
	R_1	$-\frac{F(ig) \cos[gt]}{g^2 G(ig)}$
	R_2	$\sum_{s=1}^{\infty} \frac{2 \cos[a_s t] \sinh[\frac{1}{2} \sqrt{a^2 - 4a_s^2}] \sqrt{a^2 - 4a_s^2}}{(g^2 - a_s^2) (a_s (-2a_s ((2+a) \cosh[\frac{1}{2} \sqrt{a^2 - 4a_s^2}] + \sqrt{a^2 - 4a_s^2}) \sinh[\frac{1}{2} \sqrt{a^2 - 4a_s^2}]))}$
	R_3	$\frac{\sinh[a/2]}{a(\cosh[a/2] + \sinh[a/2])g^2}$
$P_2(t)$	$v(l, t) = \frac{2e^a P_0}{E_0 A_0} (R_1 + R_2 + R_3)$	
	R_1	0
	R_2	$\sum_{s=1}^{\infty} \frac{2 \cos[a_s t] \sinh[\frac{1}{2} \sqrt{a^2 - 4a_s^2}] \sqrt{a^2 - 4a_s^2}}{(a_s (-2a_s ((2+a) \cosh[\frac{1}{2} \sqrt{a^2 - 4a_s^2}] + \sqrt{a^2 - 4a_s^2}) \sinh[\frac{1}{2} \sqrt{a^2 - 4a_s^2}]))}$
	R_3	$\frac{\sinh[a/2]}{a(\cosh[a/2] + \sinh[a/2])}$
$P_3(t)$	$v(l, t) = \frac{2e^a P_0 g}{E_0 A_0} (R_1 + R_2 + R_3)$	
	R_1	$-\frac{F(-g) e^{-gt}}{g G(-g)}$
	R_2	$\sum_{s=1}^{\infty} \frac{(2a_s \sin[a_s t] + 2g \cos[a_s t]) \sinh[\frac{1}{2} \sqrt{a^2 - 4a_s^2}] \sqrt{a^2 - 4a_s^2}}{(g^2 + a_s^2) (a_s (-2a_s ((2+a) \cosh[\frac{1}{2} \sqrt{a^2 - 4a_s^2}] + \sqrt{a^2 - 4a_s^2}) \sinh[\frac{1}{2} \sqrt{a^2 - 4a_s^2}]))}$
	R_3	$\frac{\sinh[a/2]}{g a(\cosh[a/2] + \sinh[a/2])}$

3.4.5 Mode-Superposition Analysis

In this section we use mode-superposition analysis for finding the displacements of these rods under dynamic loading.

In mode-superposition analysis, we must follow certain steps. These are:

- Determine Mode Shapes and Frequencies:

For these fixed-free rods, the expressions were found in previous stages

- Compute Generalized Mass and Loading:

$$M_n = \int_0^1 c^2 V_n^2(h) m(h) dh$$

$$P_n(t) = \int_0^1 L V_n(h) q(h,t) dh$$

where

$$q(x,t) = P(t) \delta(x-L)$$

After using dimensionless variables and applying Delta function, $q(x,t)$ becomes;

$$q(h,t) = P(t) \frac{1}{L} \delta(h-1)$$

- Solve The Normal-Coordinate Response:

In this analysis, the Duhamel integral equation can be used to evaluate the response of an undamped SDOF system to any form of dynamic loading $P(t)$

$$Y_n(t) = \frac{1}{M_n a_n} \int_0^t P_n(t^*) \sin[w_n(t-t^*)] dt^*$$

- Evaluate Displacement:

$$v(h,t) = \sum_{n=1}^{\infty} V_n(h) Y_n(t)$$

If we want to use mode-superposition analysis, firstly the forces, which we applied to the rod, must be determined. These forces must be dynamic and the following forces will be used:

- Cosine Type Force : $P_1(t) = P_0(1 - \cos[gt])$
- Step Force : $P_2(t) = P_0$
- Exponential Type Force : $P_3(t) = P_0(1 - e^{-gt})$

Also, only the displacement expression for the end point $h = 1$ will be obtained and the behavior of the end point under dynamic load will be examined.

Table 3.10. Mode-superposition analysis expressions for step force loading.

For the form:	$(1 + a h)^2$
a_n	k_n
$V_n(h)$	$\frac{\text{Sin}[k_n h]}{(1 + a h)}$
M_n	$\frac{c^2 r_O A_O}{4 k_n} (2 k_n - \text{Sin}[2 k_n])$
$P_n(t)$	$P_O \frac{\text{Sin}[k_n]}{(1 + a)}$
$Y_n(t)$	$\frac{P_O}{M_n a_n^2} \frac{\text{Sin}[k_n]}{(1 + a)} (1 - \text{Cos}[a_n t])$
$v(1, t)$	$\frac{P_O}{(1 + a)^2} \sum_{n=1}^m \frac{\text{Sin}^2[k_n]}{M_n a_n^2} (1 - \text{Cos}[a_n t])$
For the form:	$\text{Sin}^2[ah + b]$
a_n	$\sqrt{k_n^2 - a^2}$
$V_n(h)$	$\frac{\text{Sin}[k_n h]}{\text{Sin}[ah + b]}$
M_n	$\frac{c^2 r_O A_O}{4 k_n} (2 k_n - \text{Sin}[2 k_n])$
$P_n(t)$	$P_O \frac{\text{Sin}[k_n]}{\text{Sin}[a + b]}$
$Y_n(t)$	$\frac{P_O}{M_n a_n^2} \frac{\text{Sin}[k_n]}{\text{Sin}[a + b]} (1 - \text{Cos}[a_n t])$
$v(1, t)$	$\frac{P_O}{\text{Sin}^2[a + b]} \sum_{n=1}^m \frac{\text{Sin}^2[k_n]}{M_n a_n^2} (1 - \text{Cos}[a_n t])$
For the form:	$e^{-a h}$
a_n	$\sqrt{k_n^2 + \frac{a^2}{4}}$
$V_n(h)$	$e^{\frac{a}{2} h} \text{Sin}[k_n h]$
M_n	$\frac{c^2 r_O A_O}{4 k_n} (2 k_n - \text{Sin}[2 k_n])$
$P_n(t)$	$P_O e^{a/2} \text{Sin}[k_n]$
$Y_n(t)$	$\frac{P_O}{M_n a_n^2} \text{Sin}[k_n] e^{a/2} (1 - \text{Cos}[a_n t])$
$v(1, t)$	$P_O e^a \sum_{n=1}^m \frac{\text{Sin}^2[k_n]}{M_n a_n^2} (1 - \text{Cos}[a_n t])$

Table 3.11. Mode-superposition analysis expressions for cosine type force loading

For the form:	$(1 + a h)^2$
a_n	k_n
$V_n(h)$	$\frac{\text{Sin}[k_n h]}{(1 + a h)}$
M_n	$\frac{c^2 r_O A_O}{4 k_n} (2 k_n - \text{Sin}[2 k_n])$
$P_n(t)$	$P_O (1 - \text{Cos}[g t]) \frac{\text{Sin}[k_n]}{(1 + a)}$
$Y_n(t)$	$\frac{P_O}{M_n a_n} \frac{\text{Sin}[k_n]}{(1 + a)} \left(\frac{1 - \text{Cos}[a_n t]}{a_n} + \frac{a_n (\text{Cos}[a_n t] - \text{Cos}[g t])}{a_n - g^2} \right)$
$v(1, t)$	$\frac{P_O}{(1 + a)^2} \sum_{n=1}^m \frac{\text{Sin}^2[k_n]}{M_n a_n} \left(\frac{1 - \text{Cos}[a_n t]}{a_n} + \frac{a_n (\text{Cos}[a_n t] - \text{Cos}[g t])}{a_n - g^2} \right)$
For the form:	$\text{Sin}^2[ah + b]$
a_n	$\sqrt{k_n^2 - a^2}$
$V_n(h)$	$\frac{\text{Sin}[k_n h]}{\text{Sin}[ah + b]}$
M_n	$\frac{c^2 r_O A_O}{4 k_n} (2 k_n - \text{Sin}[2 k_n])$
$P_n(t)$	$P_O (1 - \text{Cos}[g t]) \frac{\text{Sin}[k_n]}{\text{Sin}[a + b]}$
$Y_n(t)$	$\frac{P_O}{M_n a_n} \frac{\text{Sin}[k_n]}{\text{Sin}[a + b]} \left(\frac{1 - \text{Cos}[a_n t]}{a_n} + \frac{a_n (\text{Cos}[a_n t] - \text{Cos}[g t])}{a_n - g^2} \right)$
$v(1, t)$	$\frac{P_O}{\text{Sin}^2[a + b]} \sum_{n=1}^m \frac{\text{Sin}^2[k_n]}{M_n a_n} \left(\frac{1 - \text{Cos}[a_n t]}{a_n} + \frac{a_n (\text{Cos}[a_n t] - \text{Cos}[g t])}{a_n - g^2} \right)$
For the form:	e^{-ah}
a_n	$\sqrt{k_n^2 + a^2 / 4}$
$V_n(h)$	$\frac{a}{e^2} \text{Sin}[k_n h]$
M_n	$\frac{c^2 r_O A_O}{4 k_n} (2 k_n - \text{Sin}[2 k_n])$
$P_n(t)$	$P_O (1 - \text{Cos}[g t]) e^{a/2} \text{Sin}[k_n]$
$Y_n(t)$	$\frac{P_O}{M_n a_n} \text{Sin}[k_n] e^{a/2} \left(\frac{1 - \text{Cos}[a_n t]}{a_n} + \frac{a_n (\text{Cos}[a_n t] - \text{Cos}[g t])}{a_n - g^2} \right)$
$v(1, t)$	$P_O e^a \sum_{n=1}^m \frac{\text{Sin}^2[k_n]}{M_n a_n} \left(\frac{1 - \text{Cos}[a_n t]}{a_n} + \frac{a_n (\text{Cos}[a_n t] - \text{Cos}[g t])}{a_n - g^2} \right)$

Table 3.12. Mode-superposition analysis expressions for exp. type force loading

For the form:	$(1 + a h)^2$
a_n	k_n
$V_n(h)$	$\frac{\text{Sin}[k_n h]}{(1 + a h)}$
M_n	$\frac{c^2 r_O A_O}{4 k_n} (2 k_n - \text{Sin}[2 k_n])$
$P_n(t)$	$P_O (1 - e^{-gt}) \frac{\text{Sin}[k_n]}{(1 + a)}$
$Y_n(t)$	$\frac{P_O \text{Sin}[k_n]}{M_n a_n (1 + a)} \left(\frac{a_n^2 - e^{-gt} a_n^2 + g^2 - g^2 \text{Cos}[a_n t] - a_n g \text{Sin}[a_n t]}{a_n (a_n + g^2)} \right)$
$v(1, t)$	$\frac{P_O}{(1 + a)^2} \sum_{n=1}^m \frac{\text{Sin}^2[k_n]}{M_n a_n^2} \left(\frac{a_n^2 - e^{-gt} a_n^2 + g^2 - g^2 \text{Cos}[a_n t] - a_n g \text{Sin}[a_n t]}{a_n + g^2} \right)$
For the form:	$\text{Sin}^2[ah + b]$
a_n	$\sqrt{k_n^2 - a^2}$
$V_n(h)$	$\frac{\text{Sin}[k_n h]}{\text{Sin}[ah + b]}$
M_n	$\frac{c^2 r_O A_O}{4 k_n} (2 k_n - \text{Sin}[2 k_n])$
$P_n(t)$	$P_O (1 - e^{-gt}) \frac{\text{Sin}[k_n]}{\text{Sin}[a + b]}$
$Y_n(t)$	$\frac{2 P_O \text{Sin}[k_n]}{M_n a_n \text{Sin}[a + b]} \left(\frac{a_n^2 - e^{-gt} a_n^2 + g^2 - g^2 \text{Cos}[a_n t] - a_n g \text{Sin}[a_n t]}{a_n (a_n + g^2)} \right)$
$v(1, t)$	$\frac{P_O}{\text{Sin}^2[a + b]} \sum_{n=1}^m \frac{\text{Sin}^2[k_n]}{M_n a_n^2} \left(\frac{a_n^2 - e^{-gt} a_n^2 + g^2 - g^2 \text{Cos}[a_n t] - a_n g \text{Sin}[a_n t]}{a_n + g^2} \right)$
For the form:	e^{-ah}
a_n	$\sqrt{k_n^2 + a^2 / 4}$
$V_n(h)$	$e^{\frac{a}{2} h} \text{Sin}[k_n h]$
M_n	$\frac{c^2 r_O A_O}{4 k_n} (2 k_n - \text{Sin}[2 k_n])$
$P_n(t)$	$P_o (1 - e^{-gt}) e^{a/2} \text{Sin}[k_n]$
$Y_n(t)$	$\frac{P_o \text{Sin}[k_n]}{M_n a_n} e^{a/2} \left(\frac{a_n^2 - e^{-gt} a_n^2 + g^2 - g^2 \text{Cos}[a_n t] - a_n g \text{Sin}[a_n t]}{a_n (a_n + g^2)} \right)$
$v(1, t)$	$P_o e^a \sum_{n=1}^m \frac{\text{Sin}^2[k_n]}{M_n a_n^2} \left(\frac{a_n^2 - e^{-gt} a_n^2 + g^2 - g^2 \text{Cos}[a_n t] - a_n g \text{Sin}[a_n t]}{a_n (a_n + g^2)} \right)$

3.5 Free Vibration Analysis of FGM Beam

A functionally graded beam of constant thickness of “h” with rectangular cross-sectional dimensions “L” and unit depth is considered and shown in Figure 3.4. A Cartesian coordinate system $O(x,y,z)$ is defined on the bottom axis of the beam, where the x-axis is taken along the bottom axis, the y-axis in the width direction and the z-axis in the depth direction. The nomenclature developed by (Sankar, 2001) will be closely followed. It is assumed that the Young’s modulus of FG beam varies through the thickness according to exponential form. The exponential form is given by

$$E(z) = E_b \text{Exp}\left[I \frac{z}{h}\right], \quad I = \text{Log}\left[\frac{E_t}{E_b}\right], \quad E_t / E_b = r_t / r_b \quad (3.240)$$

where E_t, E_b and r_t, r_b denote values of the elasticity modulus and density at the top and bottom of the beam. A typical material used in applications is metal-ceramic FGM. According to this distribution, bottom surface ($z=0$) of functionally graded beam is pure metal, whereas the top surface ($z=h$) is pure ceramics. Figure 3.5 shows the variation of Young’s modulus of metal in the thickness direction of FG beam. In this thesis we analyze the free vibration analysis of FG beams using plane strain elasticity. The results will then be compared to those from beam theories.

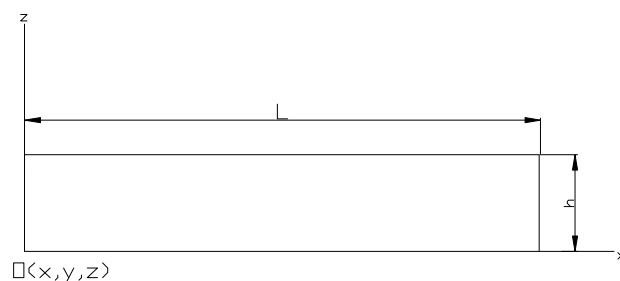


Figure 3.4. A FGM beam

3.5.1 Elasticity Analysis

The beam is assumed to be in a state of plane strain normal to the xz plane, and the width in the y -direction is taken as unity. The boundary conditions are similar to that of a simply supported beam. The upper and lower surfaces are completely free of tractions.

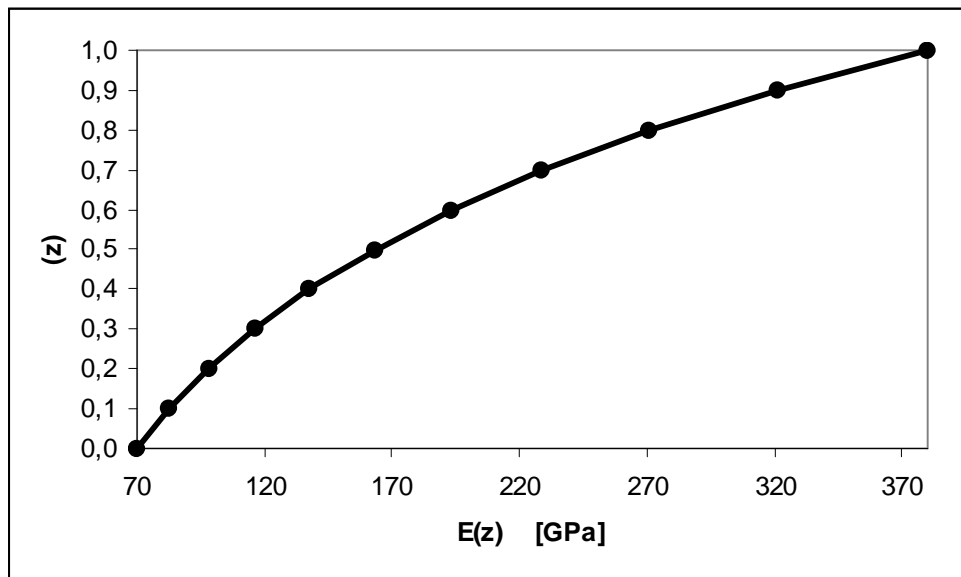


Figure 3.5. Variation of Young's modulus in the thickness direction.

The differential equations of equilibrium are:

$$\frac{\partial s_{xx}}{\partial x} + \frac{\partial t_{xz}}{\partial z} = r(z) \frac{\partial^2 u}{\partial t^2} \quad (3.241)$$

$$\frac{\partial t_{xz}}{\partial x} + \frac{\partial s_{zz}}{\partial z} = r(z) \frac{\partial^2 w}{\partial t^2} \quad (3.242)$$

Assuming that the material is orthotropic at every point and also that the principal material directions coincide with the x and z axes, the constitutive relations are:

$$\begin{Bmatrix} \mathbf{s}_{xx} \\ \mathbf{s}_{zz} \\ \mathbf{t}_{xz} \end{Bmatrix} = \begin{bmatrix} c_{11} & c_{13} & 0 \\ c_{13} & c_{33} & 0 \\ 0 & 0 & c_{55} \end{bmatrix} \begin{Bmatrix} \mathbf{e}_{xx} \\ \mathbf{e}_{zz} \\ \mathbf{g}_{xz} \end{Bmatrix} \quad (3.243)$$

Assuming that all elastic stiffness coefficients vary exponentially in the z direction, the elasticity matrix can be written as:

$$[c_{ij}(z)] = e^{\frac{Iz}{h}} \begin{bmatrix} c_{11}^0 & c_{13}^0 & 0 \\ c_{13}^0 & c_{33}^0 & 0 \\ 0 & 0 & c_{55}^0 \end{bmatrix} \quad (3.244)$$

where $c_{ij}^0 = c_{ij}(0)$. Substituting from Eq.(3.243) into (3.241) and (3.242), than using strain-displacement relations we obtain the following two equations in $u(x,z,t)$ and $w(x,z,t)$:

$$\frac{\partial}{\partial x} \left(c_{11} \frac{\partial u}{\partial x} + c_{13} \frac{\partial w}{\partial z} \right) + \frac{\partial}{\partial z} \left(c_{55} \frac{\partial u}{\partial z} + c_{55} \frac{\partial w}{\partial x} \right) = r(z) \frac{\partial^2 u}{\partial t^2} \quad (3.245)$$

$$\frac{\partial}{\partial x} \left(c_{55} \frac{\partial u}{\partial z} + c_{55} \frac{\partial w}{\partial x} \right) + \frac{\partial}{\partial z} \left(c_{13} \frac{\partial u}{\partial x} + c_{33} \frac{\partial w}{\partial z} \right) = r(z) \frac{\partial^2 w}{\partial t^2} \quad (3.246)$$

where $r(z) = r_b e^{\frac{Iz}{h}}$. We will assume solutions of the form:

$$\begin{aligned} u(x, z, t) &= U(z, t) \cos[\mathbf{x} x] \\ w(x, z, t) &= W(z, t) \sin[\mathbf{x} x] \end{aligned} \quad (3.247)$$

where $\mathbf{x} = n\mathbf{p} / L$.

From the forms of the displacements one can note that the boundary conditions at the left and right end faces of the beam are given by:

$$\begin{aligned}
w(0, z, t) = w(L, z, t) = 0 \\
S_{xx}(0, z, t) = S_{xx}(L, z, t) = 0
\end{aligned} \tag{3.248}$$

which is typical of simply supported beams. Substituting from Eqs. (3.244) and (3.247) into Eqs. (3.245) and (3.246) we obtain a pair of ordinary differential equations for $U(z,t)$ and $W(z,t)$:

$$\begin{aligned}
-c_{11}^0 U x^2 + c_{13}^0 x W' + \frac{I}{h} c_{55}^0 U' + c_{55}^0 U'' + x c_{55}^0 \frac{I}{h} W \\
+ x c_{55}^0 W' = r_b{}^{oo} U
\end{aligned} \tag{3.249}$$

$$\begin{aligned}
-c_{55}^0 U' x - c_{55}^0 W x^2 - c_{13}^0 x \frac{I}{h} U - c_{13}^0 x U' + c_{33}^0 \frac{I}{h} W' \\
+ c_{33}^0 W'' = r_b{}^{oo} W
\end{aligned} \tag{3.250}$$

where $(.)' \equiv \frac{\partial(.)}{\partial z}$ and $(.)^o \equiv \frac{\partial(.)}{\partial t}$.

Taking the Laplace transforms of Eqs. (3.249) and (3.250) yields

$$\begin{aligned}
-c_{11}^0 \bar{U} x^2 + c_{13}^0 x \bar{W}' + \frac{I}{h} c_{55}^0 \bar{U}' + c_{55}^0 \bar{U}'' + x c_{55}^0 \frac{I}{h} \bar{W} \\
+ x c_{55}^0 \bar{W}' - r_b p^2 \bar{U} = 0
\end{aligned} \tag{3.251}$$

$$\begin{aligned}
-c_{55}^0 \bar{U}' x - c_{55}^0 \bar{W} x^2 - c_{13}^0 x \frac{I}{h} \bar{U} - c_{13}^0 x \bar{U}' + c_{33}^0 \frac{I}{h} \bar{W}' \\
+ c_{33}^0 \bar{W}'' - r_b p^2 \bar{W} = 0
\end{aligned} \tag{3.252}$$

where $\bar{U}(z, p) = L\{U(z, t)\}$ and $\bar{W}(z, p) = L\{W(z, t)\}$, p being the complex Laplace parameter.

To simplify the calculations, we will assume that the FGM is isotropic at every point. Further we will assume that the Poisson's ratio is a constant through the thickness. Then the variation of Young's modulus is given by $E(z) = E_b e^{1 \frac{z}{h}}$. The elasticity matrix $[c]$ is related to the Young's modulus and Poisson's ratio by:

$$[c] = \frac{E}{(1+\nu)(1-2\nu)} \begin{bmatrix} 1-\nu & \nu & 0 \\ \nu & 1-\nu & 0 \\ 0 & 0 & \frac{1-2\nu}{2} \end{bmatrix} \quad (3.253)$$

The solution of Eqs. (3.251) and (3.252) can be derived as:

$$\begin{aligned} \bar{U}(z, p) &= \sum_{i=1}^4 a_i e^{a(p)_i \frac{z}{h}} \\ \bar{W}(z, p) &= \sum_{i=1}^4 b_i e^{a(p)_i \frac{z}{h}} \end{aligned} \quad (3.254)$$

where a_i and b_i are arbitrary constants to be determined from the traction boundary conditions on the top and bottom surfaces, also at this stage free vibration analysis can easily be performed, the Laplace parameter p in Eqs. (3.251) and (3.252) are replaced by ib to get

$$\begin{aligned} a_i \left(-c_{11}^0 x^2 + \frac{l}{h} c_{55}^0 \frac{a(b)_i}{h} + c_{55}^0 \frac{a(b)_i^2}{h^2} + r_b b^2 \right) \\ + b_i \left(c_{13}^0 x \frac{a(b)_i}{h} + x c_{55}^0 \frac{l}{h} + x c_{55}^0 \frac{a(b)_i}{h} \right) = 0 \end{aligned} \quad (3.255)$$

$$\begin{aligned} a_i \left(-c_{55}^0 x \frac{a(b)_i}{h} - c_{13}^0 x \frac{l}{h} - c_{13}^0 x \frac{a(b)_i}{h} \right) + b_i \left(-c_{55}^0 x^2 \right. \\ \left. + c_{33}^0 \frac{l}{h} \frac{a(b)_i}{h} + c_{33}^0 \frac{a(b)_i^2}{h^2} + r_b b^2 \right) = 0 \end{aligned} \quad (3.256)$$

$a(b)_i$ are the roots of the characteristic equation for $a(b)$

$$\begin{vmatrix} A_{11} & A_{12} \\ A_{21} & A_{22} \end{vmatrix} = 0 \quad (3.257)$$

where

$$\begin{aligned} A_{11} &= -c_{11}^0 x^2 + \frac{l}{h} c_{55}^0 \frac{a(b)_i}{h} + c_{55}^0 \frac{a(b)_i^2}{h^2} + r_b b^2 \\ A_{12} &= c_{13}^0 x \frac{a(b)_i}{h} + x c_{55}^0 \frac{l}{h} + x c_{55}^0 \frac{a(b)_i}{h} \\ A_{21} &= -c_{55}^0 x \frac{a(b)_i}{h} - c_{13}^0 x \frac{l}{h} - c_{13}^0 x \frac{a(b)_i}{h} \\ A_{22} &= -c_{55}^0 x^2 + c_{33}^0 \frac{l}{h} \frac{a(b)_i}{h} + c_{33}^0 \frac{a(b)_i^2}{h^2} + r_b b^2 \end{aligned} \quad (3.258)$$

Note that the characteristic equation (3.257) is a quadratic equation in $a(b)$ and will result in four roots, and that is why we have four terms in the complementary solution given in Eq.(3.254). The arbitrary constants a_i and b_i are related by

$$r_i = \frac{b_i}{a_i} = - \frac{-c_{11}^0 x^2 + \frac{l}{h} c_{55}^0 \frac{a(b)_i}{h} + c_{55}^0 \frac{a(b)_i^2}{h^2} + r_b b^2}{c_{13}^0 x \frac{a(b)_i}{h} + x c_{55}^0 \frac{l}{h} + x c_{55}^0 \frac{a(b)_i}{h}} \quad (3.259)$$

The four arbitrary constants a_i can be found from the traction boundary conditions on the top and bottom surface of the beam:

$$\begin{aligned}
t_{xz}(x,0,t) &= c_{55} \left. \frac{\partial u}{\partial z} \right|_{z=0} + c_{55} \left. \frac{\partial w}{\partial x} \right|_{z=0} = 0 \\
t_{xz}(x,h,t) &= c_{55} \left. \frac{\partial u}{\partial z} \right|_{z=h} + c_{55} \left. \frac{\partial w}{\partial x} \right|_{z=h} = 0 \\
s_{zz}(x,0,t) &= c_{13} \left. \frac{\partial u}{\partial x} \right|_{z=0} + c_{33} \left. \frac{\partial w}{\partial z} \right|_{z=0} = 0 \\
s_{zz}(x,h,t) &= c_{13} \left. \frac{\partial u}{\partial x} \right|_{z=h} + c_{33} \left. \frac{\partial w}{\partial z} \right|_{z=h} = 0
\end{aligned} \tag{3.260}$$

Substituting for u and w from Eq. (3.248), we obtain the BCs in terms of U and W :

$$\begin{aligned}
U'(0,t) + \alpha W(0,t) &= 0 \\
U'(h,t) + \alpha W(h,t) &= 0 \\
-c_{13}^0 \alpha U(0,t) + c_{33}^0 W'(0,t) &= 0 \\
-c_{13}^h \alpha U(h,t) + c_{33}^h W'(h,t) &= 0
\end{aligned} \tag{3.261}$$

where $c_{ij}^h = c_{ij}(h)$. Taking the Laplace transform of Eq. (3.261) to get

$$\begin{aligned}
\bar{U}'(0,p) + \alpha \bar{W}(0,p) &= 0 \\
\bar{U}'(h,p) + \alpha \bar{W}(h,p) &= 0 \\
-c_{13}^0 \alpha \bar{U}(0,p) + c_{33}^0 \bar{W}'(0,p) &= 0 \\
-c_{13}^h \alpha \bar{U}(h,p) + c_{33}^h \bar{W}'(h,p) &= 0
\end{aligned} \tag{3.262}$$

Substituting for U and W from Eqs. (3.254) into (3.262) and replaced Laplace parameter p with ib , we obtain four equations for a_i :

$$\begin{aligned}
\sum_{i=1}^4 a_i \left(\frac{\mathbf{a}(b)_i}{h} + \mathbf{x} r_i \right) &= 0 \\
\sum_{i=1}^4 a_i \left(\frac{\mathbf{a}(b)_i}{h} + \mathbf{x} r_i \right) e^{a(b)_i} &= 0 \\
\sum_{i=1}^4 a_i \left(-c_{13}^0 \mathbf{x} + c_{33}^0 r_i \frac{\mathbf{a}(b)_i}{h} \right) &= 0 \\
\sum_{i=1}^4 a_i \left(-c_{13}^0 \mathbf{x} + c_{33}^0 r_i \frac{\mathbf{a}(b)_i}{h} \right) e^{a(b)_i} e^l &= 0
\end{aligned} \tag{3.263}$$

Eq. (3.263) can be written as

$$\begin{vmatrix} S_{11} & S_{12} & S_{13} & S_{14} \\ S_{21} & S_{22} & S_{23} & S_{24} \\ S_{31} & S_{32} & S_{33} & S_{34} \\ S_{41} & S_{42} & S_{43} & S_{44} \end{vmatrix} \begin{vmatrix} a_1 \\ a_2 \\ a_3 \\ a_4 \end{vmatrix} = 0 \tag{3.264}$$

in which S_{ij} represents constants which includes b . For finding free vibration frequencies, the determinant of constant matrix S_{ij} is set equal to zero.

In the present work, since the beam is modelled as a continuum, infinitely many frequencies may be obtained. Table 3.13 shows the first ten natural frequencies for FGM beam with $\nu=0.3$, $r_b = 2707 \text{ kg/m}^3$, $E_b = 70 \text{ GPa}$, $L/h=5,10,20$ and $n=1,3,5$.

3.5.2. Mode Shapes

$\mathbf{a}(b)$ values related to natural frequencies can be obtained from equation (3.257) in imaginary form.

$$\begin{aligned}
\mathbf{a}(b)_1 &= p_1 + q_1 i & , & & \mathbf{a}(b)_3 &= p_1 - q_1 i \\
\mathbf{a}(b)_2 &= p_2 + q_2 i & , & & \mathbf{a}(b)_4 &= p_2 - q_2 i
\end{aligned} \tag{3.265}$$

For obtaining the $a(b)$ values in real form, Eq.(3.254) is rewritten as

$$\begin{aligned}\bar{U}(z, p) &= a_1 e^{p_1 \frac{z}{h}} \cos[q_1 \frac{z}{h}] + a_3 e^{p_1 \frac{z}{h}} \sin[q_1 \frac{z}{h}] \\ &\quad + a_2 e^{p_2 \frac{z}{h}} \cos[q_2 \frac{z}{h}] + a_4 e^{p_4 \frac{z}{h}} \sin[q_2 \frac{z}{h}]\end{aligned}\quad (3.266)$$

$$\begin{aligned}\bar{W}(z, p) &= b_1 e^{p_1 \frac{z}{h}} \cos[q_1 \frac{z}{h}] + b_3 e^{p_1 \frac{z}{h}} \sin[q_1 \frac{z}{h}] \\ &\quad + b_2 e^{p_2 \frac{z}{h}} \cos[q_2 \frac{z}{h}] + b_4 e^{p_4 \frac{z}{h}} \sin[q_2 \frac{z}{h}]\end{aligned}$$

Substituting Eq.(3.266) into Eq.(3.251) and following the same steps as in the section 3.5.1, the values of a_i and b_i will be obtained. Mode shapes will be found for different values of “z” by using these constants.

Table 3.13. Exact natural frequencies for FGM beam, using elasticity theory.

L/h	20			10			5		
	1	3	5	1	3	5	1	3	5
Elasticity Theory (ET)	0,00893	0,07795	0,20497	0,03530	0,28538	0,67918	0,13516	0,90212	1,85277
	0,21179	0,63454	1,05460	0,42338	1,26295	1,76117	0,84503	1,92887	2,49016
	0,55681	0,96443	1,24508	0,78745	1,36391	2,45257	1,11363	2,90299	3,66944
	0,71326	1,32485	1,29714	0,81733	1,41712	3,40277	1,13311	3,67621	4,74260
	1,26934	2,68590	1,46068	1,28994	1,60791	4,50087	1,37701	4,50523	4,82574
	2,60600	4,73453	2,83432	2,63647	2,92917	5,91537	2,75253	6,14326	7,13686
	4,83398	5,22375	4,63721	4,78691	4,59607	7,55695	4,68378	7,57213	7,76168
	5,08512	7,54838	5,39989	5,14687	5,49558	9,76948	5,30891	9,89271	10,3736
	7,54940	9,49227	7,54730	7,54898	7,54725	10,1202	7,54775	10,1539	10,5149
	9,46614	10,0547	9,54357	9,47598	9,57814	12,6350	9,51486	12,6735	12,9128

3.5.3 Beam Theory

In the present thesis, free vibration of simply supported FG beams using classical beam theory (CBT) and parabolic shear deformation beam theory (PSDBT) and first order shear deformation beam theory (FSDBT) will also be given from the literature (Aydogdu and Taskin, 2007). Governing equations of FG beam for free vibration problem were found by applying Hamilton principle and Navier type solution method was used to solve vibration problem.

The state of stress in the beam is given by the generalised Hooke's law as follows:

$$s_x = Q_{11} e_x \quad , \quad t_{xz} = Q_{55} g_{xz} \quad (3.267)$$

where Q_{ij} are the transformed stiffness constants in the beam co-ordinate system and are defined as

$$Q_{11} = \frac{E(z)}{1-\nu^2} \quad , \quad Q_{55} = \frac{E(z)}{2(1+\nu^2)} \quad (3.268)$$

Assuming that the deformations of the beam are in the x-z plane and denoting the displacement components along the x, y and z-directions by U, V and W [Timarci and Soldatos, 1995]:

$$\begin{aligned} U(x, z, t) &= u(x, t) - z w_{,x} + \Phi(z) u_1(x, t) \\ V(x, z, t) &= 0 \\ W(x, z, t) &= w(x, t) \end{aligned} \quad (3.269)$$

It may be noted that u and w denotes the displacement of points on the bottom surfaces of the beam, and not points in the mid-plane. u_1 is an unknown function that represents the effect of transverse shear strain on the beam bottom surface, and

Φ represents the shape function determining the distribution of the transverse strain and stress through the thickness.

Classical beam theory is obtained as a particular case by taking the shape function as zero. Although different shape functions are applicable, only the ones which convert the present theory to the corresponding parabolic shear deformation beam theory (PSDBT) and first order shear deformation beam theory (FSDBT) are employed in the present thesis. This is achieved by choosing the shape function as follows:

$$\begin{aligned}
 CBT : \Phi(z) &= 0 \\
 FSDBT : \Phi(z) &= z \\
 PSDBT : \Phi(z) &= z(1 - 4z^2/3h^2)
 \end{aligned} \tag{3.270}$$

The displacement equations yields the following kinematic relations:

$$\begin{aligned}
 e_x &= u_{,x} - z w_{,xx} + \Phi(z) u_{1,x} \\
 g_{xz} &= \Phi'(z) u_1
 \end{aligned} \tag{3.271}$$

where a prime denotes the derivative with respect to z and “ x ” represents the partial derivative with respect to x . By substituting the stress-strain relations into the definitions of the force and moment resultants of the theory given in [Soldatos and Timarci, 1993] and using the notation given by [Soldatos and Sophocleous, 2001], the following constitutive equations are obtained:

$$\begin{bmatrix} N_x^c \\ M_x^c \\ M_x^a \end{bmatrix} = \begin{bmatrix} A_{11}^c & B_{11}^c & B_{11}^a \\ B_{11}^c & D_{11}^c & D_{11}^a \\ B_{11}^a & D_{11}^a & D_{11}^{aa} \end{bmatrix} \begin{bmatrix} u_{,x} \\ -w_{,xx} \\ u_{1,x} \end{bmatrix} \tag{3.272}$$

$$Q_x^a = A_{55}^a u_1 \tag{3.273}$$

The extensional, coupling and bending rigidities appearing in Eq. (3.272) are, respectively, defined as follows:

$$\begin{aligned}
 A_{11}^c &= \int_0^h Q_{11} dz \\
 (B_{11}^c, B_{11}^a) &= \int_0^h Q_{11} [z, \Phi(z)] dz \\
 (D_{11}^c, D_{11}^a, D_{11}^{aa}) &= \int_0^h Q_{11} [z^2, z \Phi(z), \Phi^2(z)] dz
 \end{aligned} \tag{3.274}$$

Moreover, the transverse shear rigidity appearing in Eq. (3.273) is defined according to

$$A_{55}^a = \int_0^h Q_{55} \Phi'(z)^2 dz \tag{3.275}$$

It should be pointed out that the extensional A_{11}^c , coupling B_{11}^c and bending D_{11}^c rigidities are the ones usually appearing even in the classical beam theories. Among the additional rigidities in Eq. (3.272), the one denoted as B_{11}^a is considered as additional coupling rigidity while the ones denoted as D_{11}^a and D_{11}^{aa} are considered as additional bending rigidities.

Upon employing the Hamilton's principle, the three variationally consistent equilibrium equations of the beam are obtained as:

$$\begin{aligned}
 N_{x,x}^c &= (r_0 u + r_{01} u_1 - r_1 w_{,x})_{,t} \\
 M_{x,xx}^c &= (r_1 u_{,x} + r_{11} u_{1,x} + r_0 w - r_2 w_{,xx})_{,t} \\
 M_{x,x}^a - Q_x^a &= (r_{01} u + r_{02} u_1 - r_{11} w_{,x})_{,t}
 \end{aligned} \tag{3.276}$$

Here, $_{,t}$ denotes time derivatives and the r 's are defined as:

$$r_i = \int_0^h r(z) z^i dz, \quad (i = 0,1,2)$$

$$r_{jm} = \int_0^h r(z) z^j \Phi_j^m(z) dz, \quad (j = 0,1; m = 1,2)$$
(3.277)

where $r(z) = r_b \text{Exp}[I \frac{z}{h}]$. The force and moment components are

$$(N_x^c, M_x^c) = \int_0^h \mathbf{s}_x(1, z) dz$$

$$Q_x^a = \int_0^h t_{xz} \Phi'(z) dz$$

$$M_x^a = \int_0^h \mathbf{s}_x \Phi(z) dz$$
(3.278)

Here, the appearance of the higher order moment M_x^a and the transverse shear force resultant Q_x^a in Eq.(3.278) is due to the particular form of the displacement field (3.269). In particular, the superscript “a” in these definitions is used only for a distinction between higher order transverse shear resultants and the corresponding conventional ones used in classical beam theory.

Moreover, the following sets of boundary conditions at the edges of the beam are obtained by the application of Hamilton’s principle: at $x=0,L$.

$$\text{Either } u \text{ or } N_x^c = \overline{N}_x \text{ prescribed,}$$

$$\text{Either } w \text{ or } M_{x,x}^c = \overline{Q}_x \text{ prescribed,}$$

$$\text{Either } w_{,x} \text{ or } M_x^c = \overline{M}_x \text{ prescribed,}$$

$$\text{Either } u_1 \text{ or } M_x^a = \overline{M}_x^a \text{ prescribed,}$$
(3.279)

Here, the over-barred quantities appearing in the right sides of natural boundary conditions denote prescribed force and moment resultants acting on the beam boundaries .

The simply supported boundary conditions are

$$N_x^c = w = M_x^c = M_x^a = 0 \quad (3.280)$$

Navier-type solutions to Eq. (3.276) that satisfy the boundary conditions Eq. (3.280) can be expressed in the form of

$$\begin{aligned} u &= A_n \cos\left[\frac{n\pi x}{L}\right] \sin[bt] \\ Lu_1 &= B_n \cos\left[\frac{n\pi x}{L}\right] \sin[bt] \\ w &= C_n \sin\left[\frac{n\pi x}{L}\right] \sin[bt] \end{aligned} \quad (3.281)$$

where “n” is the wave number in the x direction and A_n, B_n and C_n are undetermining coefficients. Inserting Eq. (3.281) in Eq. (3.276) leads to following problem.

$$\begin{vmatrix} K_{11} & K_{12} & K_{13} \\ K_{21} & K_{22} & K_{23} \\ K_{31} & K_{32} & K_{33} \end{vmatrix} \begin{vmatrix} A_n \\ B_n \\ C_n \end{vmatrix} = 0 \quad (3.282)$$

in which K_{ij} represents costants which includes b . For finding free vibration frequencies, the determinant of constant matrix K_{ij} is set equal to zero.

Table 3.14 shows the fundamental natural frequencies for FGM beam with $\nu=0.3$, $r_b = 2707 \text{ kg / m}^3$, $E_b = 70 \text{ GPa}$, $L/h=5,10,20$ and $n=1,3,5$.

Table 3.14. Natural frequencies for FGM beam from beam theories.

n	L/h	CBT	FSDBT	PSDBT	ET
1	5	0,141475	0,137088	0,141107	0.13516
	10	0,035745	0,035446	0,035720	0.03530
	20	0,00896	0,008941	0,008959	0.00893
3	5	1,151350	0,966028	1,134500	0.90212
	10	0,312914	0,293397	0,311228	0.28538
	20	0,08007	0,078611	0,079949	0.07795
5	5	2,737690	2,061590	2,681100	1.85277
	10	0,825849	0,718196	0,816126	0.67916
	20	0,219342	0,209255	0,218483	0.20497

The result from Elasticity Theory (ET) corresponding to “m” and “L/h” values used in beam theories are also included for comparison purposes.

4. RESULTS AND DISCUSSIONS

For non-uniform rods and heterogeneous rods, the end-point displacements will be calculated using the various methods outlined in previous sections and the results will be compared to assure the efficiency of the Laplace transform method as it is applied to the particular problem on hand.

The results are presented graphically using the following analyses for each loading type:

A1 (MSM): The resulting end-point displacement equations summarized in Table-3.10 to Table-3.12 are used directly.

A2 (DURBIN): Inverse Laplace transformation of the end-point displacement expressions given in Table-3.4 to Table-3.6 are obtained. Durbin's Inverse Transform Method is used to obtain the values in the time domain

A3 (RESIDUE): The numerical results obtained from Residue theorem summarized in Table-3.7 to Table-3.9 are used directly.

First ten frequencies have been taken in the calculations. Figs. 4.1 - 4.27 show the results for given variations subjected to dynamic loads $P_1(t) = P_0(1 - \cos[gt])$, $P_2(t) = P_0$ and $P_3(t) = P_0(1 - e^{-gt})$, respectively. A g value of 0.6 has been used throughout. Increasing a causes an increase in displacement. In all loading cases, for $a = 2$, a noticeable difference was present between the exact and MSM results. To achieve the accuracy of the exact results, up to a hundred frequencies were needed in MSM.

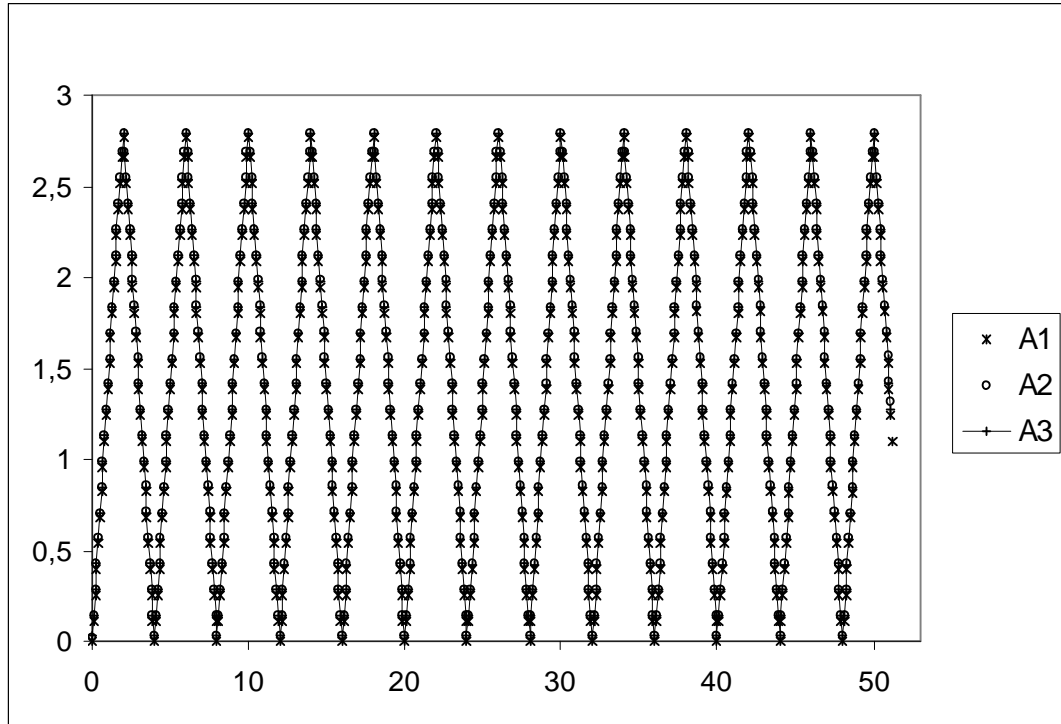


Figure 4.1. End Displacement for the form $\sin^2[ah + b]$ under $P_2(t) = P_0$, $a=0$, $m=10$.

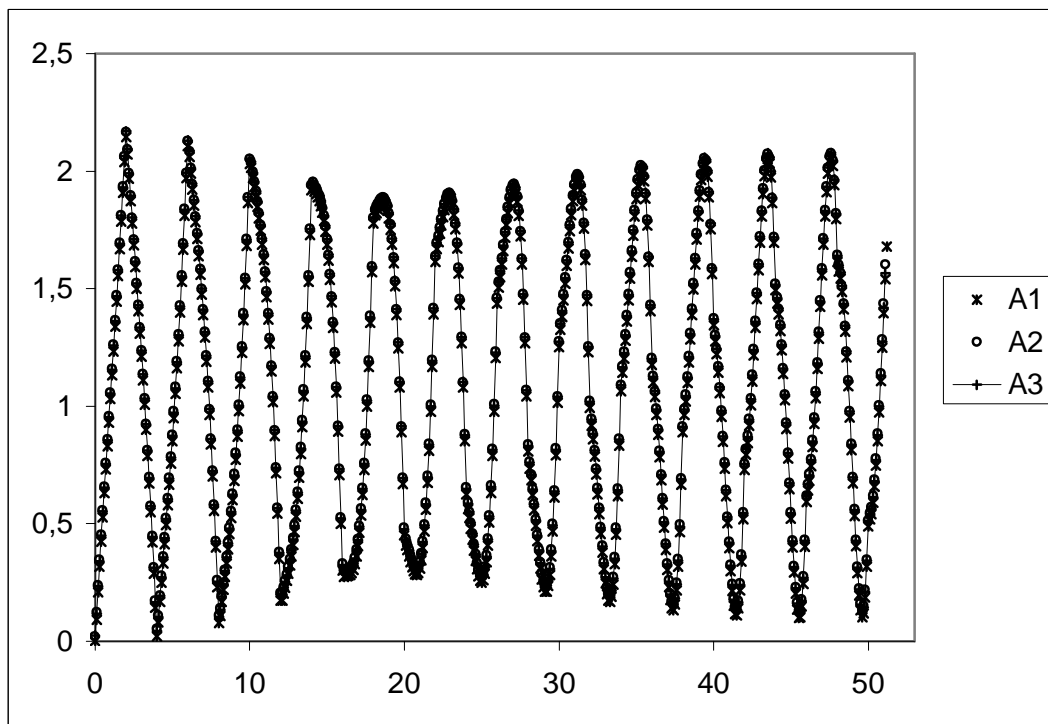


Figure 4.2. End Displacement for the form $\sin^2[ah + b]$ under $P_2(t) = P_0$, $a=1$, $m=10$.

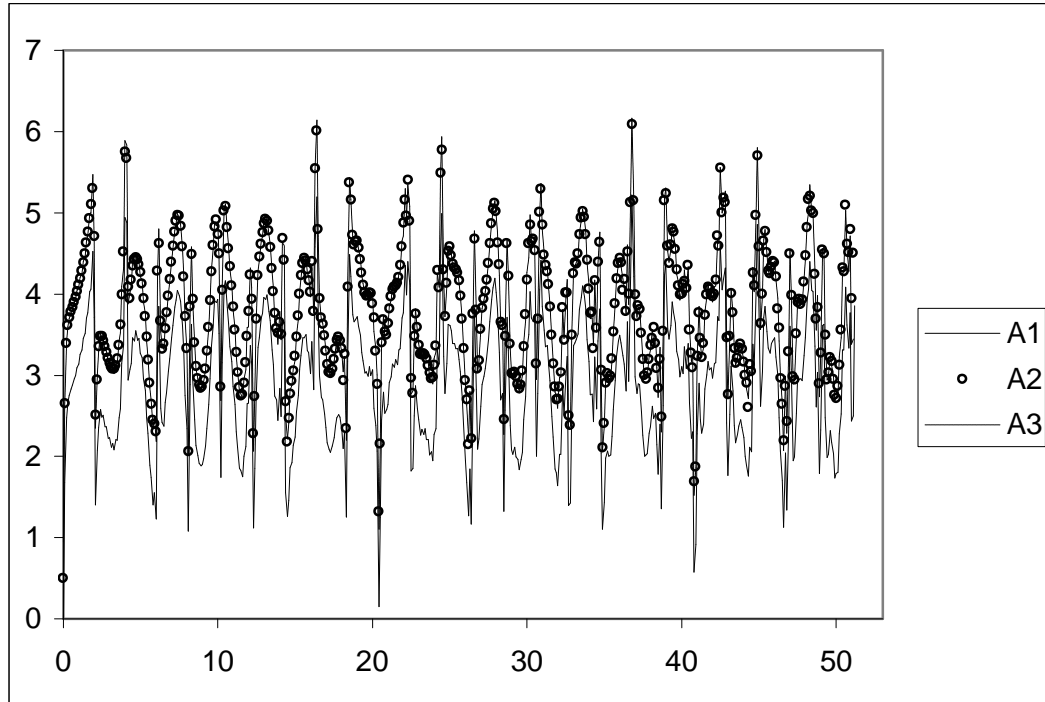


Figure 4.3. End Displacement for the form $\sin^2[ah + b]$ under $P_2(t) = P_0$, $a=2$, $m=10$.

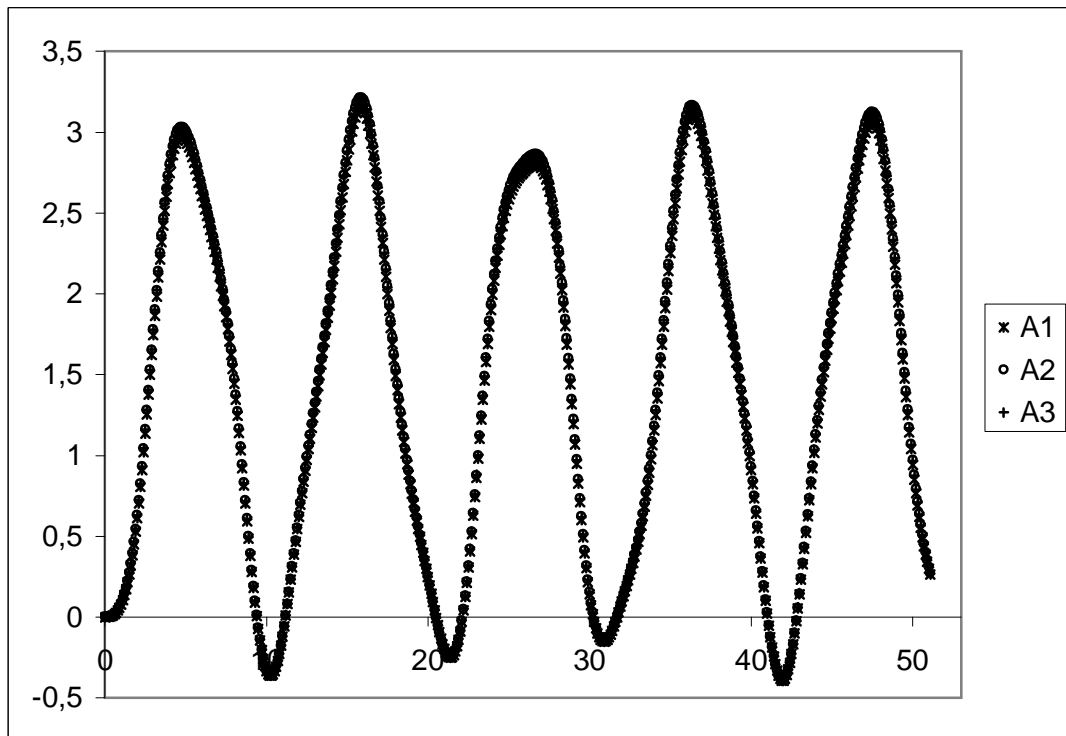


Figure 4.4. End displacement for the form $\sin^2[ah + b]$ under $P_1(t) = P_0(1 - \cos[gt])$, $a=0$, $m=10$, $g=0.6$.

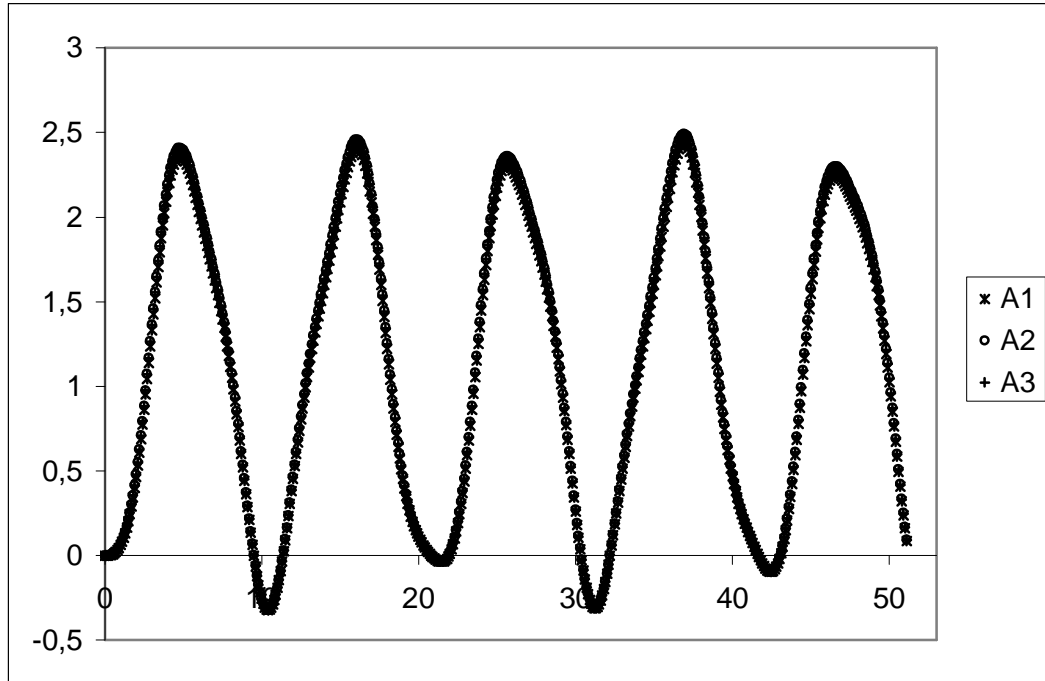


Figure 4.5. End displacement for the form $\sin^2[ah + b]$ under $P_1(t) = P_0(1 - \cos[gt])$, $a=1, m=10, g=0.6$.

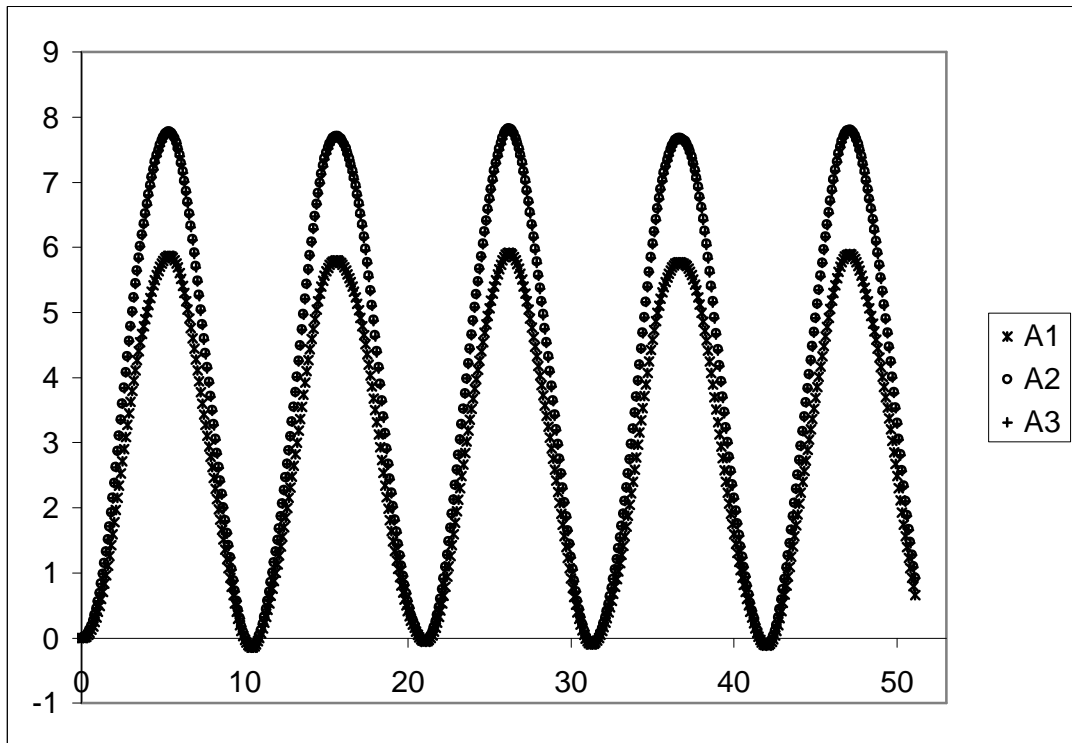


Figure 4.6. End displacement for the form $\sin^2[ah + b]$ under $P_1(t) = P_0(1 - \cos[gt])$, $a=2, m=10, g=0.6$.

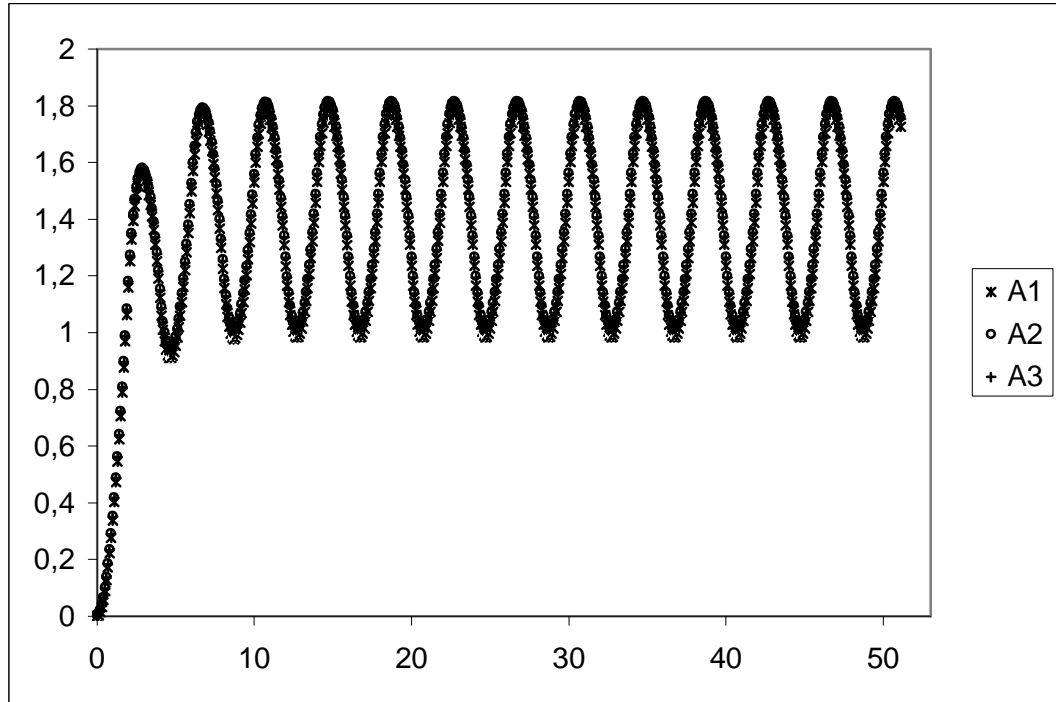


Figure 4.7. End displacement for the form $\sin^2[ah + b]$ under $P_3(t) = P_0(1 - e^{-gt})$, $a=0$, $m=10$, $g=0.6$.

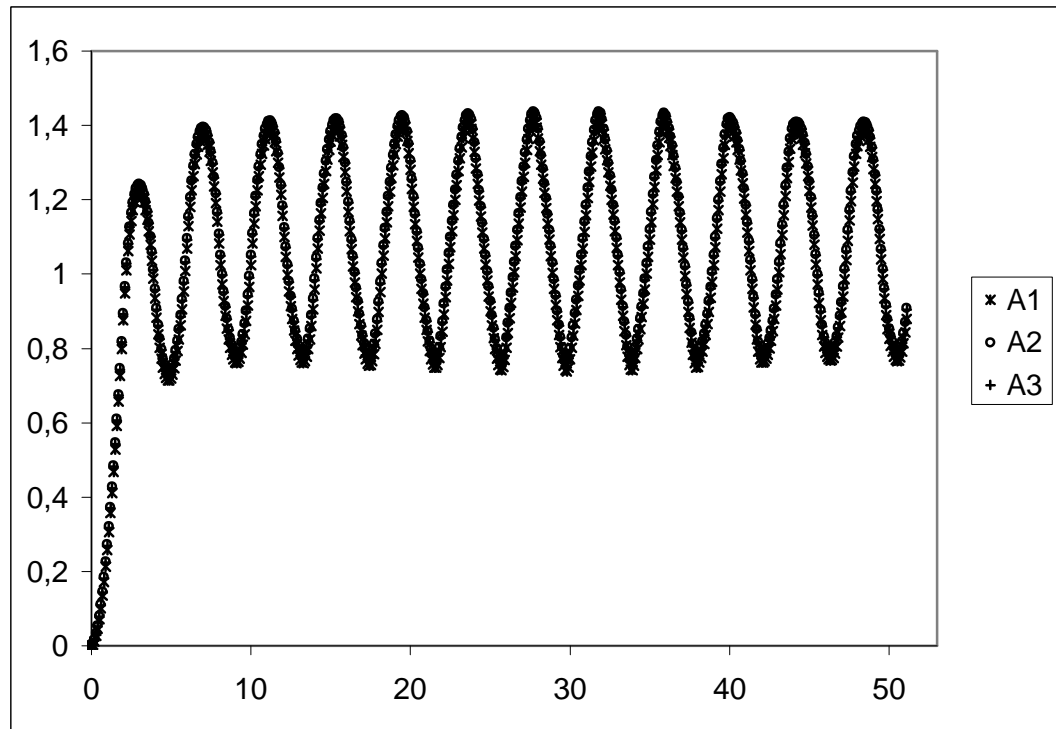


Figure 4.8. End displacement for the form $\sin^2[ah + b]$ under $P_3(t) = P_0(1 - e^{-gt})$, $a=1$, $m=10$, $g=0.6$.

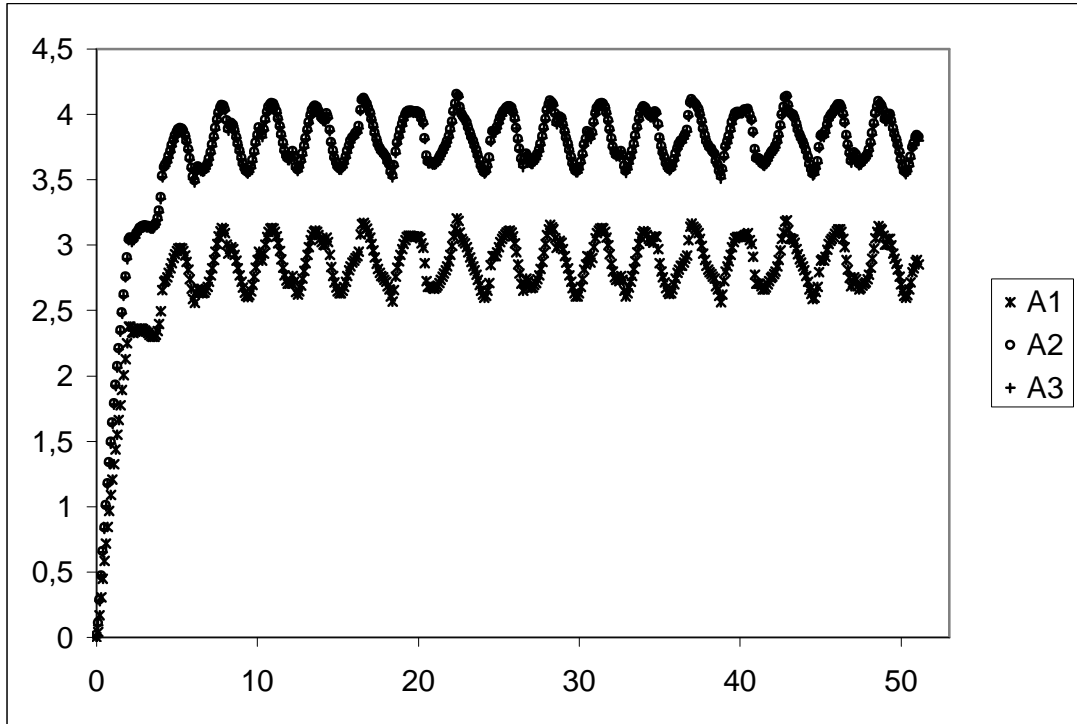


Figure 4.9. End displacement for the form $\sin^2[ah + b]$ under $P_3(t) = P_0(1 - e^{-gt})$, $a=2, m=10, g=0.6$.

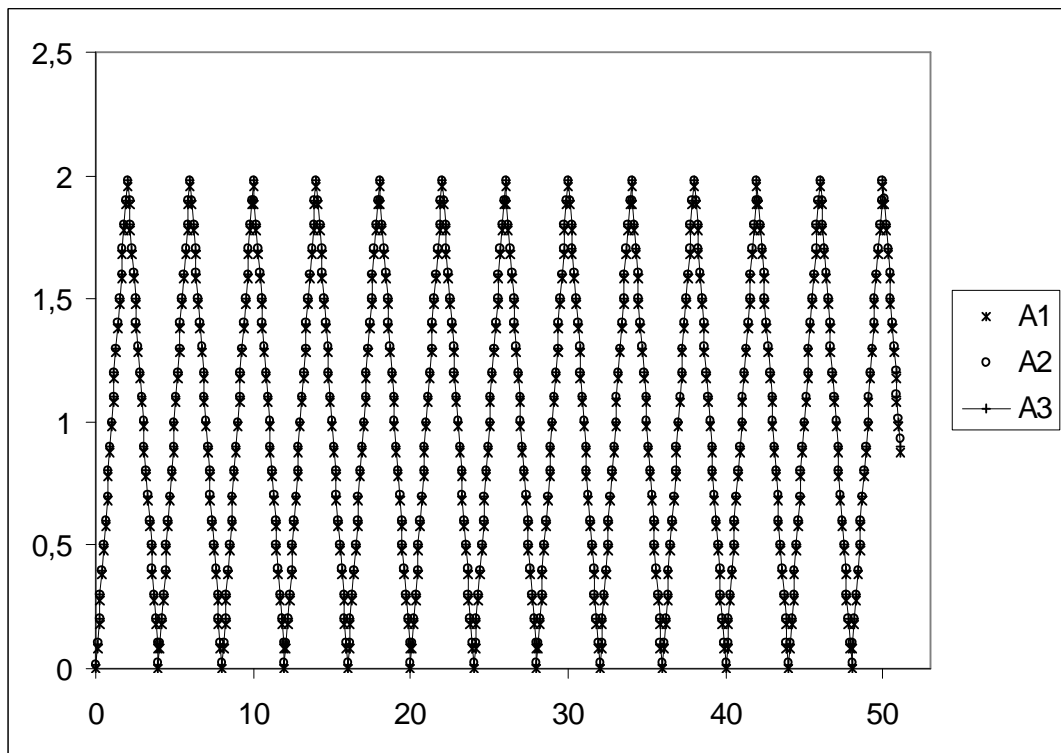


Figure 4.10. End displacement. for the form $(1 + ah)^2$ under $P_2(t) = P_0$, $a=0, m=10$.

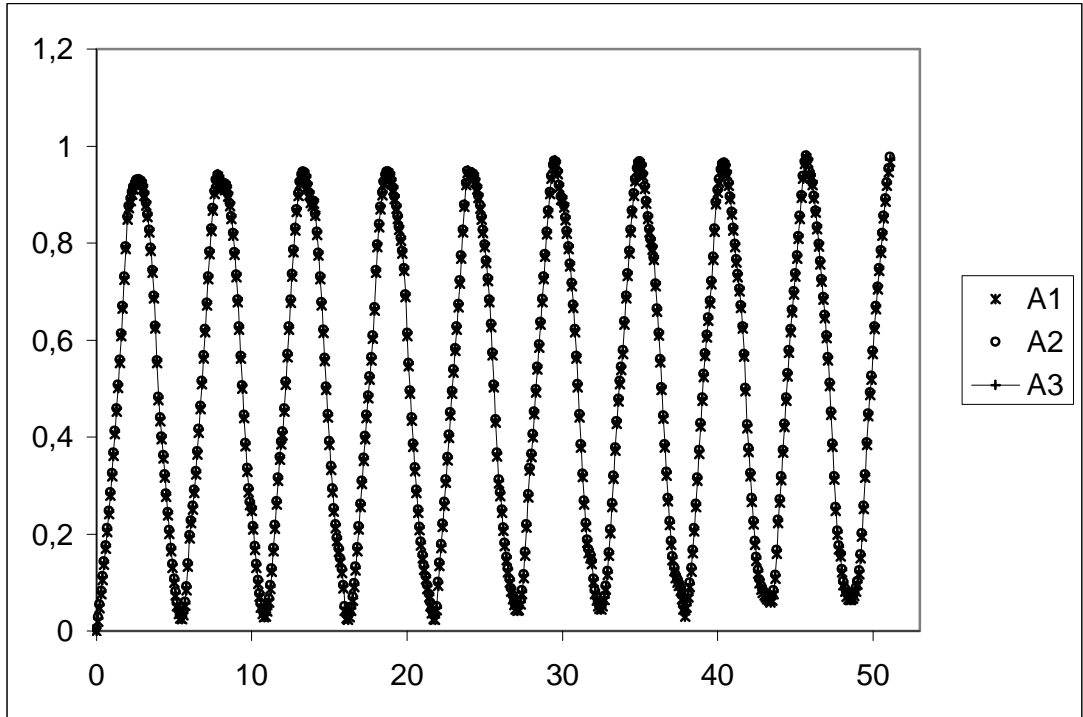


Figure 4.11. End displacement for the form $(1 + ah)^2$ under $P_2(t) = P_0$, $a=1$, $m=10$.

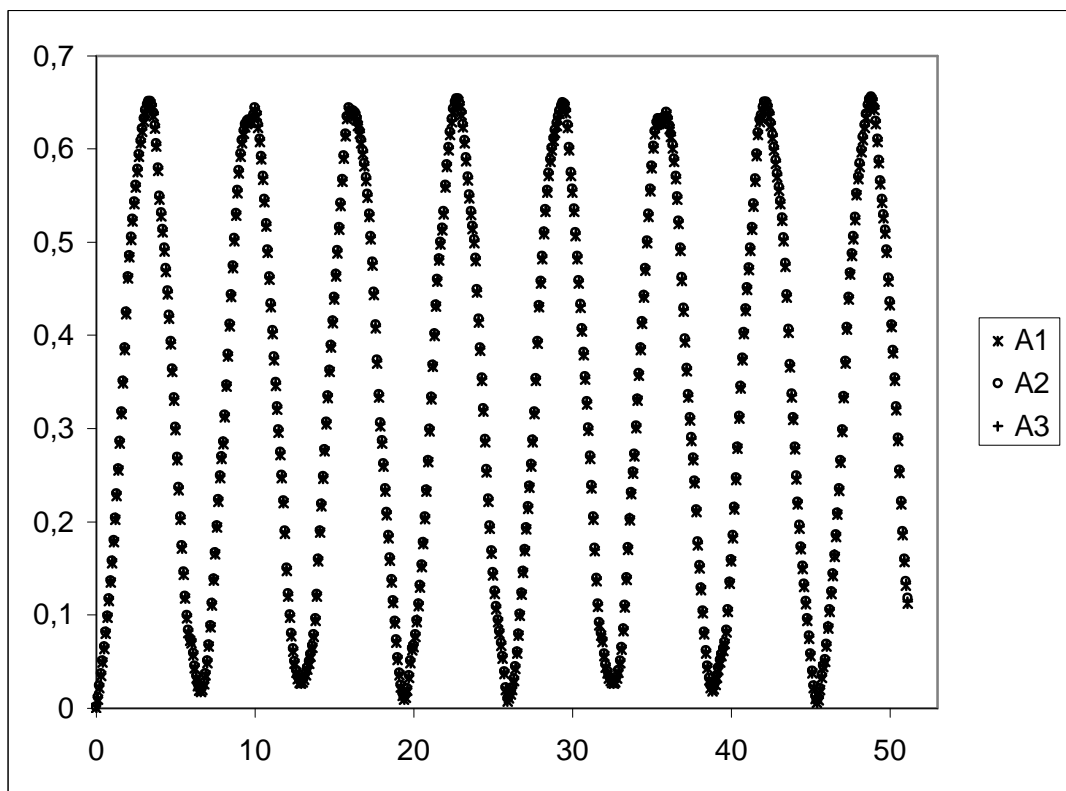


Figure 4.12. End displacement for the form $(1 + ah)^2$ under $P_2(t) = P_0$, $a=2$, $m=10$.

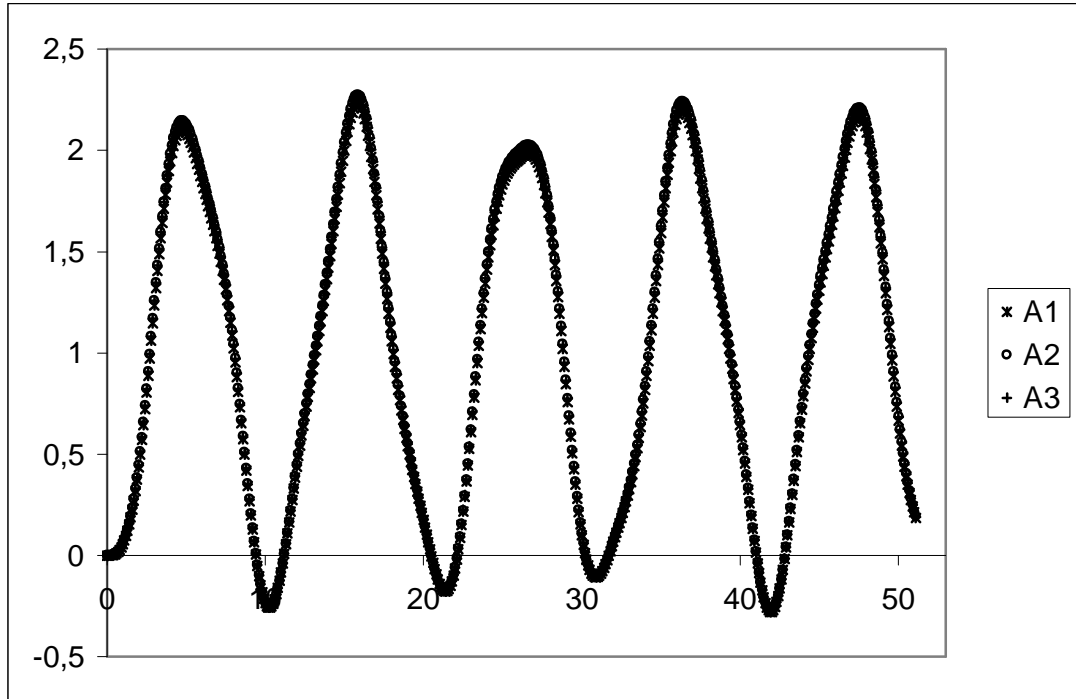


Figure 4.13. End displacement for the form $(1+ah)^2$ under $P_1(t) = P_0(1 - \cos[gt])$, $a=0$, $m=10$, $g=0.6$.

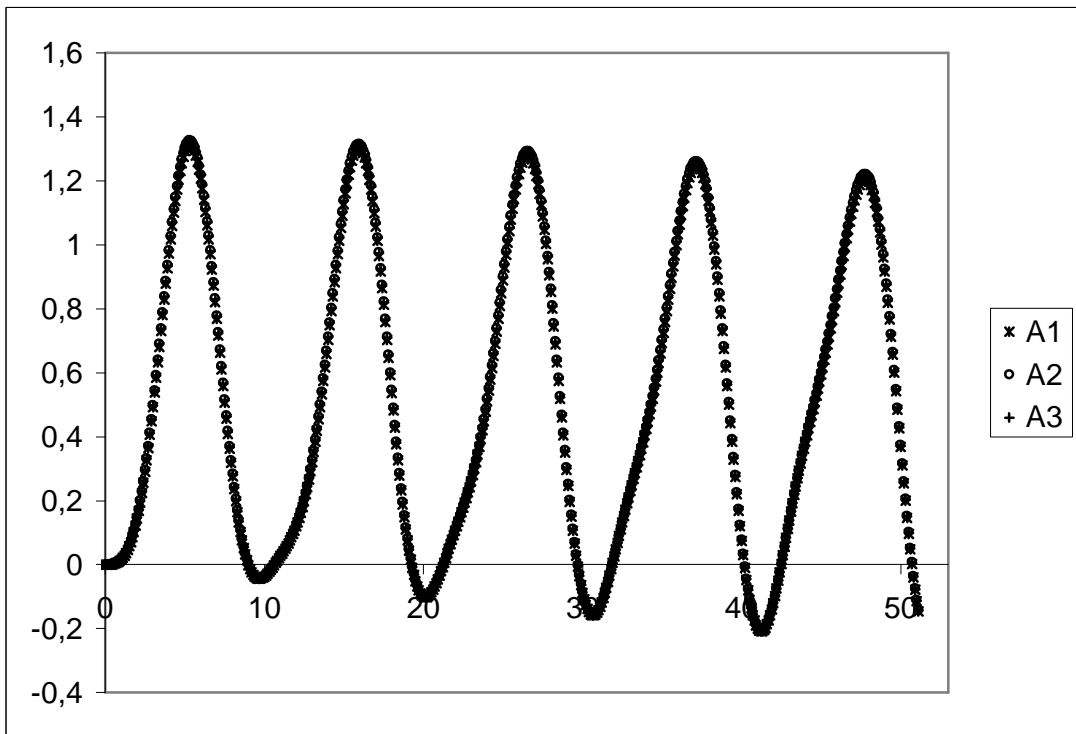


Figure 4.14. End displacement for the form $(1+ah)^2$ under $P_1(t) = P_0(1 - \cos[gt])$, $a=1$, $m=10$, $g=0.6$.

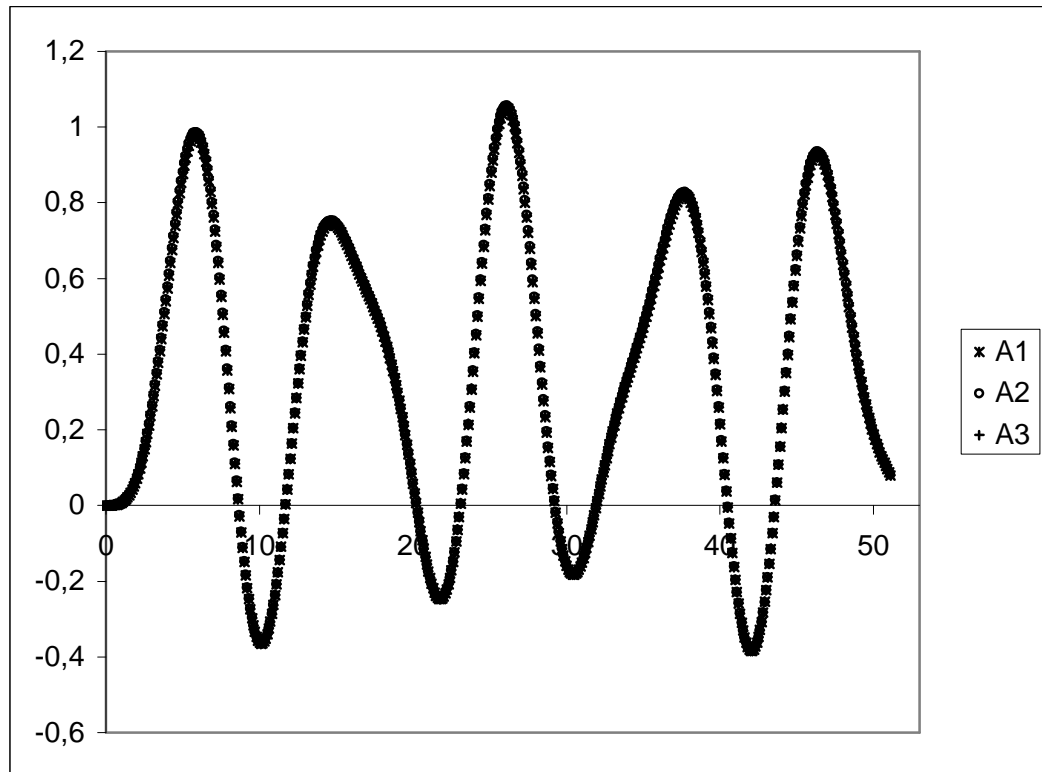


Figure 4.15. End displacement for the form $(1+ah)^2$ under $P_1(t) = P_0(1 - \cos[gt])$, $a=2$, $m=10$, $g=0.6$.

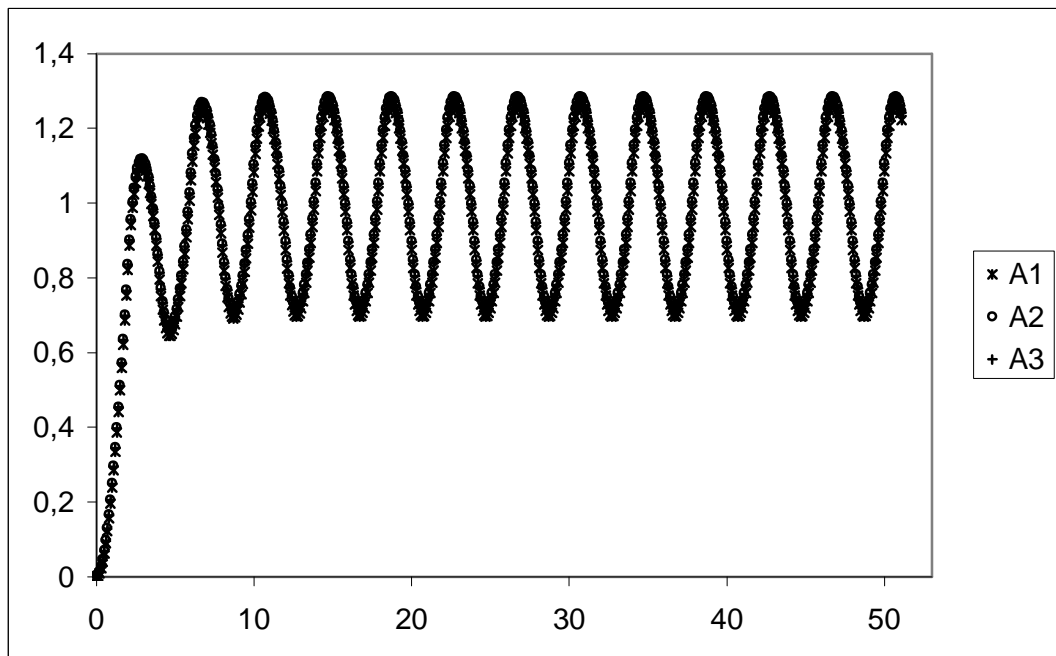


Figure 4.16. End displacement for the form $(1+ah)^2$ under $P_3(t) = P_0(1 - e^{-gt})$, $a=0$, $m=10$, $g=0.6$.

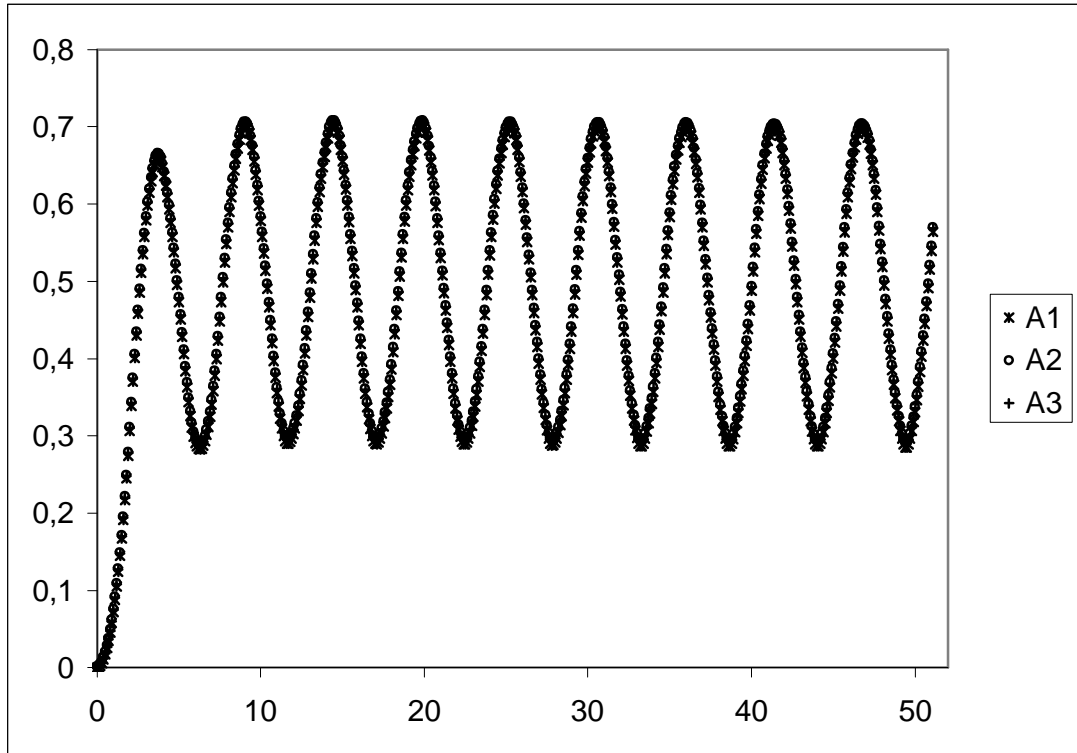


Figure 4.17. End displacement for the form $(1 + ah)^2$ under $P_3(t) = P_0(1 - e^{-gt})$, $a=1, m=10, g=0.6$.

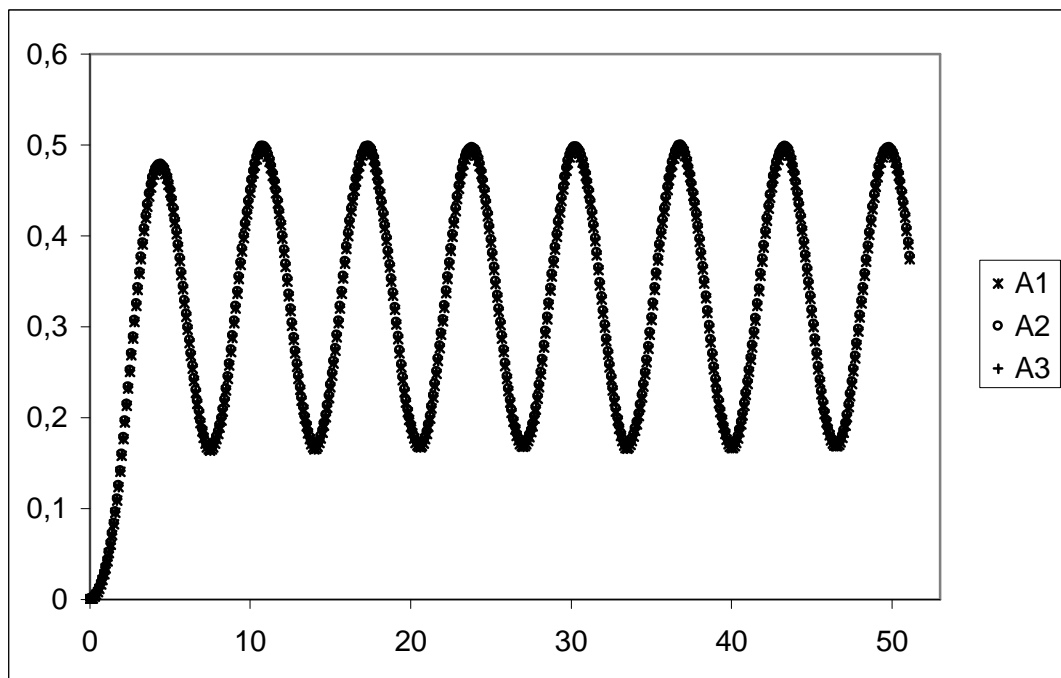


Figure 4.18. End displacement for the form $(1 + ah)^2$ under $P_3(t) = P_0(1 - e^{-gt})$, $a=2, m=10, g=0.6$.

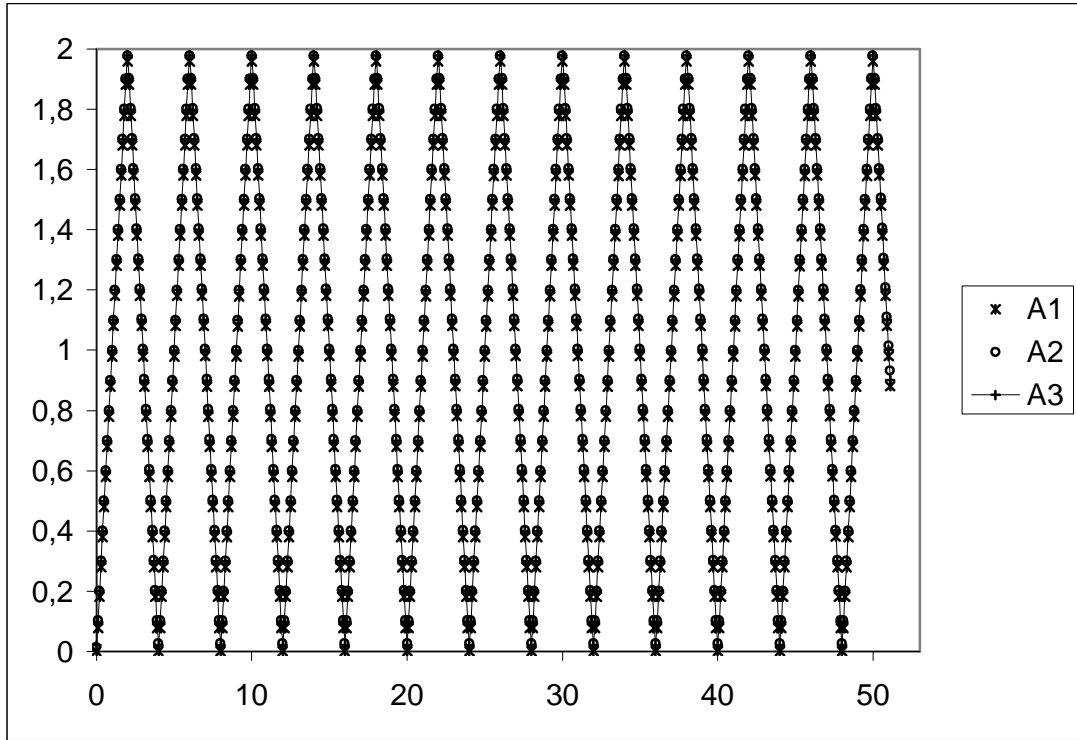


Figure 4.19. End displacement for the form e^{-ah} under $P_2(t) = P_0$, $a=0$, $m=10$.

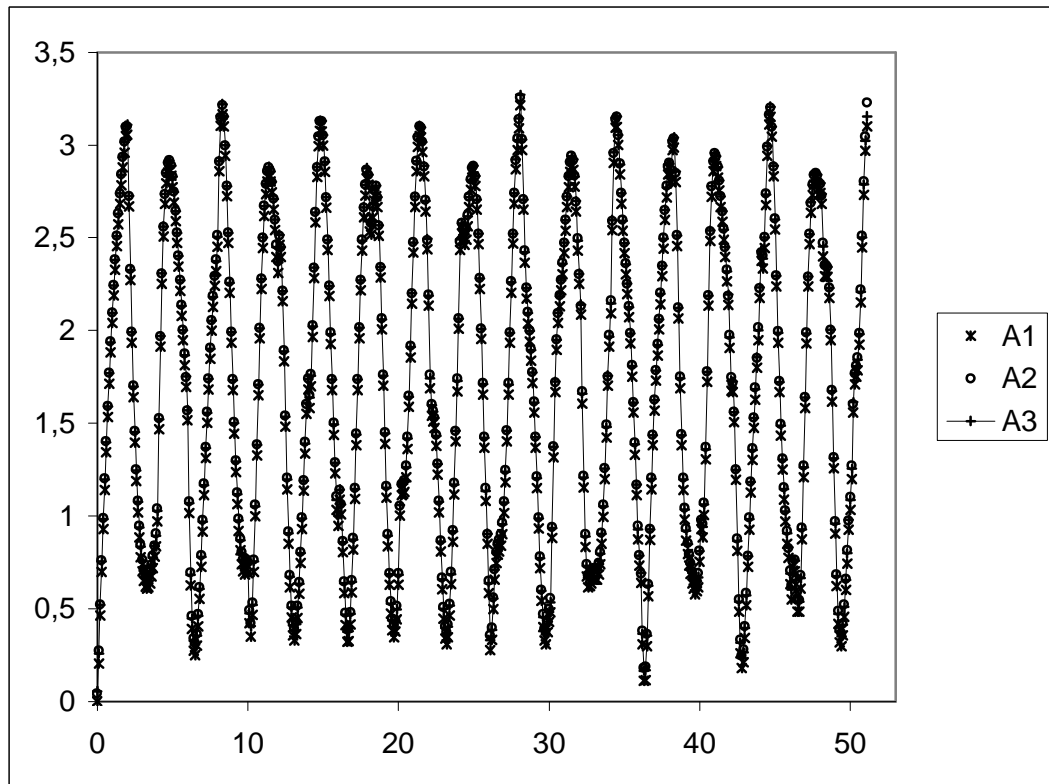


Figure 4.20. End displacement for the form e^{-ah} under $P_2(t) = P_0$, $a=1$, $m=10$.

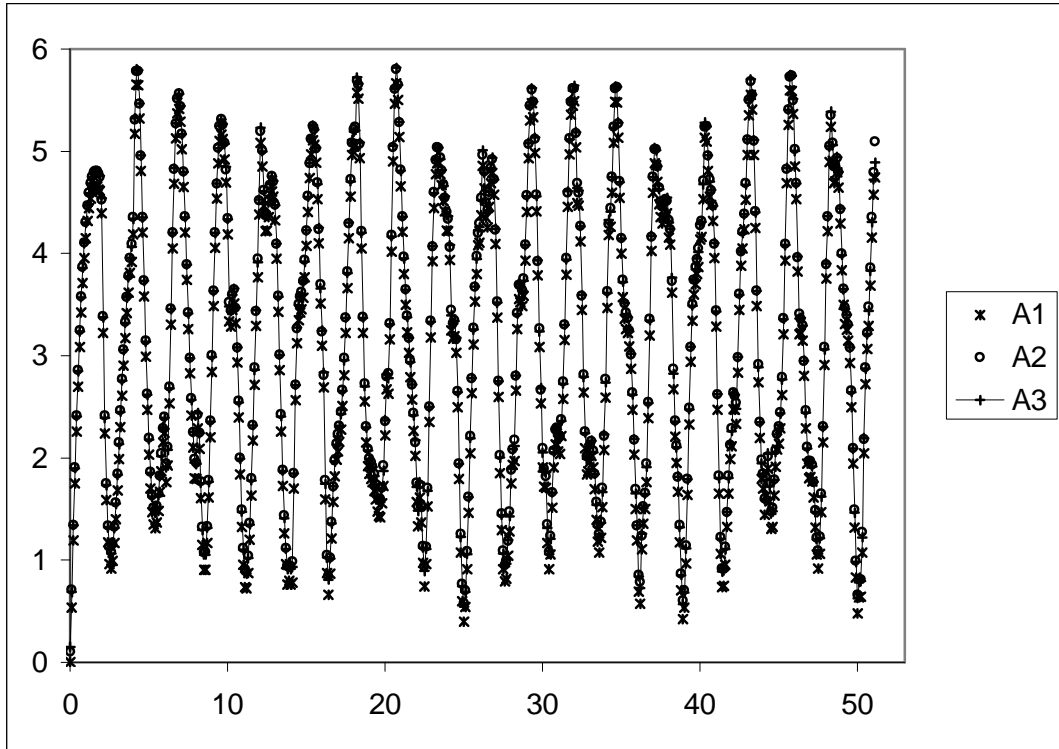


Figure 4.21. End displacement for the form e^{-ah} under $P_2(t) = P_0$, $a=2$, $m=10$.

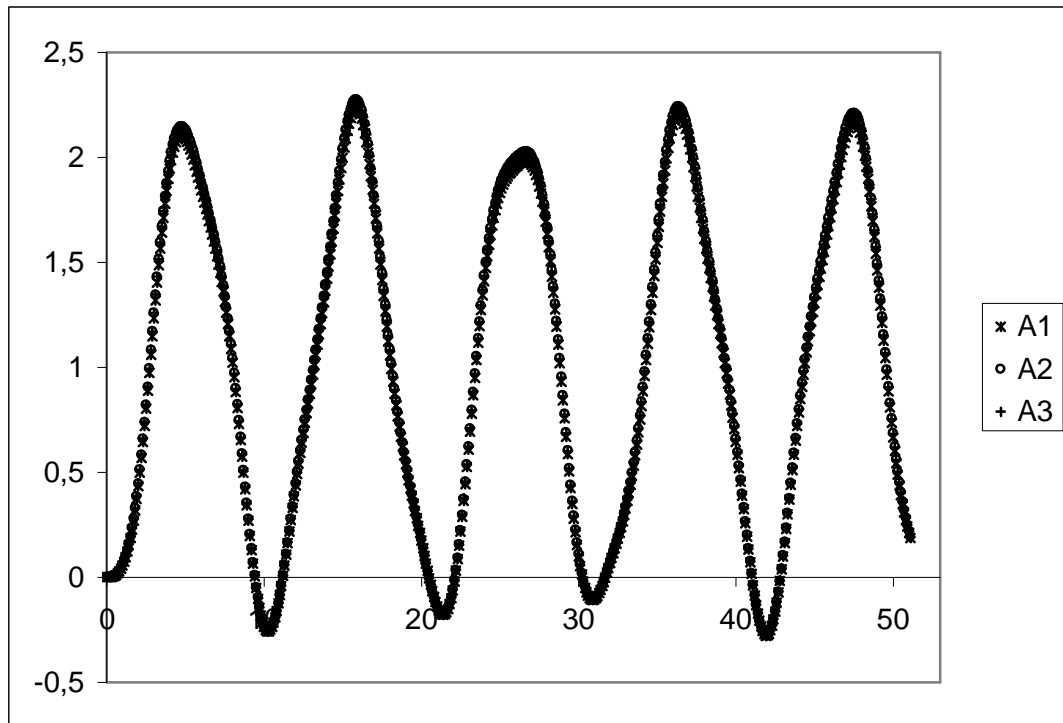


Figure 4.22. End displacement for the form e^{-ah} under $P_1(t) = P_0(1 - \cos[gt])$, $a=0$, $m=10$, $g=0.6$.

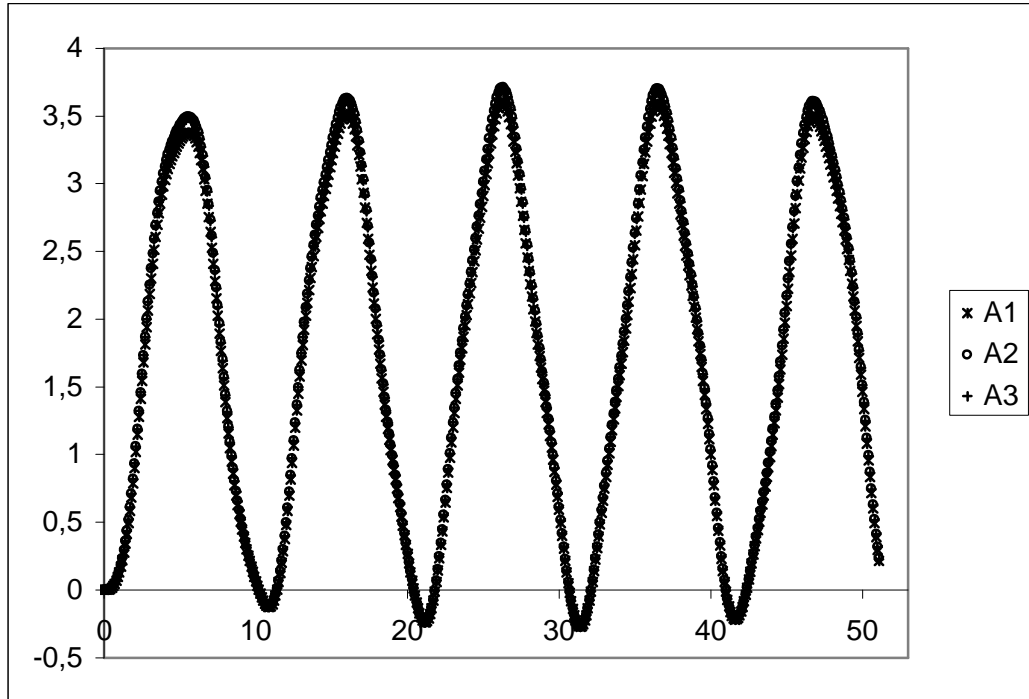


Figure 4.23. End displacement for the form e^{-ah} under $P_1(t) = P_0(1 - \cos[gt])$,
 $a=1, m=10, g=0.6$.

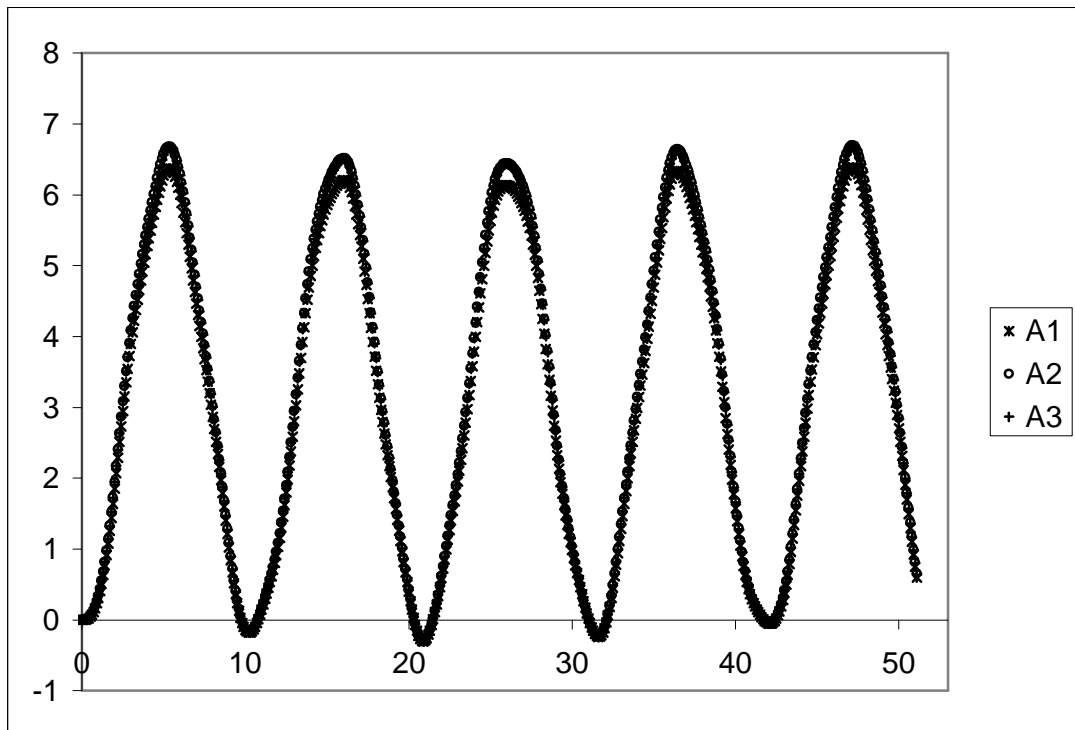


Figure 4.24. End displacement for the form e^{-ah} under $P_1(t) = P_0(1 - \cos[gt])$,
 $a=2, m=10, g=0.6$.

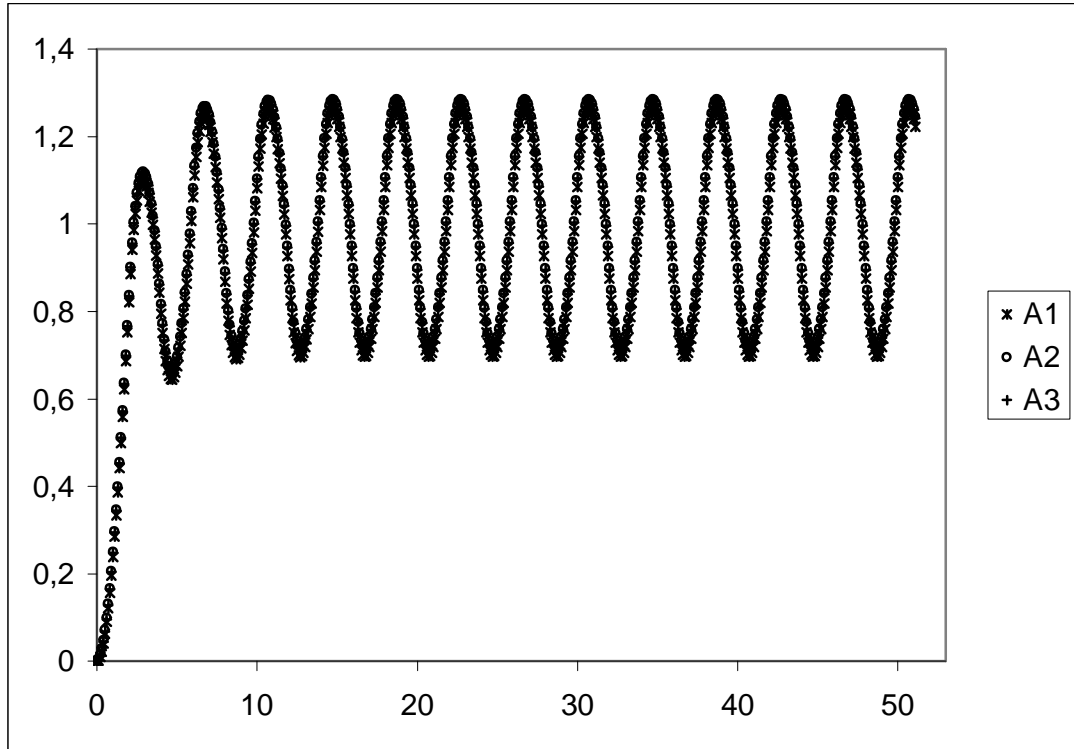


Figure 4.25. End displacement for the form e^{-ah} under $P_3(t) = P_0(1 - e^{-gt})$, $a=0$, $m=10, g=0.6$.

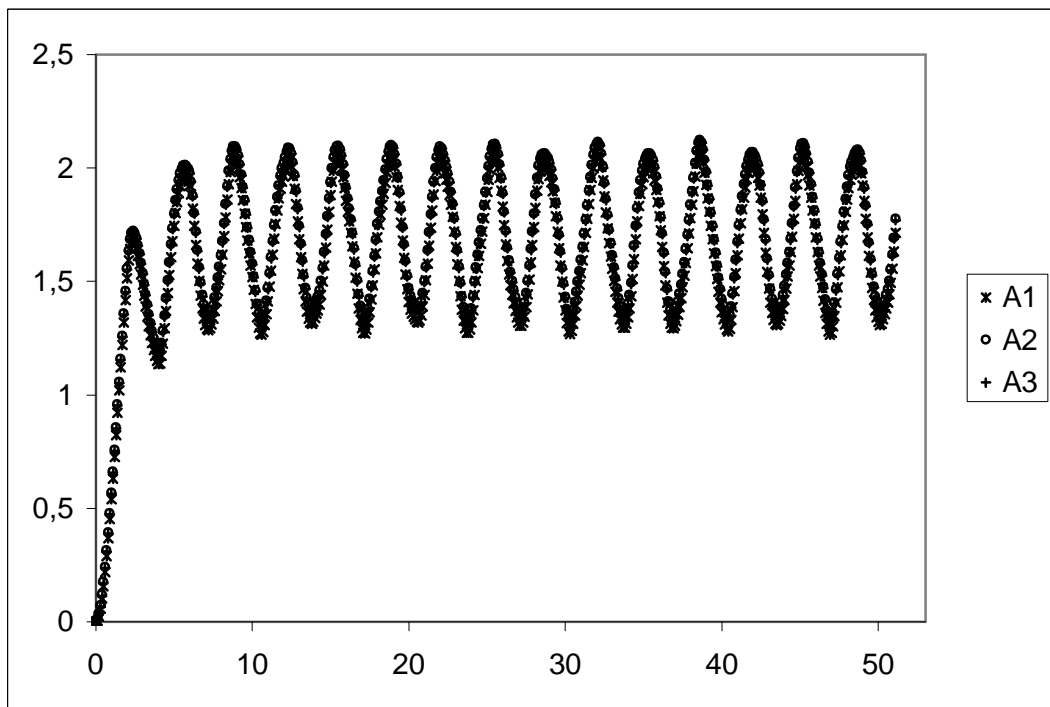


Figure 4.26. End displacement for the form e^{-ah} under $P_3(t) = P_0(1 - e^{-gt})$, $a=1$, $m=10, g=0.6$.

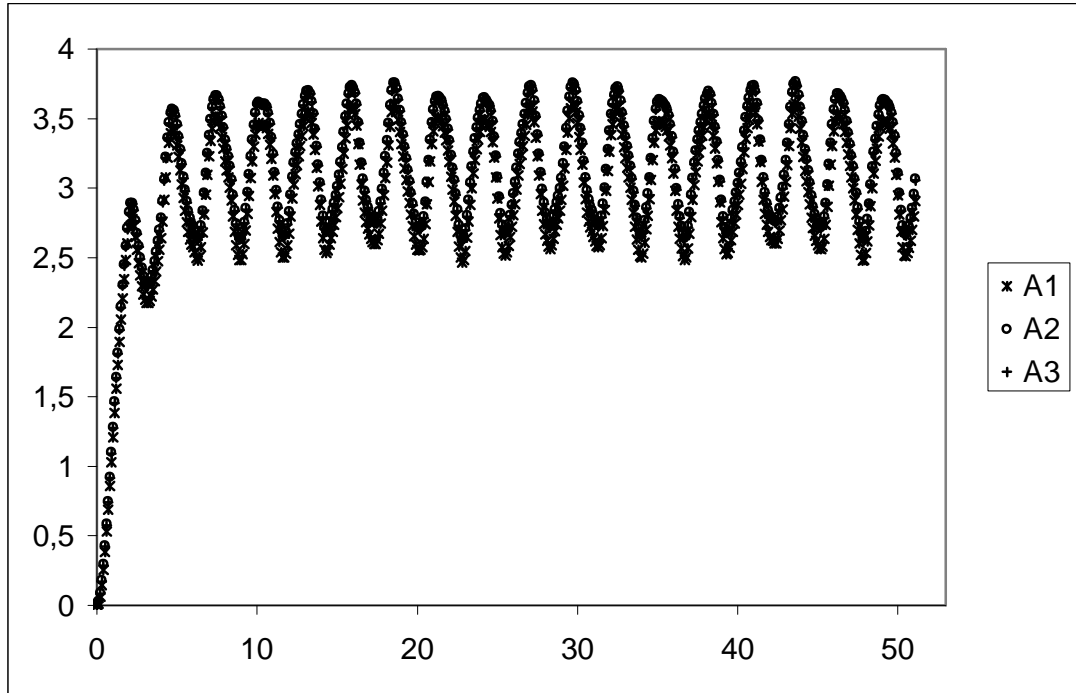


Figure 4.27. End displacement for the form e^{-ah} under $P_3(t) = P_0(1 - e^{-gt})$, $a=2$, $m=10$, $g=0.6$.

In numerical analysis, fundamental frequencies of FG beams with clamped-free support are given in tabular form for different values of slenderness ratio ($L/h=5, 10, 20$) and wave number ($n=1,3,5$). Assume that the FG beam is a mixture of two materials and material properties were chosen as follows:

$$E_b = 70 \text{ GPa} \quad , \quad \nu_b = 0.3 \quad , \quad r_b = 2707 \text{ kg/m}^3$$

$$E_t = 380 \text{ GPa} \quad , \quad \nu_t = 0.3 \quad , \quad r_t = 14695 \text{ kg/m}^3$$

For the given material properties $E_t / E_b = r_t / r_b$.

The results are presented graphically using the following analyses for each L/h ratio and wave number (n).

B1: Elasticity solution (ET)

B2: Classical beam theory (CBT)

B3: First order shear deformation beam theory (FSDBT)

B4: Parabolic shear deformation beam theory (PSDBT)

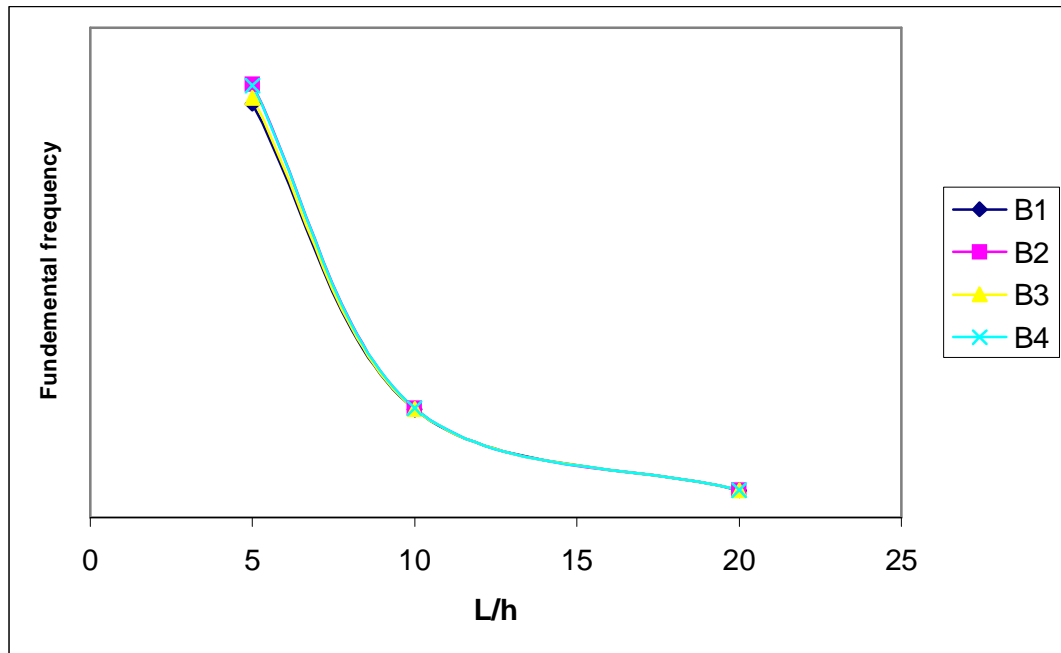


Figure 4.28. Variation of the fundamental frequency of FGM beam with L/h ratio for n=1

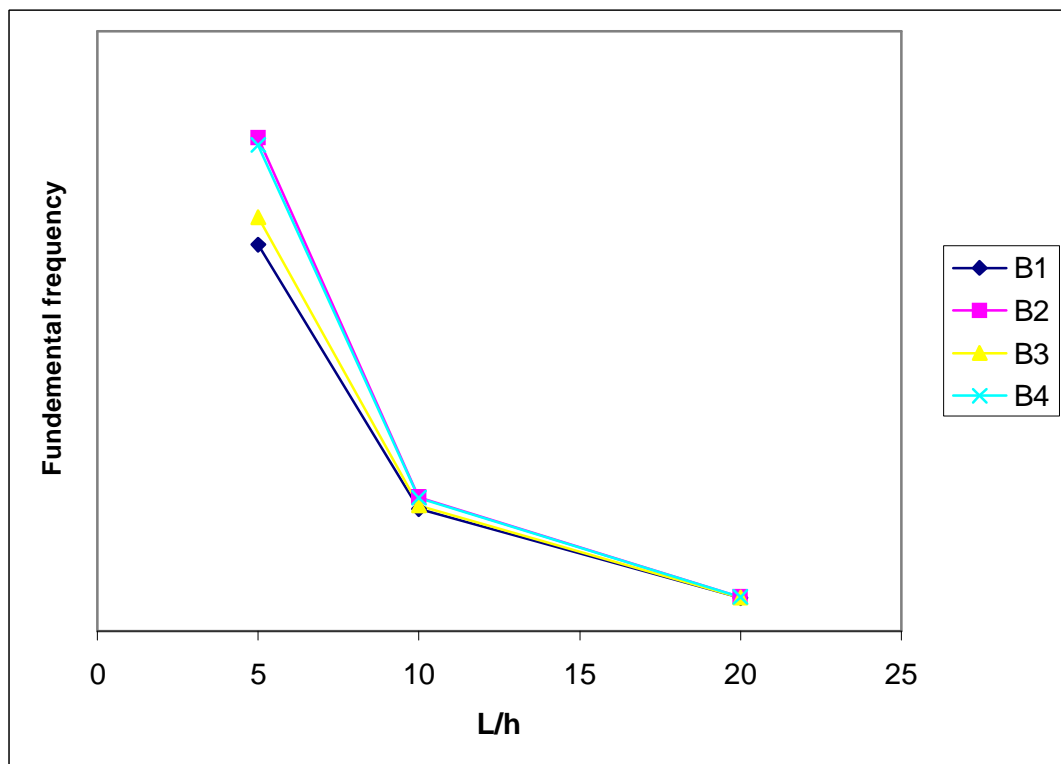


Figure 4.29. Variation of the fundamental frequency of FGM beam with L/h ratio for n=3

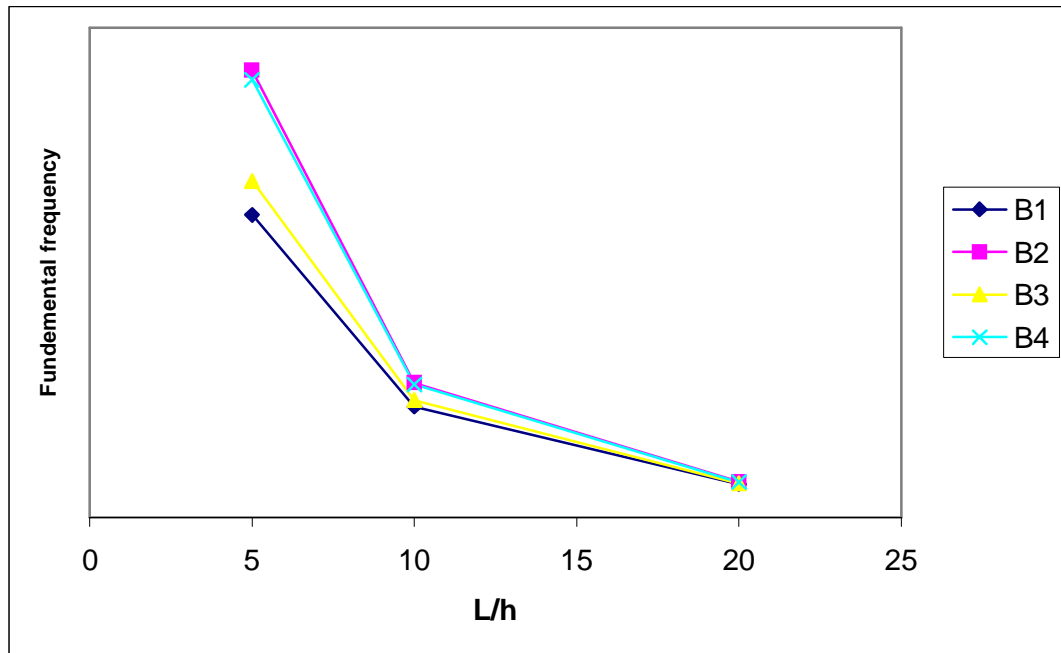


Figure 4.30. Variation of the fundamental frequency of FGM beam with L/h ratio for n=5

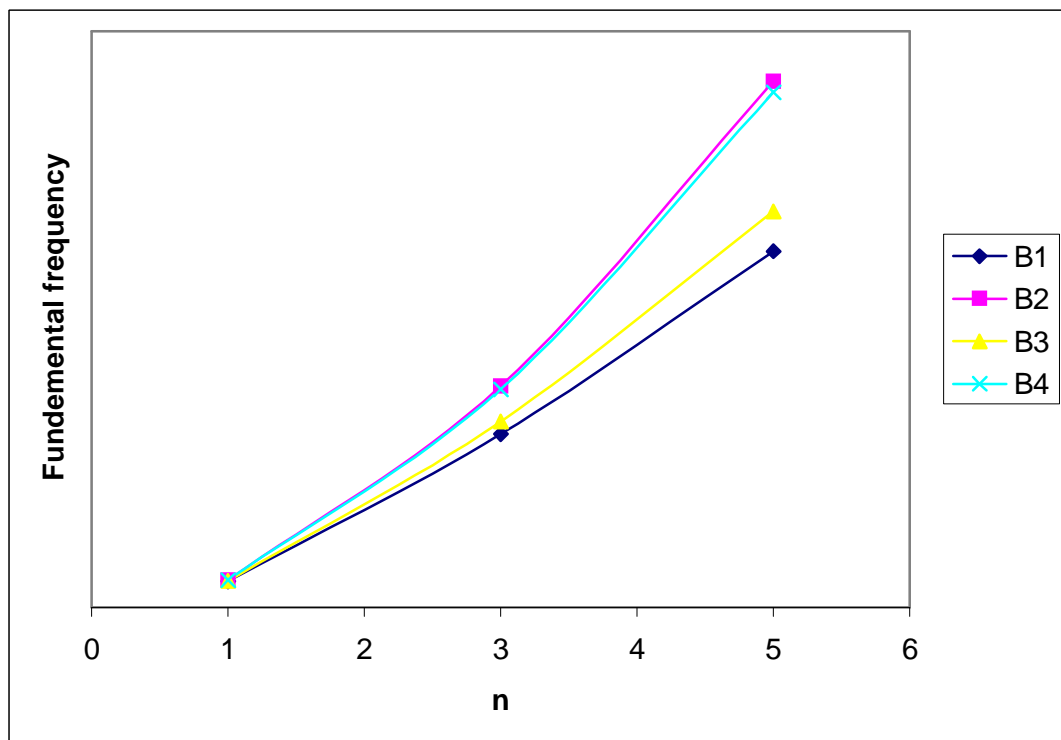


Figure 4.31. Variation of the fundamental frequency of FGM beam with n for L/h=5

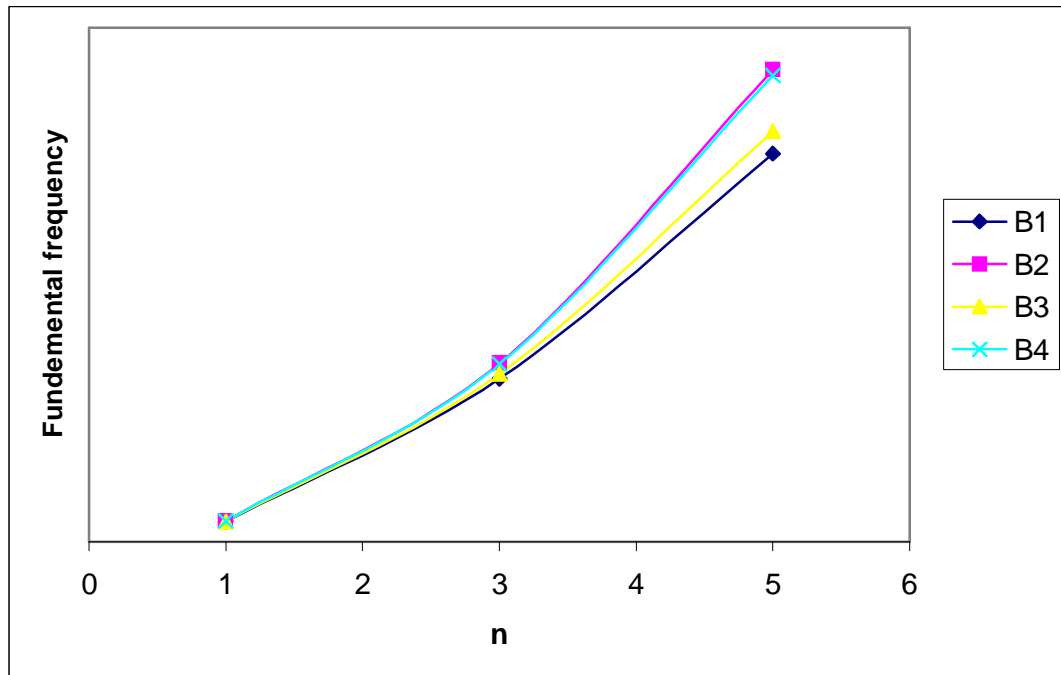


Figure 4.32. Variation of the fundamental frequency of FGM beam with n for $L/h=10$

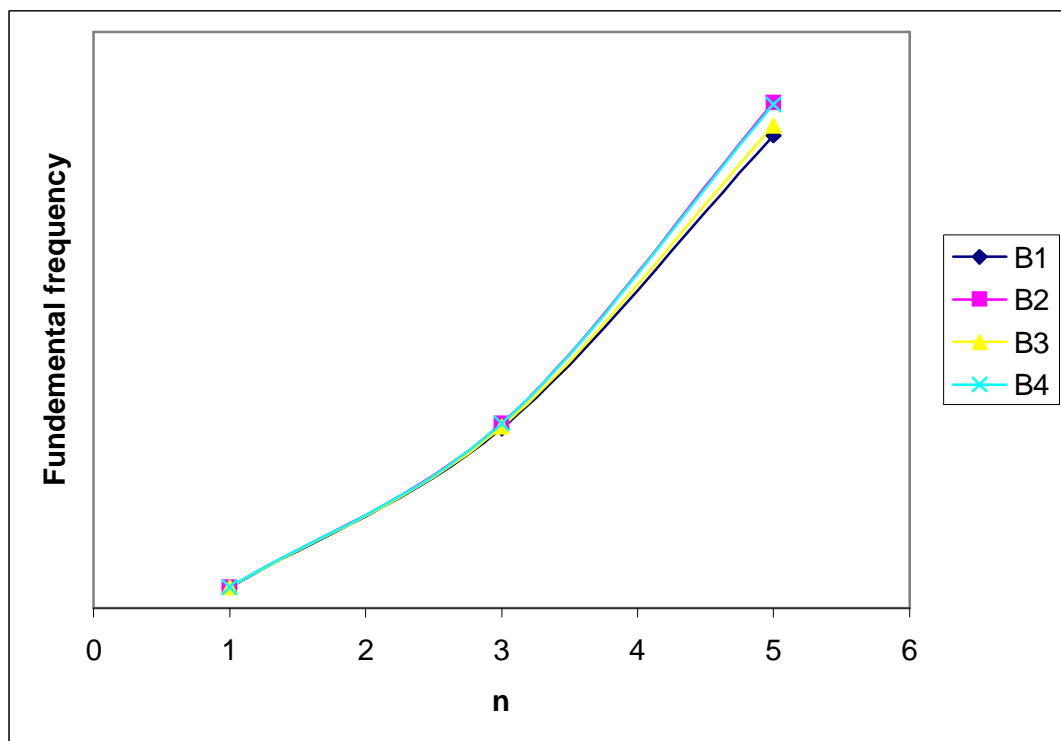


Figure 4.33. Variation of the fundamental frequency of FGM beam with n for $L/h=20$

Figures 4.28 - 4.33 show the fundamental frequencies of FG beams for different values of slenderness ratio and wave number. As it seen from the figures, L/h ratio is more effective for higher modes. The differences between analysis are increasing with increasing mode number and decreasing L/h ratio.

In Figure 4.34, the first, third and fifth flexural mode shapes of FGM beam using elasticity theory are shown for different L/h ratios. It is clear that mode shapes are affected by the variations of L/h ratio.

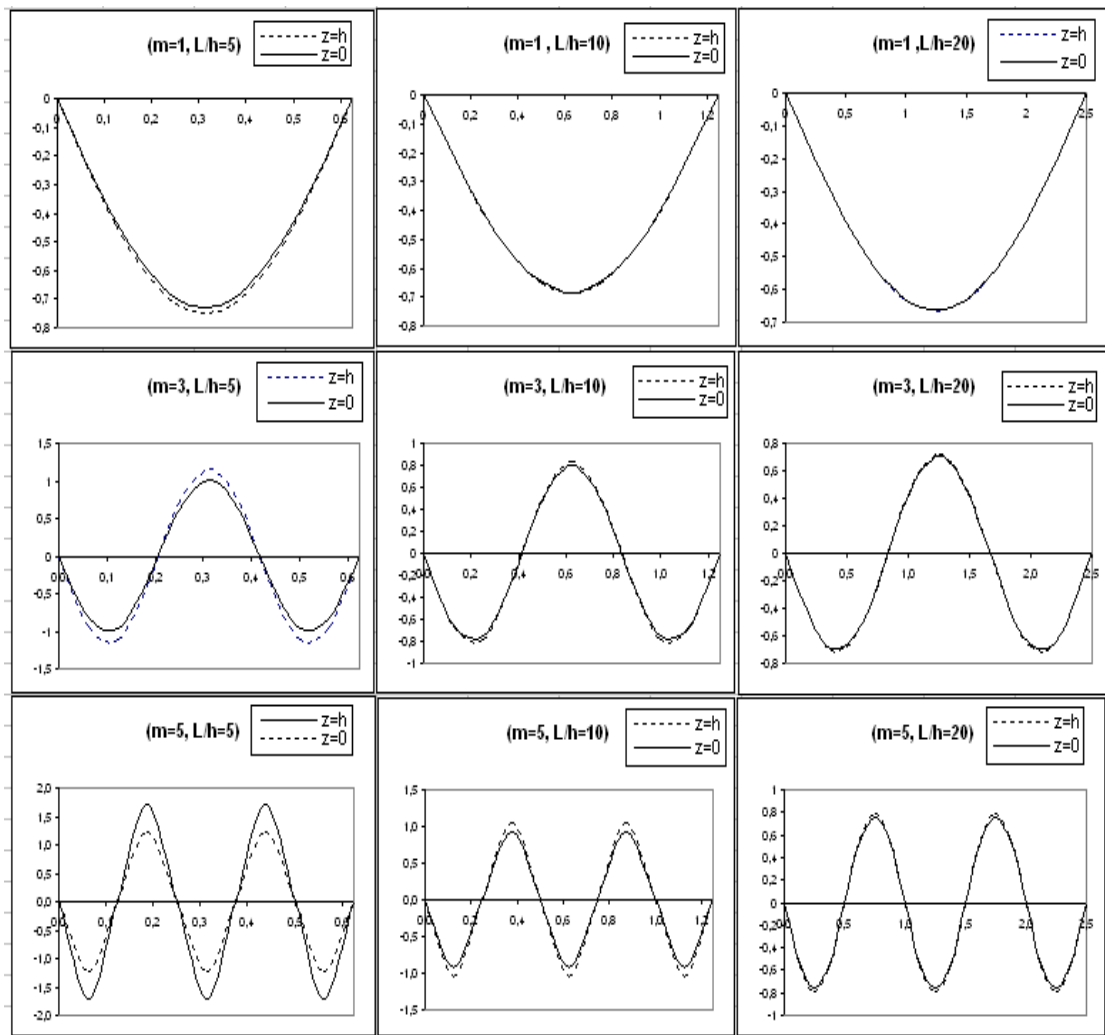


Figure 4.34. Flexural mode shapes at the bottom surface and upper surface of the FGM beam.

5. CONCLUSIONS

Closed-form solutions for free and forced vibration analyses of a non-uniform rod and heterogeneous rod have been performed using Laplace transform technique. The problem is solved in the Laplace domain and the inversion into the time domain is done exactly by the residue theorem and modified Durbin's inverse transform method. The numerical results obtained from Residue theorem and Durbin's inverse transform method are compared with those from Mode Superposition Method (MSM). It is seen that when use of first ten frequencies in the analytical solutions gave six-digit accuracy, for certain cases, up to a hundred frequencies were needed in MSM. In addition to their efficient use, exact solutions give adequate insight into the physics of the problem. In optimization problems using closed-form solutions will greatly reduce the solution time. The inhomogeneity parameter "a" used in rod models is found to be effective in the response of the material such that increasing the inhomogeneity parameter consistently caused a decrease in the amplitude of displacements.

Free vibration analysis of FG beam has been performed using elasticity analysis and beam theory. The advantage of using elasticity theory is, since the beam is modelled as a continuum, infinitely many frequencies may be obtained. But in beam theories, only limited number of natural frequencies are obtained. Figure 4.28-4.33 show the variation of the fundamental frequencies of FGM beam. The most important observation is the fact that the frequencies are increased when the value of L/h decreased or value of n increased. The difference between the frequencies of CBT and those of the other higher-order beam theories and elasticity solution is significant when $L/h < 20$. The results of the higher-order beam theories and elasticity solution are very close to each other when $L/h > 20$. The difference between the results increases with increasing value of n and decreasing value of L/h .

Also similar situation is valid for mode shapes; the difference between the mode shapes of upper and lower surfaces increases with decreasing L/h . For long slender beams, there is no variation through the thickness. In short and thick beams,

however, the flexural mode shape for top and bottom surfaces are different. Because of this, for short and thick beams, beam theory should not be used.

REFERENCES

- ABBASI, M., ESLAMI, M.R. and SABBAGHIAN, M., 2008. Coupled Thermoelastic Vibrations Analysis of Functionally Graded Timoshenko Beams Using the Galerkin Finite Element Method. 2008 ASME International Mechanical Engineering Congress and Exposition, October 31-November 6, Boston, Massachusetts, USA.
- ABRAMOWITZ, M. and STEGUN, I.A., 1982. Handbook of Mathematical Functions. Dover, USA.
- ABRATE, S., 1995. Vibration of Non-Uniform Rods and Beams. *Journal of Sound and Vibration*, 185, 703-716.
- AYDOGDU, M., 2005. Vibration Analysis of Cross-ply Laminated Beams with General Boundary Conditions by Ritz Method. *International Journal of Mechanical Science*, 47, 1740-1755.
- AYDOGDU, M. and TASKIN, V., 2007. Free Vibration Analysis of Functionally Graded Beams with Simply Supported Edges. *Materials and Design*, 28, 1651- 1656.
- BESKOS, D.E. and NARAYANAN, G.V., 1981. Dynamic Response of Frameworks by Numerical Laplace Transform. *Computer Methods in Applied Mechanics and Engineering*, 37, 289-307.
- CALIM, F.F., 2009. Free and Forced Vibrations of Non-uniform Composite Beams. *Composite Structures*, 88, 413-423.
- CALIO, I. and ELISHAKOFF, I., 2005. Closed-form Solutions for Axially Graded Beam-Columns. *Journal of Sound and Vibration*, 280, 1083-1094.
- CANDAN, S. and ELISHAKOFF, I., 2001. Constructing the Axial Stiffness of Longitudinally Vibrating Rod from Fundamental Mode Shape. *International Journal of Solids and Structures*, 38, 3443-3452.
- CELEBI, K., KELES, I. and TUTUNCU, N., 2009. Homojen Olmayan Çubuk, disk ve Silindirlerin Laplace Transformasyonu ile Zorlanmış Titreşim Analizi. XVI. Ulusal Mekanik Kongresi, 22-26 Haziran, Erciyes Üniversitesi, Kayseri.

- COOLEY, W. and TUKEY, J.W., 1965. An Algorithm for Machine Calculation of Complex Fourier Series, *Math. Computation*, 19, 297-301.
- CLOUGH, R.W. and PENZIEN, J., 1993. *Dynamics of Structures*, McGraw-Hill, USA.
- DURBIN, F., 1974. Numerical Inversion of Laplace Transforms: An Efficient Improvement to Dubner and Abate's Method. *Commissariat a l'Energie Atomique Centre U-Service Electronique*, 17, 371-376.
- EISENBERGER, M., 1991. Exact Longitudinal Vibration Frequencies of a Variable Cross-Section Rod. *Applied Acoustics*, 34, 123-130.
- ELISHAKOFF, I. and CANDAN, S., 2001. Apparently First Closed-Form Solution for Vibrating: Inhomogeneous Beam. *International Journal of Solids and Structures*, 38, 3411-3441.
- HORGAN, C.O. and CHAN, A.M., 1999. Vibration of Inhomogeneous strings, rods and membranes. *Journal of Sound and Vibration*, 225, 503-513.
- KADOLI, R., AKHTAR, K. and GANESAN, N., 2008. Static Analysis of Functionally Graded Beams Using Higher Order Shear Deformation Theory. *Applied Mathematical Modelling*, 32, 2509-2525.
- KUMAR, B.M. and SUJITH, R.I., 1997. Exact Solutions for the Longitudinal Vibrations of Non-Uniform Rods. *Journal of Sound and Vibration*, 207, 721 - 729.
- LI, Q.S., FANG, J.Q. and JEARY, A.P., 1998. Calculation of Vertical Dynamic Characteristics of Tall Buildings with Viscous Damping. *International Journal of Solids Structures*, 35 (24), 3165-3176.
- LI, Q.S., LI, G.Q. and LIU, D.K., 1999. Exact Solutions for Longitudinal Vibration of Rods Coupled by Translational Springs. *International Journal of Mechanical Sciences*, 42, 1135-1152.
- LI, Q.S., 2000. Free Longitudinal Vibration analysis of Multi-Step Non-Uniform Bars Based on Piecewise Analytical Solutions. *Engineering Structures*, 22, 1205-1215.

- LI, Q.S., WU, J.R. and XU, J., 2002. Longitudinal Vibration of Multi-Step Non-Uniform Structures with Lumped Masses and Spring Supports. *Applied Acoustics*, 63, 333-350.
- LI, X.F., 2008. A Unified Approach for Analyzing Static and Dynamic Behaviors of Functionally Graded Timoshenko and Euler-Bernoulli Beams. *Journal of Sound and Vibration*, 313, 1210-1229.
- MANOLIS, R.W. and BESKOS, D.E., 1981. Dynamic Stress Concentration Studies by Boundary Integrals and Laplace Transform. *International Journal of Numerical Methods for Engineering*, 17, 573-599.
- NACHUM, S. and ALTUS, E., 2007. Natural Frequencies and Mode Shapes of Deterministic and Stochastic Non-homogeneous Rods and Beams. *Journal of Sound and Vibration*, 302, 903-924.
- NARAYANAN, G.V., 1977. Use of Dynamic Influence Coefficients in Forced Vibration Problems with the Aid of Fast Fourier Transform. *Computers and Structures*, 9, 145-150.
- QIUSHENG, L., HONG, C. and GUIGING, L., 1996. Static and Dynamic Analysis of Straight Bars with Variable Cross-Section, 59, 1185-1191.
- RAJ, A. and SUJITH, R.I., 2005. Closed-form Solutions for the Free Longitudinal Vibration of Inhomogeneous Rods. *Journal of Sound and Vibration*, 283, 1015- 1030.
- SANKAR, B.V., 2001. An Elasticity Solution for Functionally Graded Beams. *Composites Science and Technology*, 61, 689-696.
- SANKAR, B.V. and TZENG, J.T., 2002. Thermal Stresses in Functionally Graded Beams. *AIAA Journal*, 40, 1228-1232.
- SINA, S.A., NAVAZI, H.M. and HADDADPOUR, H., 2009. An Analytical Method for Free Vibration Analysis of Functionally Graded Beams. *Materials and Design*, 30, 741-747.
- SIMSEK, M. and KOCATURK, T., 2009. Free and Forced Vibration of a Functionally Graded Beam Subjected to a Concentrated Moving Harmonic Load. *Composite Structures*, 90, 465-473.

- SIMSEK, M., 2009. Static Analysis of a Functionally Graded Beam Under a Uniformly Distributed Load by Ritz Method. *International Journal of Engineering and Applied Science*, 1, 1-11.
- SIMSEK, M., 2010. Vibration Analysis of a Functionally Graded Beam Under a Moving Mass by Using Different Beam Theories. *Composite Structures*, Article in press.
- SOLDATOS, K.P. and SOPHOCLEOUS, C., 2001. On Shear Deformable Beam Theories: The Frequency and Normal Mode Equations of the Homogeneous Orthotropic Bickford Beam. *Journal of Sound and Vibration*, 242, 215-245.
- TEMEL, B., 1996. Dinamik Zemin-Yapı Etkileşimi Problemlerinin Sonlu-Sonsuz Elemanlar ve Laplace Dönüşüm Yöntemi ile Analizi. Çukurova University Civil Engineering Department, Adana, 82-83.
- YING, J., LU, C.F. and CHEN, W.Q., 2008. Two-Dimensional Elasticity Solutions for Functionally Graded Beams Resting on Elastic Foundations. *Composite Structures*, 84, 209-219.
- ZHONG, Z. and Yu, T., 2007. Analytical Solution of a Cantilever Functionally Graded Beam. *Composites Science and Technology*, 67, 689-696.

CURRICULUM VITAE

The author was born in ADANA in 1978. He graduated from Yeni College in 1995. He registered to have his BS education at the Mechanical Engineering Department of Çukurova University in 1996. He completed his BS education and started his MS education in 2001. He started his PhD study at the Mechanical Engineering Department of Çukurova University in 2004. He has been working as a R&D Engineer at the Temsa Global A.Ş.

APPENDIX A.

Fast Fourier Transforms

The Fast Fourier transform, which allows very efficient and accurate evaluations of the discrete Fourier transforms, is based on an algorithm developed by Cooley and Tukey. Since the algorithm is used in exactly the same way in evaluating both the direct and inverse FFTs, let us now consider only the direct FFT, namely

$$A_n \equiv P_n N = \sum_{m=0}^{N-1} p_m e^{-i \frac{2\pi n m}{N}}, \quad n = 1, 2, 3, \dots, (N-1) \quad (1)$$

in which p_m denotes $p(t = t_m)$. In the present work, p_m corresponds to $f(t_m) e^{-at_m}$ from Equation (3.99). A straightforward evaluation of this summation for all values of n requires N^2 complex multiplications. This number would be prohibitive for most practical solutions requiring large values of N , say $N > 1000$, thus providing the incentive to develop the FFT algorithm.

The FFT algorithm based on letting $N = 2^g$ where g is an integer. In this case, each value of n and m in their common range from zero to $N-1$ can be expressed in terms of binary coefficients as given by

$$n = 2^{g-1} n_{g-1} + 2^{g-2} n_{g-2} + \dots + n_0 \quad (2)$$

$$m = 2^{g-1} m_{g-1} + 2^{g-2} m_{g-2} + \dots + m_0$$

in which each binary coefficient is either +1 or 0 depending upon the particular value of n or m being represented. Using these relations and letting $W_N \equiv e^{-i\frac{2p}{N}}$, Equation (1) can be expressed as

$$A(n_{g-1}, n_{g-2}, \dots, n_0) = \sum_{m_0=0}^1 \sum_{m_1=0}^1 \dots \sum_{m_{g-1}=0}^1 p_0(m_{g-1}, m_{g-2}, \dots, m_0) W_N^{nm} \quad (3)$$

Note that each coefficient A_n for $n=0,1,2,\dots,N-1$ is represented by $A(n_{g-1}, n_{g-2}, \dots, n_0)$ and each load ordinate p_m for $m=0,1,2,\dots,N-1$ is represented by $p_0(m_{g-1}, m_{g-2}, \dots, m_0)$. The subscript zero has been added to p only to indicate the multiplier of the W_N^{nm} term in the first summation. The reason for introducing this addition to the notation will become apparent as the algorithm develops.

Consider now the term W_N^{nm} of Equation (3) in the form

$$W_N^{nm} = W_N^{(2^{g-1} n_{g-1} + 2^{g-2} n_{g-2} + \dots + n_0)(2^{g-1} m_{g-1} + 2^{g-2} m_{g-2} + \dots + m_0)} \quad (4)$$

Making use of $W_N^{(a+b)} = W_N^a W_N^b$, this equation can be modified to

$$\begin{aligned} W_N^{nm} &= W_N^{(2^{g-1} n_{g-1} + 2^{g-2} n_{g-2} + \dots + n_0)(2^{1-1} m_{g-1})} \\ &\quad * W_N^{(2^{g-1} n_{g-1} + 2^{g-2} n_{g-2} + \dots + n_0)(2^{g-2} m_{g-2})} \\ &\quad * \dots * W_N^{(2^{g-1} n_{g-1} + 2^{g-2} n_{g-2} + \dots + n_0)m_0} \end{aligned} \quad (5)$$

let us now examine each individual W_N term on the right hand side of this equation separately. The first term can be written

$$\begin{aligned}
& W_N^{(2^{g-1}n_{g-1} + 2^{g-2}n_{g-2} + \dots + n_0)(2^{1-1}m_{g-1})} \\
&= W_N^{2^g(2^{g-2}n_{g-1}m_{g-1})} * W_N^{2^g(2^{g-3}n_{g-2}m_{g-1})} * \dots \\
& * W_N^{2^g(2n_1m_{g-1})} * W_N^{2^{g-1}(n_0m_{g-1})} \\
&= W_N^{2^{g-1}(n_0m_{g-1})} \tag{6}
\end{aligned}$$

since each W_n term of the form

$$W_N^{2^g(\text{int eger})} = \left[e^{-i\frac{2p}{N}} \right]^{N(\text{int eger})} = 1 \tag{7}$$

writing the second term similarly and making use of Equation (7), one finds that

$$W_N^{(2^{g-1}n_{g-1} + 2^{g-2}n_{g-2} + \dots + n_0)(2^{1-2}m_{g-2})} = W_N^{2^{g-2}(2n_1 + n_0)m_{g-2}} \tag{8}$$

This pattern continues up to the last term which has no cancellations due to Equation (7); therefore, it must remain in the same form shown in Equation (5).

After substituting all W_N terms, except the last, in their reduced forms, Equation (3) becomes

$$\begin{aligned}
A(n_{g-1}, n_{g-2}, \dots, n_0) &= \sum_{m_0=0}^1 \sum_{m_1=0}^1 \dots \sum_{m_{g-1}=0}^1 p_0(m_{g-1}, m_{g-2}, \dots, m_0) * W_N^{2^{g-1}(n_0m_{g-1})} \\
& * W_N^{2^{g-2}(2n_1+n_0)m_{g-2}} * \dots * W_N^{(2^{g-1}n_{g-1} + 2^{g-2}n_{g-2} + \dots + n_0)m_0} \tag{9}
\end{aligned}$$

Carrying out all summations in this equation in succession gives

$$\sum_{m_{g-1}=0}^1 p_0(m_{g-1}, m_{g-2}, \dots, m_0) W_N^{2^{g-1}(N_0M_{g-1})} \equiv p_1(n_0, m_{g-2}, \dots, m_0)$$

$$\begin{aligned}
& \sum_{m_{g-2}=0}^1 p_1(n_0, m_{g-2}, \dots, m_0) W_N^{2^{g-2}(2n_1+n_0)m_{g-2}} \equiv p_2(n_0, n_1, m_{g-3}, \dots, m_0) \dots \\
& \dots \\
& \dots \\
& \sum_{m_0=0}^1 p_{g-1}(n_0, n_1, \dots, n_{g-2}, m_0) W_N^{(2^{g-1}n_{g-1} + 2^{g-2}n_{g-2} + \dots + n_0)m_0} \\
& \qquad \qquad \qquad = A(n_{g-1}, n_{g-2}, \dots, n_0)
\end{aligned} \tag{10}$$

these recursive equations, leading to the desired result $A(n_{g-1}, n_{g-2}, \dots, n_0)$, represent the Cooley-Tukey algorithm used in modern FFT analysis. They are extremely efficient due to the fact that each summation is used immediately in the next summation. The fact that the exponential has unit value in the first term of each summation and that $W_N^{nm} = -W_N^{nm+N/2}$ adds to the efficiency. The reduction in computational effort which results from the use of Equation (10) is enormous when the time duration T_p is divided into a large number of intervals. For example, when $N=1024$ ($g=10$), the computer time required by the FFT to obtain all $N A_n$ -values is approximately 0.5 percent of the time required to obtain the same values by direct use of Equation (1). Not only is the FFT extremely efficient but it is very accurate as well, thus making the frequency-domain approach to the dynamic-response analysis of structures very attractive indeed.

APPENDIX B

1. Residue Theorem

Consider the counter integral

$$I = \oint_C f(z) dz \quad (1)$$

where f has a finite number of singular points within C , and each of them is isolated. We do not permit singularities on the contour C , and whether or not f has singular points outside C will not be relevant.

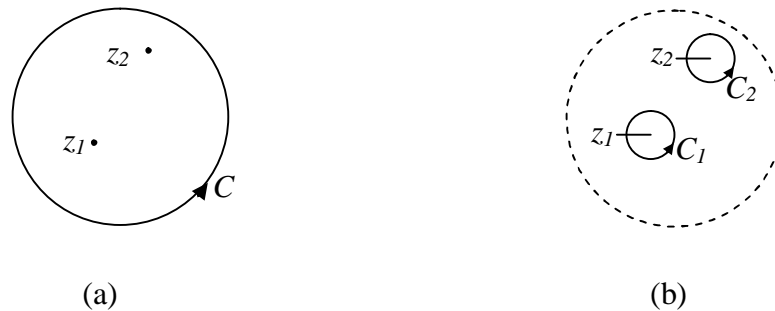


Figure 1. Deformation of contour.

For definiteness, suppose that f has two isolated singular points within C , z_1 and z_2 , as shown in Fig. 1a. Using Cauchy's theorem to deform the contour into C_1 and C_2 (fig. 1b), we have

$$I = \oint_C f(z) dz = \oint_{C_1} f(z) dz + \oint_{C_2} f(z) dz \quad (2)$$

To evaluate the latter two integrals, which we denote as I_1 and I_2 , respectively, expand f in Laurent series

$$f(z) = \sum_{n=-\infty}^{\infty} c_n^{(1)} (z - z_1)^n \text{ in } 0 < |z - z_1| < r_1 \quad (3a)$$

and

$$f(z) = \sum_{n=-\infty}^{\infty} c_n^{(2)} (z - z_2)^n \text{ in } 0 < |z - z_2| < r_2 \quad (3b)$$

and be sure that C_1 is small enough to fit entirely within the $0 < |z - z_1| < r_1$ annulus, and that C_2 is small enough to fit entirely within the $0 < |z - z_2| < r_2$ annulus. The (3a) holds on C_1 and (3b) C_2 , so we can re-express (2) as

$$I = \oint_{C_1} \sum_{n=-\infty}^{\infty} c_n^{(1)} (z - z_1)^n dz + \oint_{C_2} \sum_{n=-\infty}^{\infty} c_n^{(2)} (z - z_2)^n dz = 2\pi i c_{-1}^{(1)} + 2\pi i c_{-1}^{(2)} \quad (4)$$

where the last step follows our “important little integral”. Understand that (3a) and (3b) are two different Laurent series- of the same function of $f(z)$, but about z_1 and z_2 , respectively. Hence, their coefficients are in general different, and we denote them as $c_n^{(1)}$ and $c_n^{(2)}$, respectively.

Observe that of the infinite number of terms in the C_1 integral, only $n=-1$ term survives and contributes to the answer its contribution being $2\pi i c_{-1}^{(1)}$; similarly for the C_2 integral. Thus, the surviving coefficients in (4) $c_{-1}^{(1)}$ and $c_{-1}^{(2)}$, are called the **residues** of $f(z)$ at z_1 and z_2 , and we have found in (4) that $I = \oint_C f(z) dz$ is equal to $2\pi i$ times the sum of the residues.

The foregoing derivation is attractive in its directness, but it does beg justification of the termwise integration of two Laurent series, expressed by the equality (4). With $n=-1$, that equation gives, immediately,

$$\oint_{C_1} f(z)dz = 2\pi i c_{-1}^{(1)} \text{ and } \oint_{C_2} f(z)dz = 2\pi i c_{-1}^{(2)} \quad (5)$$

In agreement with the result obtained above. Surely the same method applies if C contains any finite number of isolated singular points so we can state the residues theorem:

Let C be a piecewise smooth simple closed curve oriented counterclockwise, and let $f(z)$ be analytic inside and on C except at finitely many points isolated z_1, \dots, z_k within C . If $c_{-1}^{(j)}$ denotes the residue of f at z_j , then

$$\oint_{C_1} f(z)dz = 2\pi i \sum_{j=1}^k c_{-1}^{(j)} \quad (6)$$

That is, the integral equals $2\pi i$ times the sum of the residues of f within C . Again, by the residue of f at z_j we mean the $c_{-1}^{(j)}$ coefficient in the Laurent expansion

$$f(z) = \sum_{n=-\infty}^{\infty} c_n^{(j)} (z - z_j)^n \quad (7)$$

of f about z_j , in some annulus $0 < |z - z_j| < r_j$.

Calculating residues:

a) Expansions

Example: Find the Laurent series expansion of $f(z) = \frac{e^{2z}}{(z-1)^3}$

Singular at $z=1$

Let $z-1 = u$, $z = u+1$

$$\frac{e^{2+2u}}{u^3} = \frac{e^2}{u^3} \cdot e^{2u} = \frac{e^2}{u^3} \left\{ 1 + 2u + \frac{(2u)^2}{2} + \frac{(2u)^3}{3!} + \dots \right\} \quad (8)$$

Substitute back ; $z-1 = u$

Residue : $2e^2$

$$\oint \frac{e^{2z}}{(z-1)^3} dz = 2\pi i 2e^2 = 4\pi i e^2 \quad (9)$$

b) Ratios of Analytic Functions:

If $f(z) = \frac{P(z)}{Q(z)}$ where P and Q are both analytic with no common factors, then

the function is not analytic at zeros of $Q(z)$.

Suppose that $Q(z)$ has a simple zero at $z=a$.

$$f(z) = \frac{P(a) + P'(a)(z-a) + \dots}{Q(a) + Q'(a)(z-a) + \dots} = \frac{P(a) / Q'(a)}{(z-a)} \quad (10)$$

$$\text{Residue}_{z=a} = \frac{P(a)}{Q'(a)} \quad (11)$$

Example: Find the residues of $f(z) = \frac{1+z^2}{z^3-1}$

Singularities are at $z^3 = 1 = e^{2\pi k i} = \cos 2\pi k + i \sin 2\pi k \quad k = 0, \pm 1$
 $z = e^{\frac{2\pi k i}{3}}$

$$\left. \begin{aligned} k=0 &\Rightarrow a_1 = 1 \\ k=1 &\Rightarrow a_2 = e^{\frac{2\pi i}{3}} = \cos\left(\frac{2\pi i}{3}\right) + i \sin\left(\frac{2\pi i}{3}\right) = -\frac{1}{2} + i \frac{\sqrt{3}}{2} \\ k=1 &\Rightarrow a_3 = e^{-\frac{2\pi i}{3}} = \cos\left(\frac{2\pi i}{3}\right) + i \sin\left(\frac{2\pi i}{3}\right) = -\frac{1}{2} - i \frac{\sqrt{3}}{2} \end{aligned} \right\} \text{Singular points (12)}$$

$$\left. \begin{aligned} P(z) &= 1 + z^2 \\ Q'(z) &= 3z^2 \end{aligned} \right\} (\text{Re } s)_{z=a} = \frac{1+a^2}{3a^2} = \frac{1}{3} \left(1 + \frac{1}{a^2}\right) \quad (13)$$

$$(\text{Re } s)_{z=1} = \frac{1}{3}(1+1) = \frac{2}{3} \quad (14)$$

$$(\text{Re } s)_{z=e^{\pm \frac{2\pi i}{3}}} = \frac{1}{3} \left(1 + e^{\pm \frac{4\pi i}{3}}\right) = \frac{1}{3} \left(\frac{1}{2} \pm i \frac{\sqrt{3}}{2}\right) \quad (15)$$

$$\oint \frac{1+z^2}{z^3-1} = 2\pi i \left(\frac{2}{3} + \frac{1}{3} \left(\frac{1}{2} + i \frac{\sqrt{3}}{2}\right)\right) \quad (16)$$

c) Residue of a Pole

$$(\text{Re } s)_{z=a} = \lim_{z \rightarrow a} \left[\frac{1}{(m-1)!} \frac{d^{m-1}}{dz^{m-1}} \left\{ (z-a)^m f(z) \right\} \right] \quad (17)$$

If $m = 1$ it's called a simple pole. $m =$ Pole of order.

Example:

Find the residue of $f(z) = \frac{e^z \cos z}{z(z-p)^3}$.

Singularities are at $z = 0 \quad m = 1$
 $z = p \quad m = 3$

$z = 0, m = 1$

$$(\text{Res } s)_{z=0} = \lim_{z \rightarrow 0} \left[\frac{1}{0!} \frac{d^0}{dz^0} \left\{ z \frac{e^z \cos z}{z(z-p)^3} \right\} \right] = -\frac{1}{p^3} \quad (18)$$

$z = p, m = 3$

$$(\text{Res } s)_{z=p} = \lim_{z \rightarrow p} \left[\frac{1}{2!} \frac{d^2}{dz^2} \left\{ (z-p)^3 \frac{e^z \cos z}{z(z-p)^3} \right\} \right] = \frac{e^p}{p^2} \left(1 - \frac{1}{p} \right) \quad (19)$$

$$\oint \frac{e^z \cos z}{z(z-p)^3} dz = 2\pi i \left\{ -\frac{1}{p^3} + \frac{e^p}{p^2} \left(1 - \frac{1}{p} \right) \right\} \quad (20)$$

Determining the points, Singular point or Branch Point

The displacement equation of sinusoidal rod under cosinus type force is

$$y = \frac{P_0 g^2}{E A_0 \sin[a+b]} \frac{F(p)}{p(p^2 + g^2)G(p)} \quad (21)$$

where

$$F(p) = \sin[\sqrt{a^2 - p^2}] \quad (22)$$

$$G(p) = \sqrt{a^2 - p^2} \sin[a+b] \cos[\sqrt{a^2 - p^2}] - a \cos[a+b] \sin[\sqrt{a^2 - p^2}] \quad (23)$$

If same value of $y(p)$ are obtained by successively encircling $p = 0$ and $p = \pm ig$, we call $p = 0$ and $p = \pm ig$ are singular points, otherwise they are

branch points. In order to keep the function single-valued, we set up an artificial barrier such as OB where B is at infinity. This barrier is called a branch line-cut and point “O” is called a branch point. But in our solutions, these points are singular points.

For $p = 0$, we assume that

$$p = r_1 e^{iq_1} \quad (24)$$

then we have

$$y(p) = \frac{P_0 g^2}{E A_0 \sin[a+b]} \frac{\sin[\sqrt{a^2 - r_1^2 e^{2iq_1}}]}{r_1 e^{iq_1} (r_1 e^{iq_1} - ig)(r_1 e^{iq_1} + ig)} \quad (25)$$

$$\frac{1}{\sqrt{a^2 - r_1^2 e^{2iq_1}} \cos[\sqrt{a^2 - r_1^2 e^{2iq_1}}] \sin[a+b] - a \cos[a+b] \sin[\sqrt{a^2 - r_1^2 e^{2iq_1}}]}$$

As q increases from q_1 to $q_1 + 2p$, which is what happens when one complete circuit counter clockwise around the origin is made, we find

$$y(p) = \frac{P_0 g^2}{E A_0 \sin[a+b]} \frac{\sin[\sqrt{a^2 - r_1^2 e^{2iq_1}}]}{r_1 e^{iq_1} e^{2pi} (r_1 e^{iq_1} e^{2pi} - ig)(r_1 e^{iq_1} e^{2pi} + ig)} \quad (26)$$

$$\frac{1}{\sqrt{a^2 - r_1^2 e^{2iq_1} e^{4pi}} \cos[\sqrt{a^2 - r_1^2 e^{2iq_1} e^{4pi}}] \sin[a+b] - a \cos[a+b] \sin[\sqrt{a^2 - r_1^2 e^{2iq_1} e^{4pi}}]}$$

where $e^{2pi} = e^{4pi} = 1$, Equation (26) is equal to Equation (25). Thus there is actually only one branch to the function, and so $p = 0$ can not be a branch point.

For $p = ig$, we assume that

$$p - ig = r_1 e^{iq_1} \quad (27)$$

then we have

$$y(p) = \frac{P_0 g^2}{E A_0 \sin[a+b]} \frac{\sin[\sqrt{a^2 - r_1^2 e^{2iq_1} - 2ig r_1 e^{iq_1} + g^2}]}{(r_1 e^{iq_1} + ig)(r_1 e^{iq_1})(r_1 e^{iq_1} + 2ig)} \frac{1}{\sqrt{a^2 - r_1^2 e^{2iq_1} - 2ig r_1 e^{iq_1} + g^2} \cos[\sqrt{a^2 - r_1^2 e^{2iq_1} - 2ig r_1 e^{iq_1} + g^2}] \sin[a+b] - a \cos[a+b] \sin[\sqrt{a^2 - r_1^2 e^{2iq_1} - 2ig r_1 e^{iq_1} + g^2}]} \quad (28)$$

As q increases from q_1 to $q_1 + 2p$, which is what happens when one complete circuit counter clockwise around the origin is made, we find

$$y(p) = \frac{P_0 g^2}{E A_0 \sin[a+b]} \frac{\sin[\sqrt{a^2 - r_1^2 e^{2iq_1} e^{4pi} - 2ig r_1 e^{iq_1} e^{2pi} + g^2}]}{(r_1 e^{iq_1} e^{2pi} + ig)(r_1 e^{iq_1} e^{2pi})(r_1 e^{iq_1} e^{2pi} + 2ig)} \frac{1}{\sqrt{a^2 - r_1^2 e^{2iq_1} e^{4pi} - 2ig r_1 e^{iq_1} e^{2pi} + g^2} \cos[\sqrt{a^2 - r_1^2 e^{2iq_1} e^{4pi} - 2ig r_1 e^{iq_1} e^{2pi} + g^2}] \sin[a+b] - a \cos[a+b] \sin[\sqrt{a^2 - r_1^2 e^{2iq_1} e^{4pi} - 2ig r_1 e^{iq_1} e^{2pi} + g^2}]} \quad (29)$$

where $e^{2pi} = e^{4pi} = 1$, Equation (29) is equal to Equation (28). Thus there is actually only one branch to the function, and so $p = ig$ can not be a branch point.

For $p = -ig$, we assume that

$$p + ig = r_1 e^{iq_1} \quad (30)$$

then we have

$$y(p) = \frac{P_0 g^2}{E A_0 \sin[a+b]} \frac{\sin[\sqrt{a^2 - r_1^2 e^{2iq_1} + 2ig r_1 e^{iq_1} + g^2}]}{(r_1 e^{iq_1} - ig)(r_1 e^{iq_1} - 2ig)(r_1 e^{iq_1})} \frac{1}{\sqrt{a^2 - r_1^2 e^{2iq_1} + 2ig r_1 e^{iq_1} + g^2} \cos[\sqrt{a^2 - r_1^2 e^{2iq_1} + 2ig r_1 e^{iq_1} + g^2}] \sin[a+b] - a \cos[a+b] \sin[\sqrt{a^2 - r_1^2 e^{2iq_1} + 2ig r_1 e^{iq_1} + g^2}]} \quad (31)$$

As q increases from q_1 to $q_1 + 2p$, which is what happens when one complete circuit counter clockwise around the origin is made, we find

$$y(p) = \frac{P_0 g^2}{E A_0 \sin[a+b]} \frac{\sin[\sqrt{a^2 - r_1^2 e^{2iq_1} e^{4pi} + 2ig r_1 e^{iq_1} e^{2pi} + g^2}]}{(r_1 e^{iq_1} e^{2pi} - ig)(r_1 e^{iq_1} e^{2pi} - 2ig)(r_1 e^{iq_1} e^{2pi})} \frac{1}{\sqrt{a^2 - r_1^2 e^{2iq_1} e^{4pi} + 2ig r_1 e^{iq_1} e^{2pi} + g^2} \cos[\sqrt{a^2 - r_1^2 e^{2iq_1} e^{4pi} + 2ig r_1 e^{iq_1} e^{2pi} + g^2}] \sin[a+b] - a \cos[a+b] \sin[\sqrt{a^2 - r_1^2 e^{2iq_1} e^{4pi} + 2ig r_1 e^{iq_1} e^{2pi} + g^2}]} \quad (32)$$

where $e^{2pi} = e^{4pi} = 1$, Equation (32) is equal to Equation (31). Thus there is actually only one branch to the function, and so $p = -ig$ can not be a branch point.